

Summer 8-2-2023

SENSING THE RHIZOSPHERE: MICROBIAL TRANSCRIPTOME RESPONSES TO ROOT EXUDATES AND REDOX-ACTIVE METABOLITES

Ankita Bhattacharyya

Follow this and additional works at: <https://aquila.usm.edu/dissertations>



Part of the [Environmental Microbiology and Microbial Ecology Commons](#), and the [Molecular Genetics Commons](#)

Recommended Citation

Bhattacharyya, Ankita, "SENSING THE RHIZOSPHERE: MICROBIAL TRANSCRIPTOME RESPONSES TO ROOT EXUDATES AND REDOX-ACTIVE METABOLITES" (2023). *Dissertations*. 2141.
<https://aquila.usm.edu/dissertations/2141>

This Dissertation is brought to you for free and open access by The Aquila Digital Community. It has been accepted for inclusion in Dissertations by an authorized administrator of The Aquila Digital Community. For more information, please contact aquilastaff@usm.edu.

SENSING THE RHIZOSPHERE: MICROBIAL TRANSCRIPTOME RESPONSES TO
ROOT EXUDATES AND REDOX-ACTIVE METABOLITES

by

Ankita Bhattacharyya

A Dissertation
Submitted to the Graduate School,
the College of Arts and Sciences
and the School of Biological, Environmental, and Earth Sciences
at The University of Southern Mississippi
in Partial Fulfillment of the Requirements
for the Degree of Doctor of Philosophy

Approved by:

Dr. Dmitri Mavrodi, Committee Chair

Dr. Alex S. Flynt

Dr. Micheal A. Davis

Dr. Kevin A. Kuehn

Dr. Fengwei Bai

August 2023

COPYRIGHT BY

Ankita Bhattacharyya

2023

Published by the Graduate School



THE UNIVERSITY OF
SOUTHERN
MISSISSIPPI®

ABSTRACT

The term “rhizosphere” describes the dynamic interface between plant roots and soil influenced by root exudates. It is a hotspot of microbial activity, plant-microbe, and microbe-microbe interactions. Distinct variations in bacterial diversity are thought to be driven by plant root exudates. However, the molecular details of these processes still remain unclear.

I addressed this gap by focusing on two strains, *Pseudomonas synxantha* 2-79 and *Burkholderia lata* 383, representing diverse groups of Gammaproteobacteria comprised of species with environmental, agricultural, and medical significance. In the first part of this project, we used a combination of metabolomics and RNA-seq to characterize transcriptome responses of *P. synxantha* 2-79 to the root exudates of barley. Our results revealed that root exudates perturb bacterial genes that function in the uptake and catabolism of C and N sources, synthesis of antimicrobials, and biofilm formation. The second part of my project explored exudate-mediated interactions between 2-79 and wheat under water stress. Metabolomic profiling of root exudates from wheat showed that the water-stressed plants exude significantly higher amounts of osmoprotectants called quaternary ammonium compounds (QACs). Transcriptome profiling of 2-79 grown in the presence of these exudates revealed changes in the expression of genes for the catabolism of QACs. These results portray the effects of drought on the rhizosphere microbiome and demonstrate that plant root exudates play a significant role in the survival of root-associated microorganisms in water-deprived conditions.

My final aim dealt with redox-active secondary phenazine metabolites produced by *B. lata* 383. Using a combination of transposon mutagenesis and RNA-seq, we

identified multiple genes that function in the phenazine biosynthesis, its cell density-dependent regulation, and inherent tolerance to these redox-active metabolites. This is the first study to demonstrate that phenazine production in *Burkholderia* is regulated in response to quorum sensing. Finally, we analyzed transcriptome responses to phenazine methosulfate in *B. lata* 383 and two closely related phenazine-non-producing *Burkholderia* strains. Our results revealed that *Burkholderia* spp. cope with phenazine toxicity by upregulating pathways involved in oxidative stress response, iron-sulfur cluster biogenesis, and multidrug efflux. Collectively, these results will provide new insight into interspecies interactions with rhizosphere communities and molecular processes underpinning the adaptation of plants and their associated microbes to abiotic stress.

ACKNOWLEDGMENTS

My heartfelt gratitude and appreciation go out to my advisors and mentors, Drs. Dmitri and Olga Mavrodi. Their support and mentorship were indispensable in my Ph.D. journey. I hope to carry forward the ideals of the Mavrodi Lab in my future endeavors and will be forever thankful for their kindness, trust, and caring support. I also thank Dr. Mavrodi for designing research-intensive courses and giving me the opportunity to teach them, which will help me flourish in the future.

My research would not have been possible without the hard work and support of the past and present members of the Mavrodi Lab. Janiece and Sam's research has been a foundation for my studies, and without Yetunde and Clint's support, friendship, and mentoring, I don't think I would have been able to persevere. I thank Niladri for being an indispensable support throughout my Ph.D. journey, and Anushka for helping me in teaching and mentoring undergrads. My undergraduate research mentees, Ashley, Cole, Mallory, Jessie, Angelly, and Cynthia have given me the opportunity to flourish as a graduate student mentor and have helped me tremendously in my projects. I would like to especially mention Ashley Grantham and Cole Hinson for their hard work and sincerity in the research, and for supporting me throughout.

I thank my committee members, Dr. Alex Flynt, Dr. Micheal Davis, Dr. Kevin Kuehn, and Dr. Fengwei Bai, for setting out the time from their busy schedules to be on my committee. I appreciate the feedback they gave me to improve my research and their support in my future endeavors. Dr. Flynt and his lab have been instrumental in my RNA-seq analyses, for which I am grateful to him. I also thank our collaborators, Dr.

Linda Thomashow, Dr. David Weller, and Dr. Tim Paulitz, for their valuable input in my research.

I appreciate Dr. Jonathan Lindner for sharing the knowledge of any instrument in the entire INBRE facility that I needed for my research. I also thank him for being a great friend and providing mental support to a lot of graduate students like me. I also thank Jordan Laster and Mary Ann McRaney for their work in MS-INBRE which benefits our research tremendously. Additionally, I would like to thank the director of the School of BEES, Dr. Jake Schaefer, and the entire administrative staff (special mention to Angela Williams) who are responsible for running the program efficiently.

I would like to thank my family, without whose support, any of this would not have been possible. My parents, Asok Kumar Bhattacharyya and Santa Bhattacharyya have brought me up in the best way possible, and I thank them for their incredible support in everything I chose to do in my life. My sister, Arinjita Bhattacharyya and brother-in-law Soham Mukherjee, have inspired me and supported me while I stepped into a new country. I don't have enough words to thank my partner in the lab, and life, Niladri Bhowmik, for his support and belief in me. I also thank my extended family in India and US for their help, encouragement, and support. Lastly, I would like to thank my friends in India and US, Shreya, Kaustav, Tapadyuti, Raima, Faiyaz, Lavanya, Stephen, and Rebekah, for being by my side and encouraging me always.

The main funding for this project was provided through the NSF IOS award 1656872. I also acknowledge the Mississippi INBRE, funded by an Institutional Development Award (IDeA) from the National Institute of General Medical Sciences of NIH under grant P20GM103476.

DEDICATION

To my family, who made me who I am today.

To Sir Jagadish Chandra Bose and Dr. Ananda Mohan Chakrabarty, the two Bengali scientists, whose pioneering works on plant physiology and pseudomonads, respectively, have inspired me in pursuing this research.

TABLE OF CONTENTS

ABSTRACT ii

ACKNOWLEDGMENTS iv

DEDICATION vi

LIST OF TABLES xi

LIST OF ILLUSTRATIONS xii

LIST OF ABBREVIATIONS xvi

CHAPTER I- INTRODUCTION 1

 1.1 Importance of rhizosphere microbiome 1

 1.2 The role of rhizodeposits in the selection of rhizosphere microbiome 3

 1.3 The role of redox-active metabolites in shaping the rhizosphere microbiome 7

 1.4 Research purpose, aims, and significance 9

 1.5 References 11

CHAPTER II- TRANSCRIPTOMIC RESPONSES OF THE MODEL RHIZOSPHERE
BACTERIUM PSEUDOMONAS SYNXANTHA 2-79 TO BARLEY ROOT

EXUDATES 28

 2.1 Abstract 28

 2.2 Introduction 29

 2.3 Materials and Methods 32

 2.3.1 Microorganisms and culture conditions 32

2.3.2	Collection of barley root exudates	33
2.3.3	Metabolome profiling of root exudates.....	34
2.3.4	Effect of phosphate and root exudates on 2-79 growth and <i>phzA</i> gene expression	36
2.3.5	Transcriptome responses of 2-79 to barley root exudates	37
2.3.6	Bioinformatic analysis of expression data	38
2.4	Results and Discussion	38
2.4.1	An axenic culture system for infecting barley roots with <i>R. solani</i>	38
2.4.2	Metabolome profiling of root exudates.....	39
2.4.3	The effect of phosphate and root exudates on <i>phzA</i> gene expression.....	42
2.4.4	Transcriptome responses of 2-79 to barley root exudates	43
2.5	References.....	52

CHAPTER III- EFFECT OF WATER STRESS ON ROOT EXUDATION AND ITS
ROLE IN THE ALTERATION OF GENE EXPRESSION AND PHYSIOLOGY OF
THE MODEL RHIZOSPHERE BACTERIUM PSEUDOMONAS SYNXANTHA 2-79

.....	63	
3.1	Abstract.....	63
3.2	Introduction.....	64
3.3	Materials and Methods.....	67
3.3.1	Bacterial strains and culture conditions	67

3.3.2	Collection of wheat root exudates.....	67
3.3.3	Metabolomic profiling of root exudates	68
3.3.4	Bacterial osmoprotection assays	70
3.3.5	RNA extraction and processing	70
3.3.6	Transcriptomic and gene expression studies.....	71
3.3.7	RT-qPCR assays	72
3.4	Results and Discussion	73
3.4.1	Water stress significantly alters the composition of wheat root exudates	73
3.4.2	Root exudates rescue the growth of 2-79 under water stress.....	74
3.4.3	Transcriptome responses of 2-79 to wheat root exudates	75
3.5	References.....	82
CHAPTER IV- GENES INVOLVED IN THE REGULATION OF BIOSYNTHESIS		
AND RESISTANCE TO REDOX-ACTIVE PHENAZINES IN THE MODEL SOIL		
BACTERIUM BURKHOLDERIA LATA 383.....		
4.1	Abstract.....	91
4.2	Introduction.....	92
4.3	Materials and Methods.....	94
4.3.1	Microorganisms and culture conditions.....	94
4.3.2	Transposon mutagenesis of <i>B. lata</i> 383	95
4.3.3	Mapping of transposon insertion sites in pigment-deficient mutants	96

4.3.4 Comparison of phenazine gene expression in pigment-deficient mutants.....	96
4.3.5 Construction of <i>B. lata</i> isogenic mutants and complementation	97
4.3.6 Phenotypic assays	99
4.3.7 Transcriptomic responses of <i>B. lata</i> 383 mutants.....	100
4.3.8 Effect of phenazine metabolites on <i>Burkholderia</i> transcriptome	101
4.4 Results and Discussion	102
4.4.1 Phenazine synthesis in <i>B. lata</i> 383 involves diverse regulatory and metabolic pathways	102
4.4.2 Phenazine gene expression in <i>Burkholderia</i> mutants	107
4.4.3 The effect of quorum sensing on the physiology of <i>B. lata</i> 383.....	108
4.4.4 Transcriptomic responses of <i>B. lata</i> 383 and mutants	109
4.4.5 Effect of phenazine on <i>Burkholderia</i> transcriptome.....	112
4.5 References.....	120
CHAPTER V- CONCLUSIONS	129
5.1 References.....	131

LIST OF TABLES

Table 4.1 Summary of <i>B. lata</i> 383 genes with mutations associated with the loss of phenazine pigmentation.	104
Table 4.1 (continued).....	105
Table 4.1 (continued).....	106
Table 4.2 Shared differentially expressed genes and their predicted functions in <i>Burkholderia</i> strains exposed to phenazine methosulfate. ^a	116
Table 4.2 (continued).....	117
Table 4.2 (continued).....	118

LIST OF ILLUSTRATIONS

Figure 1.1 Overview of the beneficial and pathogenic aspects of plant rhizosphere microbiome	1
Figure 1.2 Plant roots, border cells and microbes produce and secrete numerous metabolites that shape the rhizosphere and endosphere microbiomes by recruiting certain taxa from the soil seedbank.....	4
Figure 1.3 Some phenazine RAMs produced by Gram-negative and Gram-positive soil and rhizosphere bacteria.	8
Figure 2.1 Axenic culture system used for collecting roots exudates from Rhizoctonia-infected barley. The left panel shows seedlings incubated on water agar with and without <i>R. solani</i> AG-8. The right panel shows a stained control root (top) and an infected root (bottom) covered with a network of Rhizoctonia hyphae.....	39
Figure 2.2 Concentrations (mean \pm SD) of primary and secondary metabolites and quaternary ammonium compounds (QACs) in exudates of healthy and Rhizoctonia-infected barley cv. Golden Promise.....	41
Figure 2.3 The bacterial growth and expression of the <i>phzA::gfp</i> reporter in 2-79 cultures at two levels of phosphate (1 mM or 0.3 mM) with and without root exudates.....	42
Figure 2.4 Transcriptome responses of 2-79 to barley root exudates. (A) Volcano plots that show significantly up- and downregulated genes in red and blue. (B) Principal component analysis of biological replicates. (C) Venn diagram of differentially expressed genes (DEGs) that are unique and shared between treatments. (D) KEGG Orthology classification of proteins encoded by DEGs.	44

Figure 2.5 The response to root exudates involved induction of genes for the biogenesis of type IVb pili and fimbriae, which is consistent with surface attachment and transition to the biofilm growth mode.....	47
Figure 2.6 Gene ontology classification of differentially expressed genes of 2-79 in (left) healthy and (right) Rhizoctonia-infected root exudates compared to control conditions.	49
Figure 2.7 Results of GO term enrichment analysis of upregulated genes in (top) healthy and (bottom) Rhizoctonia-infected root exudates compared to control conditions.....	50
Figure 3.1 Concentrations (mean \pm SD) of primary metabolites and quaternary ammonium compounds (QACs) in exudates of water-replete and water-stressed spring wheat cv. Tara.	73
Figure 3.2 Root exudates of water-stressed wheat cv. Tara are rich in QACs and protect 2-79 from osmotic stress.....	76
Figure 3.3 Transcriptome responses of 2-79 to wheat root exudates. (A) Volcano plots that show significantly up- and downregulated genes in red and blue (C, culture medium; CE, control exudates; SE, water-stressed exudates). (B) Venn diagram of differentially expressed genes (DEGs) that are unique and shared between treatments. (C) Principal component analysis of biological replicates. (D) Changes in expression of selected differentially expressed genes. (E) KEGG Orthology classification of proteins encoded by DEGs.....	77
Figure 3.4 Gene ontology classification of 2-79 DEGs in (A) water-replete and (B) water-stressed root exudates compared to control conditions.....	78
Figure 3.5 The summary of <i>P. synxantha</i> 2-79 genes predicted to function in the uptake and catabolism of QACs (left), and relative expression of key QAC catabolism genes in	

response to culture medium, water replete and water-stressed root exudates as analyzed by RT-qPCR (right).	80
Figure 3.6 The distribution of QAC catabolism pathways across different bacterial phyla (A) and the proportion of bacterial families (B) and genera (C) carrying betAB, gbcAB, dgcAB, and soxBDAG genes.	81
Figure 4.1 Pigmentation associated with the synthesis of 4,9-dihydrophenazine-1,6-dicarboxylic acid dimethylester (left) and color gradient (right) observed in standing cultures of <i>B. lata</i> 383, presumably due to reduction of phenazines.	93
Figure 4.2 The loss of phenazine pigmentation in Δ cepI and cepR::Tn5 quorum sensing mutants and its restoration in the Δ cepI strain complemented with a pBBR1MCS plasmid carrying functional cepI gene.....	103
Figure 4.3 The expression of the core phenazine biosynthesis gene phzE in (A) selected non-pigmented transposon mutants and (B) Δ cepI knockout mutant of <i>B. lata</i> 383.	107
Figure 4.4 Phenotypic assays with <i>B. lata</i> 383 and quorum sensing mutants. (A) Biofilm assays demonstrate significant differences amongst treatments; (B) Siderophore assay and (C) Exoprotease assay showing zones of clearing significantly different in mutants; (D) Zone of clearing in (top) siderophore assay and (bottom) exoprotease assay of wild-type and mutant <i>B. lata</i> 383.	108
Figure 4.5 The effect of phzA and cepI mutations on the <i>B. lata</i> transcriptome. (A) Volcano plots of genes significantly up- and downregulated in both mutants in comparison to the wild-type strain (WT). (B) The significant downregulation of phenazine synthesis genes in the quorum-sensing mutant. (C) Differentially expressed genes that are shared and unique to the phzA and cepI mutants.	110

Figure 4.6 Gene ontology classification of differentially expressed genes of *B. lata* 383 in the (left) *cepI* and (right) *phzA* mutants compared to the wild-type strain. 111

Figure 4.7 Volcano plots showing significantly up- and downregulated genes in phenazine methosulfate-treated (A) *B. lata* 383, (B) *B. cepacia* ATCC 25416, and (C) *B. cenocepacia* K56-2 compared to control conditions; (D) Venn diagram showing shared and unique differentially expressed genes in the three strains..... 113

Figure 4.8 The RND-9 efflux pump genes are strongly upregulated in response to treatment of *B. lata* 383 with phenazine methosulfate (PMS)..... 114

Figure 4.9 Gene ontology classification of differentially expressed genes of phenazine methosulfate-treated (A) *B. lata* 383 and (B) *B. cepacia* ATCC 25416 compared to control conditions; (C) GO term enrichment analysis of upregulated genes in phenazine methosulfate-treated *B. cepacia* ATCC 25416 compared to control conditions. (D) A representation of defense responses in *Burkholderia* cells triggered by phenazine exposure. 119

LIST OF ABBREVIATIONS

<i>PMS</i>	Phenazine methosulfate
<i>QAC</i>	Quaternary Ammonium Compounds
<i>RAM</i>	Redox-Active Metabolite
<i>RE</i>	Root Exudate

CHAPTER I- INTRODUCTION

1.1 Importance of rhizosphere microbiome

The rhizosphere is a narrow soil region that surrounds plant roots and harbors a rich microbial ecosystem. With more than 30,000 prokaryotic species,¹ the rhizosphere can contain up to 10^{11} microbial cells per gram of plant root.² Interestingly, many general aspects of interactions between plants and rhizosphere microflora resemble the association of humans with their gut microbiome.^{3,4} These plant-microbe interactions can either be positive (mutualistic), negative (pathogenic), or neutral,⁵ and, as in humans, their importance in plant health is becoming increasingly evident (Figure 1.1).

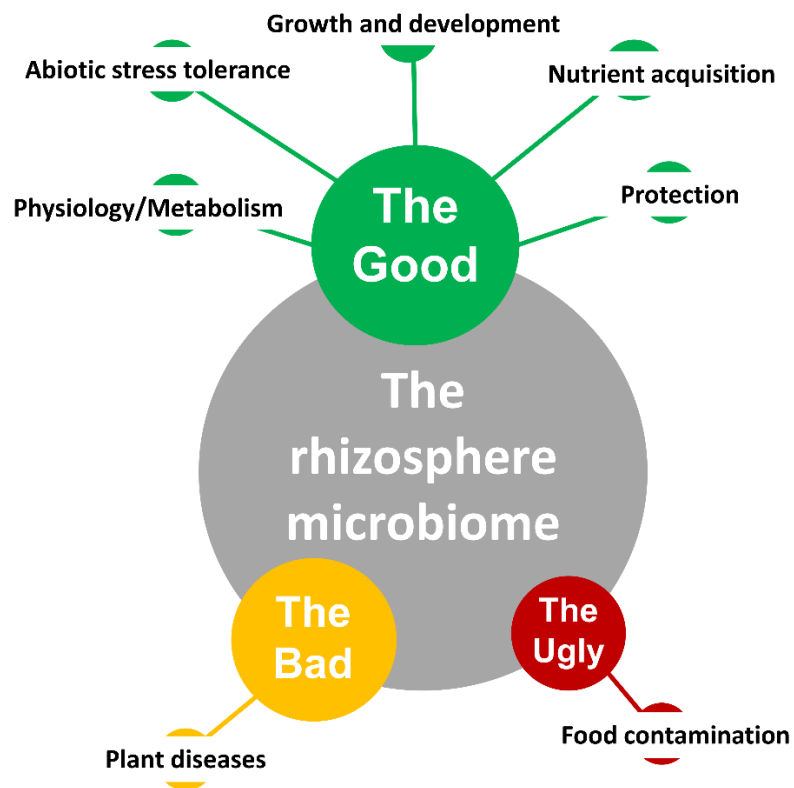


Figure 1.1 *Overview of the beneficial and pathogenic aspects of plant rhizosphere microbiome*

Adapted from Mendes et al., 2013²

This microbial community inhabiting plant surfaces and tissues (i.e., the rhizobiome) is often referred to as the plant's second genome, as its collective gene pool is much larger than that of the host.⁶ Hence, plants are viewed as superorganisms that depend on their microbiome for various functions.² The ability of mycorrhizae, *Rhizobia* and other diazotrophic bacteria to improve the plant's phosphorus and nitrogen status was recognized as early as the 1950s.^{7,8} The uptake of specific trace elements, such as iron, which is abundant in soil, but mostly in an insoluble ferric form, is facilitated by rhizosphere microorganisms via the secretion of siderophores.⁹ Mineral weathering bacteria also form a part of the rhizobiome and play an essential role in mobilizing nutrients from soil minerals.¹⁰ This includes the microorganisms capable of solubilizing inorganic phosphate, which is a critically important macronutrient required for plant growth.¹¹ Multiple species of phosphate-solubilizing rhizobacteria have been characterized and even used in agriculture as biofertilizers.¹² Rhizosphere microbiome also helps plants in the adaptation to extreme environmental conditions, such as drought stress¹³ or flooding.¹⁴ Similarly, many accounts of the beneficial microbial effects have been reported in plants exposed to elevated salinity,¹⁵ temperatures,^{16,17} soil pH,¹⁸ and the presence of toxic compounds.¹⁹

In addition to abiotic stressors, plants are attacked by various pests and pathogens. Many of these pathogens are soilborne and include fungi, oomycetes, nematodes, and certain bacteria that occur worldwide, persist in soil for a long time and cause significant yield reductions in food crops. Genetic resistance to most soilborne diseases is rare, and plants instead rely on their rhizosphere microbiome for the protection from biotic stress. The defense mechanisms associated with rhizobacteria are diverse and include the displacement of pathogens via competition for nutrients.² Many rhizosphere

microorganisms act as biological control agents by producing metabolites that directly inhibit the activity of plant pathogens. These include the highly specific bacteriocins²⁰ as well as numerous polyketides, nonribosomal peptides and other classes of broad-spectrum antibacterial and antifungal compounds.²¹ Some beneficial microorganisms emit organic volatiles that promote plant growth and inhibit the mycelial growth of phytopathogenic fungi.²²⁻²⁴ Finally, many rhizobacteria induce systemic response in plants by modulating the jasmonic acid/ethylene²⁵ and salicylic acid signaling pathways.²⁶ The activation of defense-related plant genes involves Microbe-Associated Molecular Patterns (MAMPs), siderophores, quorum-sensing molecules, various secondary metabolites and volatiles.²⁷

1.2 The role of rhizodeposits in the selection of rhizosphere microbiome

Plants secrete up to 40% of their photosynthates through their roots into the rhizosphere.²⁸ The root exudates are composed of numerous low-molecular-weight (carbohydrates, amino acids, organic acids, phenolics) and high-molecular-weight (polysaccharides, mucilages, proteins) compounds (Figure 1.2).²⁹ These rhizodeposits attract diverse microbial species from the carbon starved bulk soil to the rhizosphere, creating a phenomenon known as the 'rhizosphere effect'.³⁰ Recent ecological theories state that root exudates stimulate beneficial microorganisms resulting in better nutrient acquisition and protection against abiotic and biotic stressors.³¹ The exudation also attracts pathogens such as nematodes, which are chemotaxically driven to certain volatiles and water-soluble compounds (e.g., carbon dioxide, glutamic and ascorbic acids) secreted by plant roots.³² Plant roots generate endogenous electric field profiles due to the flow of protons and ions, which attract motile zoospores of oomycete pathogens through electrotaxis.³³ Interestingly, the rhizobiome differs substantially in its

shaped by the modifications associated with domestication and breeding.^{41,42} The process of plant domestication involves the artificial selection for desired traits and often alters root architecture, which, in turn, affects the root exudation⁴³ and the diversity and abundance of rhizosphere microbiota.^{44,45}

In nature, plant roots are constantly challenged by countless commensal, pathogenic, and symbiotic species of microorganisms. Recent studies revealed that these biotic interactions induce systemic signaling that triggers changes in the composition and amounts of metabolites exuded by plant roots. For example, Korenblum et al.⁴⁶ used a split-root hydroponic system to describe the phenomenon of systemically induced root exudation of metabolites (SIREM) in tomatoes. The authors demonstrated that treating half of the plant roots with various microorganisms resulted in the systemic secretion of acylsugars in the other part of the root system. Significantly, some acylsugars (e.g., azelaic acid) have insecticidal and fungicidal properties and have been shown to accumulate in plant tissues during a pathogen attack.⁴⁷ In another split-root study, the exposure of tomato roots to pathogen attack, wounding or osmotic stress induced secretion of unidentified plant exometabolites that acted as chemoattractants for the beneficial biocontrol fungus *Trichoderma harzianum* T22.⁴⁸ Wang et al.⁴⁹ used a similar experimental system to demonstrate that the treatment with the biocontrol agent *Bacillus cereus* AR156 significantly altered the rhizodeposition of tomato plants. The exudates of treated plants inhibited the bacterial wilt pathogen *Ralstonia solanacearum* and contained elevated levels of certain carbohydrates and organic acids, which stimulated the growth, motility, and biofilms of AR156. These and related studies show how rhizosphere plant-microbe interactions can shift the composition of root exudates and aid in the recruitment

of beneficial microbes that help plants cope with biotic stress.^{50,51} The amount and chemical makeup of exudates are strongly affected by abiotic environmental stimuli driving shifts in the composition of rhizosphere microbiome observed under changing soil composition, pH, temperature, salinity, and moisture.⁵²⁻⁵⁵ For example, the secretion of flavonoid compounds by roots of nitrogen-deficient legume plants induces the establishment of symbiosis with specific species of diazotrophic rhizobia.⁵⁶ Many rhizosphere microorganisms prefer a pH range of 6 to 7, hence changes in soil acidity or alkalinity change the microbial composition and activity.⁵⁷ However, some species tolerate lower pH, which, for example, affects the diversity and density of diazotroph communities in alpine meadow soils.⁵⁸ Soil temperature also plays an important role in shaping the root architecture and root exudation patterns⁵⁹, which in turn affects the physiology of rhizobacteria.⁶⁰ Oxygen availability in soil, mainly impacted by waterlogging⁶¹, leads to energy shortages and disruption in growth of plant roots.⁶² This affects root exudation and negatively impacts aerobic microbes, such as Actinobacteria, which are hardly seen in flood plains.⁶³ The microbiome is generally shifted towards anaerobic microorganisms in anoxic or hypoxic conditions.⁶⁴

The rhizosphere soil microbiome is also strongly affected by water stress.⁶⁵ Plant roots mitigate drought stress through osmotic adjustment, which correlates with increased overall exudation⁶⁶ and deposition of compatible solutes like amino acids and production of quaternary ammonium compounds (QACs).⁶⁷ Microbes evolved various adaptations to tolerate drought stress, which includes production and/or scavenging (from rhizosphere) of osmolytes, such as glutamine, proline, trehalose, and QACs such as glycine-betaine.^{68,69} It has been reported that under drought the plant microbiome shifts towards

Gram-positive species that produce exo- and endospores and are more resilient to desiccation.^{70,71} Bacteria also increase the synthesis of extracellular polymeric substances (EPS) as an effective drought adaptation method.⁷² Some drought-mediated changes in exudation patterns mitigate water stress effects in the rhizosphere and protect the microorganisms inhabiting plant roots.⁷³ For example, drought increases the concentration of malic acid in the root exudates of maize. The malic acid recruits *Bacillus subtilis* that increases the plant drought resistance by secreting osmolytes.^{74,75}

1.3 The role of redox-active metabolites in shaping the rhizosphere microbiome

In addition to plant-microbe interactions driven by root exudates, the rhizosphere microbiome is shaped by interspecies microbial interactions. The colonization of plant surfaces by complex communities involves cooperative, competitive, and antagonistic interactions that determine the outcome of the continuous battle for host-derived nutrients and space. Some examples of cooperation in the rhizosphere include metabolic interdependence when, in nutrient-poor environments, some microbes extend their fundamental niches by the reciprocal exchange of metabolites.^{76,77} For example, *Bacillus cereus* UW85 stimulated the growth of bacteria from the Cytophaga-Flavobacterium group in the soybean rhizosphere.⁷⁸ This interdependency led to adaptive gene loss, as the partner fidelity assured the complementation of a redundant function. Another example of cooperation is observed during the formation of mixed biofilms, which requires a coordinated secretion of exopolysaccharides, extracellular DNA, proteins and diffusible signals.⁷⁹ Competitive interactions often involve some form of interspecies competition for macro- or micronutrients. For example, the sequestration of iron by siderophores was implicated as an important mechanism that allows certain rhizobacteria to suppress plant

pathogens.⁸⁰ Finally, numerous examples of antagonistic interactions involve the in situ production of bacteriocins, protein toxins and low-molecular-weight phenolics, polyketides, non-ribosomal peptides, terpenoids or aminoglycosides. Such metabolites exhibit varying spectra of antibiotic activity and help the producing organism to compete with more closely and distantly related bacteria and fungi and to ward off bacterivorous protozoa and nematodes.^{81–85}

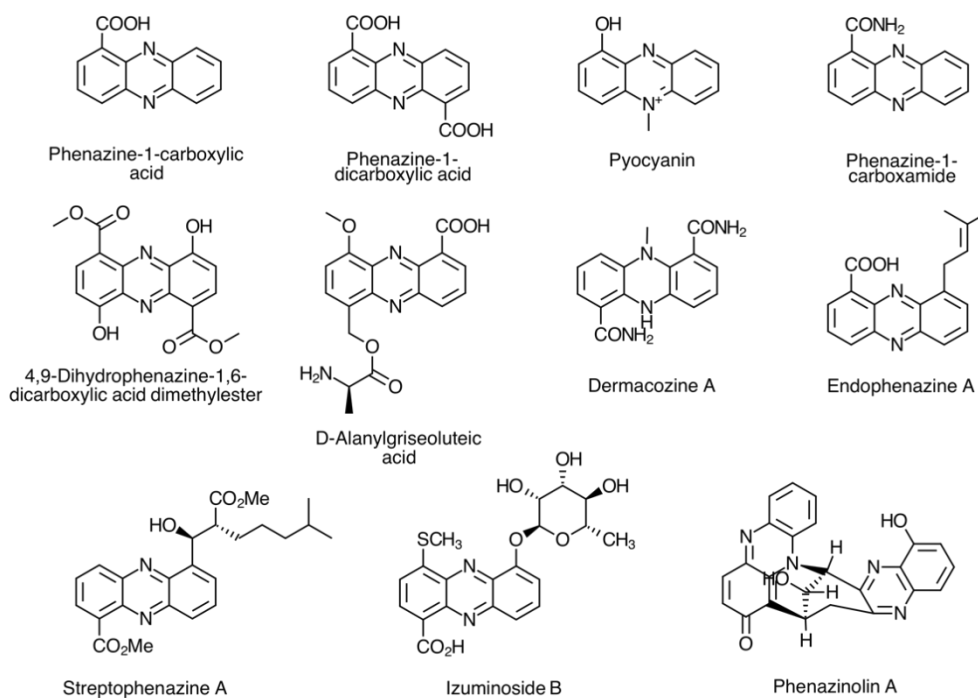


Figure 1.3 *Some phenazine RAMs produced by Gram-negative and Gram-positive soil and rhizosphere bacteria.*

Phenazines encompass a group of redox-active metabolites (RAMs) that contribute to intermicrobial competition in the rhizosphere. These compounds structurally resemble flavins and kill sensitive organisms by participating in redox cycling and generating reactive oxygen species (Figure 1.3).⁸⁶ Many phenazines have antimicrobial properties and rhizobacteria producing these metabolites include numerous biocontrol agents of diseases caused by phytopathogenic fungi and bacteria.^{87–89} Phenazine

producers are globally abundant in soil and rhizosphere microbiomes, and the redox cycling activity of these RAMs mobilizes phosphorus and iron, making them bioavailable to plants.^{90,91} Recent studies significantly extended our understanding of phenazine's role in the biology of microorganisms. In the opportunistic human pathogen *Pseudomonas aeruginosa*, phenazines modulate the cellular redox state and facilitate fermentation and survival in hypoxic environments.⁹² Phenazines also act as signals that regulate the expression of *P. aeruginosa* genes involved in antibiotic resistance and biofilm development.^{93,94} In *P. aeruginosa* and closely related species, phenazine production is regulated by quorum sensing, a cell density-dependent form of microbial communication based on autoinducing diffusible signals such as N-acyl-L-homoserine lactones (AHLs).⁹⁵ Quorum sensing is not limited to phenazine producers. It occurs in many Gram-negative and Gram-positive bacteria, where it coordinates diverse and cooperative activities relevant to symbiotic or parasitic interactions with eukaryotic hosts (i.e., motility, adhesion, biofilm formation, propagation, metabolism, virulence factors, exoenzymes and secondary metabolites).⁹⁶

1.4 Research purpose, aims, and significance

The rhizosphere microbiome positively influences plant fitness in response to the detrimental effects of diseases and climate change by stimulating nutrient uptake and organ development, suppressing pathogens, and enhancing the ability to resist heat and drought. The successful exploitation of such beneficial interactions requires a firm knowledge of the physiological and molecular processes involved in plant and microbial adaptation to biotic and abiotic stress. In contrast, our understanding of molecular mechanisms behind the rhizobiome recruitment by stressed plants, microbial interactions

in the rhizosphere, and the subsequent feedback to plant growth and fitness remains limited. My studies addressed some of these gaps by focusing on microbial transcriptome responses to root exudates and redox-active phenazine metabolites. My *central hypothesis* is that root exudates and RAMs modulate expression of metabolic, regulatory and stress response pathways critical for the adaptation of microorganisms to the rhizosphere lifestyle.

My research focused on two rhizobacteria - *Pseudomonas synxantha* 2-79 and *Burkholderia lata* 383. Pseudomonads are ubiquitous Gammaproteobacteria that catabolize various organic compounds, colonize eukaryotes, and inhibit plant and animal pathogens via the production of diverse secondary metabolites and antibiotics.^{97,98} They are divided into 14 lineages and over 180 species,⁹⁹ with a high proportion of species acting as beneficial plant growth-promoting or biocontrol organisms.¹⁰⁰ 2-79 exemplifies a complex of *P. fluorescens*-like strains specifically associated with dryland cereals grown across the Inland Pacific Northwest of the United States.¹⁰¹ These strains produce phenazine-1-carboxylic acid and protect crops against pathogenic soilborne fungi, such as *Rhizoctonia solani* and *Fusarium* spp. Last year, the Inland Pacific Northwest experienced an unprecedented heat wave and drought that resulted in record low harvests of small grains and hay. As a result, the average yield of wheat in Washington was 72.4 bushels/acre in 2020, but only 39.1 bushels/acre in 2021.¹⁰² Hence, *P. synxantha* 2-79 and dryland cereals provide an excellent model for studying the interdependence of dryland crops and their associated microbiota.

Burkholderia encompass over 100 species associated with infectious diseases and hospital-acquired infections, as well as numerous plant-associated mutualists.^{103–108} The

Mavrodi lab has recently demonstrated that strains of the *B. cepacia*, *B. pseudomallei*, and *B. glumae*/*B. gladioli* clades carry phenazine biosynthesis genes.¹⁰⁹ However, most of our current knowledge about the diverse biological functions of phenazines and their effects on other organisms is based on a single model – the opportunistic human pathogen *Pseudomonas aeruginosa*. Similar knowledge for economically important members of the *Burkholderia* group is lagging. Hence, in the third Aim, I characterized genes involved in the production, regulation, and resistance to phenazines in *B. lata* 383, a soilborne strain of the *B. cepacia* complex.

Accordingly, the specific aims of my thesis project were:

1. To characterize transcriptomic responses of *P. synxantha* 2-79 to barley root exudates;
2. To characterize the effect of water stress on root exudation and determine how exudates of water-stressed plants alter gene expression and physiology of the model rhizosphere bacterium *Pseudomonas synxantha* 2-79;
3. To characterize genes involved in the regulation of biosynthesis and resistance to redox-active phenazines in the model soil bacterium *Burkholderia lata* 383.

1.5 References

1. Egamberdieva D, Kamilova F, Validov S, Gafurova L, Kucharova Z, Lugtenberg B. High incidence of plant growth-stimulating bacteria associated with the rhizosphere of wheat grown on salinated soil in Uzbekistan. *Environ Microbiol.* 2008;10(1):1-9. doi:10.1111/j.1462-2920.2007.01424.x
2. Mendes R, Garbeva P, Raaijmakers JM. The rhizosphere microbiome: Significance of plant beneficial, plant pathogenic, and human pathogenic

- microorganisms. *FEMS Microbiol Rev.* 2013;37(5):634-663. doi:10.1111/1574-6976.12028
3. Holden N, Pritchard L, Toth I. Colonization outwith the colon: Plants as an alternative environmental reservoir for human pathogenic enterobacteria: Review article. *FEMS Microbiol Rev.* 2009;33(4):689-703. doi:10.1111/j.1574-6976.2008.00153.x
 4. Van Baarlen P, Van Belkum A, Summerbell RC, Crous PW, Thomma BPHJ. Molecular mechanisms of pathogenicity: How do pathogenic microorganisms develop cross-kingdom host jumps? *FEMS Microbiol Rev.* 2007;31(3):239-277. doi:10.1111/j.1574-6976.2007.00065.x
 5. Singh BK, Millard P, Whiteley AS, Murrell JC. Unravelling rhizosphere–microbial interactions: Opportunities and limitations. *Trends Microbiol.* 2004;12(8):386-393. doi:https://doi.org/10.1016/j.tim.2004.06.008
 6. Berendsen RL, Pieterse CMJ, Bakker PAHM. The rhizosphere microbiome and plant health. *Trends Plant Sci.* 2012;17(8):478-486. doi:10.1016/j.tplants.2012.04.001
 7. Gaby JC, Buckley DH. A global census of nitrogenase diversity. *Environ Microbiol.* 2011;13(7):1790-1799. doi:https://doi.org/10.1111/j.1462-2920.2011.02488.x
 8. Morton AG. A. G. Morton, History of botanical science, London and New York, Academic Press, 1981, 8vo, pp. xii, 474 (paperback). *Med Hist.* 1982;26(4):474. doi:10.1017/s0025727300042009
 9. Hider RC, Kong X. Chemistry and biology of siderophores. *Nat Prod Rep.*

- 2010;27(5):637-657. doi:10.1039/b906679a
10. Collignon C, Uroz S, Turpault MP, Frey-Klett P. Seasons differently impact the structure of mineral weathering bacterial communities in beech and spruce stands. *Soil Biol Biochem.* 2011;43(10):2012-2022. doi:10.1016/j.soilbio.2011.05.008
 11. Granada CE, Passaglia LMP, de Souza EM, Sperotto RA. Is phosphate solubilization the forgotten child of plant growth-promoting rhizobacteria? *Front Microbiol.* 2018;9. doi:10.3389/fmicb.2018.02054
 12. Gupta R, Kumari A, Sharma S, Alzahrani OM, Noureldeen A, Darwish H. Identification, characterization and optimization of phosphate solubilizing rhizobacteria (PSRB) from rice rhizosphere. *Saudi J Biol Sci.* 2022;29(1):35-42. doi:10.1016/j.sjbs.2021.09.075
 13. Mayak S, Tirosh T, Glick BR. Plant growth-promoting bacteria that confer resistance to water stress in tomatoes and peppers. *Plant Sci.* 2004;166(2):525-530. doi:https://doi.org/10.1016/j.plantsci.2003.10.025
 14. Grichko VP, Glick BR. Amelioration of flooding stress by ACC deaminase-containing plant growth-promoting bacteria. *Plant Physiol Biochem.* 2001;39(1):11-17. doi:10.1016/S0981-9428(00)01212-2
 15. Upadhyay SK, Singh DP, Saikia R. Genetic diversity of plant growth promoting rhizobacteria isolated from rhizospheric soil of wheat under saline condition. *Curr Microbiol.* 2009;59(5):489-496. doi:10.1007/s00284-009-9464-1
 16. Ait Barka E, Nowak J, Clément C. Enhancement of chilling resistance of inoculated grapevine plantlets with a plant growth-promoting rhizobacterium, *Burkholderia phytofirmans* strain PsJN. *Appl Environ Microbiol.*

2006;72(11):7246-7252. doi:10.1128/AEM.01047-06

17. Trivedi P, Sa T. *Pseudomonas corrugata* (NRRL B-30409) mutants increased phosphate solubilization, organic acid production, and plant growth at lower temperatures. *Curr Microbiol.* 2008;56(2):140-144. doi:10.1007/s00284-007-9058-8
18. Raudales RE, Stone E, McSpadden Gardener BB. Seed treatment with 2,4-diacetylphloroglucinol-producing pseudomonads improves crop health in low-pH soils by altering patterns of nutrient uptake. *Phytopathology.* 2009;99(5):506-511. doi:10.1094/PHYTO-99-5-0506
19. Kawasaki A, Watson ER, Kertesz MA. Indirect effects of polycyclic aromatic hydrocarbon contamination on microbial communities in legume and grass rhizospheres. *Plant Soil.* 2012;358(1-2):169-182. doi:10.1007/s11104-011-1089-z
20. Kim YS, Kim MJ, Kim P, Kim JH. Cloning and production of a novel bacteriocin, lactococcin K, from *Lactococcus lactis* subsp. *lactis* MY23. *Biotechnol Lett.* 2006;28(5):357-362. doi:10.1007/s10529-005-5935-z
21. Raaijmakers JM, de Bruijn I, Nybroe O, Ongena M. Natural functions of lipopeptides from *Bacillus* and *Pseudomonas*: More than surfactants and antibiotics. *FEMS Microbiol Rev.* 2010;34(6):1037-1062. doi:10.1111/j.1574-6976.2010.00221.x
22. Effmert U, Kalderás J, Warnke R, Piechulla B. Volatile mediated interactions between bacteria and fungi in the soil. *J Chem Ecol.* 2012;38(6):665-703. doi:10.1007/s10886-012-0135-5
23. Jamalizadeh M, Etebarian HR, Aminian H, Alizadeh A. Biological control of

- Botrytis mali on apple fruit by use of Bacillus bacteria, isolated from the rhizosphere of wheat. *Arch Phytopathol Plant Prot.* 2010;43(18):1836-1845.
doi:10.1080/03235400902830960
24. Kai M, Haustein M, Molina F, Petri A, Scholz B, Piechulla B. Bacterial volatiles and their action potential. *Appl Microbiol Biotechnol.* 2009;81:1001-1012.
doi:10.1007/s00253-008-1760-3
25. Zamioudis C, Pieterse CMJ. Modulation of host immunity by beneficial microbes. *Mol Plant-Microbe Interact.* 2012;25(2):139-150. doi:10.1094/MPMI-06-11-0179
26. van de Mortel JE, de Vos RCH, Dekkers E, et al. Metabolic and transcriptomic changes induced in Arabidopsis by the rhizobacterium *Pseudomonas fluorescens* SS101. *Plant Physiol.* 2012;160(4):2173-2188. doi:10.1104/pp.112.207324
27. Hartmann A, Schikora A. Quorum sensing of bacteria and trans-kingdom interactions of N-acyl homoserine lactones with eukaryotes. *J Chem Ecol.* 2012;38(6):704-713. doi:10.1007/s10886-012-0141-7
28. Bais HP, Weir TL, Perry LG, Gilroy S, Vivanco JM. The role of root exudates in rhizosphere interactions with plants and other organisms. *Annu Rev Plant Biol.* 2006;57:233-266. doi:10.1146/annurev.arplant.57.032905.105159
29. Kuzyakov Y, Xu X. Competition between roots and microorganisms for nitrogen: Mechanisms and ecological relevance. *New Phytol.* 2013;198(3):656-669.
doi:10.1111/nph.12235
30. Garbeva P, Silby MW, Raaijmakers JM, Levy SB, Boer W De. Transcriptional and antagonistic responses of *Pseudomonas fluorescens* Pf0-1 to phylogenetically different bacterial competitors. *ISME J.* 2011;5(6):973-985.

doi:10.1038/ismej.2010.196

31. Canarini A, Kaiser C, Merchant A, Richter A, Wanek W. Root exudation of primary metabolites: Mechanisms and their roles in plant responses to environmental stimuli. *Front Plant Sci.* 2019;10:420.
doi:10.3389/fpls.2019.00157
32. Rasmann S, Ali JG, Helder J, van der Putten WH. Ecology and evolution of soil nematode chemotaxis. *J Chem Ecol.* 2012;38(6):615-628. doi:10.1007/s10886-012-0118-6
33. Van West P, Morris BM, Reid B, et al. Oomycete plant pathogens use electric fields to target roots. *Mol Plant-Microbe Interact.* 2002;15(8):790-798.
doi:10.1094/MPMI.2002.15.8.790
34. Doornbos RF, Van Loon LC, Bakker PAHM. Impact of root exudates and plant defense signaling on bacterial communities in the rhizosphere. A review. *Agron Sustain Dev.* 2012;32(1):227-243. doi:10.1007/s13593-011-0028-y
35. Hein JW, Wolfe G V., Blee KA. Comparison of rhizosphere bacterial communities in *Arabidopsis thaliana* mutants for systemic acquired resistance. *Microb Ecol.* 2008;55(2):333-343. doi:10.1007/s00248-007-9279-1
36. Sasse J, Martinoia E, Northen T. Feed your friends: Do plant exudates shape the root microbiome? *Trends Plant Sci.* 2018;23(1):25-41.
doi:10.1016/j.tplants.2017.09.003
37. Berg G, Smalla K. Plant species and soil type cooperatively shape the structure and function of microbial communities in the rhizosphere. *FEMS Microbiol Ecol.* 2009;68(1):1-13. doi:10.1111/j.1574-6941.2009.00654.x

38. Fitzpatrick CR, Copeland J, Wang PW, Guttman DS, Kotanen PM, Johnson MTJ. Assembly and ecological function of the root microbiome across angiosperm plant species. *Proc Natl Acad Sci U S A*. 2018;115(6):E1157-E1165. doi:10.1073/pnas.1717617115
39. Hale MG, Foy CL, Shay FJ. Factors affecting root exudation. *Adv Agron*. 1971;23(C):89-109. doi:10.1016/S0065-2113(08)60151-0
40. Ling N, Wang T, Kuzyakov Y. Rhizosphere bacteriome structure and functions. *Nat Commun*. 2022;13(1):836. doi:10.1038/s41467-022-28448-9
41. Li J, Mavrodi O V., Hou J, Blackmon C, Babiker EM, Mavrodi D V. Comparative analysis of rhizosphere microbiomes of southern highbush blueberry (*Vaccinium corymbosum* L.), darrow's blueberry (*V. darrowii* Camp), and rabbiteye blueberry (*V. virgatum* Aiton). *Front Microbiol*. 2020;11:370. doi:10.3389/fmicb.2020.00370
42. Pérez-Jaramillo JE, Carrión VJ, de Hollander M, Raaijmakers JM. The wild side of plant microbiomes. *Microbiome*. 2018;6(1):143. doi:10.1186/s40168-018-0519-z
43. Iannucci A, Fragasso M, Beleggia R, Nigro F, Papa R. Evolution of the crop rhizosphere: Impact of domestication on root exudates in tetraploid wheat (*Triticum turgidum* L.). *Front Plant Sci*. 2017;8:2124. doi:10.3389/fpls.2017.02124
44. Bulgarelli D, Garrido-Oter R, Münch PC, et al. Structure and function of the bacterial root microbiota in wild and domesticated barley. *Cell Host Microbe*. 2015;17(3):392-403. doi:10.1016/j.chom.2015.01.011

45. Coleman-Derr D, Desgarences D, Fonseca-Garcia C, et al. Plant compartment and biogeography affect microbiome composition in cultivated and native *Agave* species. *New Phytol.* 2016;209(2):798-811. doi:10.1111/nph.13697
46. Korenblum E, Dong Y, Szymanski J, et al. Rhizosphere microbiome mediates systemic root metabolite exudation by root-to-root signaling. *Proc Natl Acad Sci U S A.* 2020;117(7):3874-3883. doi:10.1073/pnas.1912130117
47. Luu VT, Weinhold A, Ullah C, et al. O-Acyl sugars protect a wild tobacco from both native fungal pathogens and a specialist herbivore. *Plant Physiol.* 2017;174(1):370-386. doi:10.1104/pp.16.01904
48. Lombardi N, Vitale S, Turr A D, et al. Root exudates of stressed plants stimulate and attract trichoderma soil fungi. *Mol Plant-Microbe Interact.* 2018;31(10):982-994. doi:10.1094/MPMI-12-17-0310-R
49. Wang N, Wang L, Zhu K, et al. Plant root exudates are involved in *Bacillus cereus* AR156 mediated biocontrol against *Ralstonia solanacearum*. *Front Microbiol.* 2019;10:98. doi:10.3389/fmicb.2019.00098
50. Montiel-Rozas MM, Madejón E, Madejón P. Effect of heavy metals and organic matter on root exudates (low molecular weight organic acids) of herbaceous species: An assessment in sand and soil conditions under different levels of contamination. *Environ Pollut.* 2016;216:273-281. doi:10.1016/j.envpol.2016.05.080
51. Zhao M, Zhao J, Yuan J, et al. Root exudates drive soil-microbe-nutrient feedbacks in response to plant growth. *Plant Cell Environ.* 2021;44(2):613-628. doi:10.1111/pce.13928

52. Bali AS, Sidhu GPS, Kumar V. Root exudates ameliorate cadmium tolerance in plants: A review. *Environ Chem Lett.* 2020;18(4):1243-1275.
doi:10.1007/s10311-020-01012-x
53. Meier S, Alvear M, Borie F, Aguilera P, Ginocchio R, Cornejo P. Influence of copper on root exudate patterns in some metallophytes and agricultural plants. *Ecotoxicol Environ Saf.* 2012;75(1):8-15. doi:10.1016/j.ecoenv.2011.08.029
54. Sabrina N, Rahman NA, Wahida N, Hamid A, Nadarajah K. Effects of abiotic stress on soil microbiome. *Int J Mol Sci.* 2021;22:9036.
doi:10.3390/ijms22169036
55. Yin H, Xiao J, Li Y, et al. Warming effects on root morphological and physiological traits: The potential consequences on soil C dynamics as altered root exudation. *Agric For Meteorol.* 2013;180:287-296.
doi:10.1016/j.agrformet.2013.06.016
56. Abdel-Lateif K, Bogusz D, Hocher V. The role of flavonoids in the establishment of plant roots endosymbioses with arbuscular mycorrhiza fungi, rhizobia and Frankia bacteria. *Plant Signal Behav.* 2012;7(6):636-641. doi:10.4161/psb.20039
57. Sullivan TS, Barth V, Lewis RW. Soil acidity impacts beneficial soil microorganisms. *Washingt State Univ Ext Publ.* 2016.
58. Smercina DN, Evans SE, Friesen ML, Tiemann LK. To fix or not to fix: Controls on free-living nitrogen fixation in the rhizosphere. *Appl Environ Microbiol.* 2019;85(6):e02546-18. doi:10.1128/AEM.02546-18
59. Leuschner C, Tückmantel T, Meier IC. Temperature effects on root exudation in mature beech (*Fagus sylvatica* L.) forests along an elevational gradient. *Plant*

- Soil*. 2022;481:147-163. doi:10.1007/s11104-022-05629-5
60. Dubey A, Malla MA, Khan F, et al. Soil microbiome: a key player for conservation of soil health under changing climate. *Biodivers Conserv*. 2019;28(8-9):2405-2429. doi:10.1007/s10531-019-01760-5
61. Loreti E, Perata P. The many facets of hypoxia in plants. *Plants*. 2020;9(6):745. doi:10.3390/plants9060745
62. Li Y, Niu W, Zhang M, Wang J, Zhang Z. Artificial soil aeration increases soil bacterial diversity and tomato root performance under greenhouse conditions. *L Degrad Dev*. 2020;31(12):1443-1461. doi:10.1002/ldr.3560
63. Bhatti AA, Haq S, Bhat RA. Actinomycetes benefaction role in soil and plant health. *Microb Pathog*. 2017;111:458-467. doi:10.1016/j.micpath.2017.09.036
64. Furtak K, Grządziel J, Gałazka A, Niedźwiecki J. Prevalence of unclassified bacteria in the soil bacterial community from floodplain meadows (fluvisols) under simulated flood conditions revealed by a metataxonomic approachss. *Catena*. 2020;188. doi:10.1016/j.catena.2019.104448
65. Islam W, Noman A, Naveed H, Huang Z, Chen HYH. Role of environmental factors in shaping the soil microbiome. *Environ Sci Pollut Res*. 2020;27(33):41225-41247. doi:10.1007/s11356-020-10471-2
66. Chen Y, Yao Z, Sun Y, et al. Current studies of the effects of drought stress on root exudates and rhizosphere microbiomes of crop plant species. *Int J Mol Sci*. 2022;23(4):2374. doi:10.3390/ijms23042374
67. Karlowsky S, Augusti A, Ingrisch J, Akanda MKU, Bahn M, Gleixner G. Drought-induced accumulation of root exudates supports post-drought recovery of

- microbes in mountain grassland. *Front Plant Sci.* 2018;9:1593.
doi:10.3389/fpls.2018.01593
68. Imhoff JF, Rahn T, Künzel S, Keller A, Neulinger SC. Osmotic adaptation and compatible solute biosynthesis of phototrophic bacteria as revealed from genome analyses. *Microorganisms.* 2021;9(1):46. doi:10.3390/microorganisms9010046
69. Kakumanu ML, Ma L, Williams MA. Drought-induced soil microbial amino acid and polysaccharide change and their implications for C-N cycles in a climate change world. *Sci Rep.* 2019;9(1):10968. doi:10.1038/s41598-019-46984-1
70. Beskrovnaya P, Sexton DL, Golmohammadzadeh M, Hashimi A, Tocheva EI. Structural, metabolic and evolutionary comparison of bacterial endospore and exospore formation. *Front Microbiol.* 2021;12:630573.
doi:10.3389/fmicb.2021.630573
71. Bukar M, Sodipo O, Dawkins K, et al. Microbiomes of top and sub-layers of semi-arid soils in north-eastern Nigeria are rich in Firmicutes and Proteobacteria with surprisingly high diversity of rare species. *Adv Microbiol.* 2019;09(01):102-118. doi:10.4236/aim.2019.91008
72. Manzoni S, Katul G. Invariant soil water potential at zero microbial respiration explained by hydrological discontinuity in dry soils. *Geophys Res Lett.* 2014;41(20). doi:10.1002/2014GL061467
73. Williams A, de Vries FT. Plant root exudation under drought: implications for ecosystem functioning. *New Phytol.* 2020;225(5):1899-1905.
doi:10.1111/nph.16223
74. Gagné-Bourque F, Bertrand A, Claessens A, Aliferis KA, Jabaji S. Alleviation of

- drought stress and metabolic changes in timothy (*Phleum pratense* L.) colonized with *Bacillus subtilis* B26. *Front Plant Sci.* 2016;7:584.
doi:10.3389/fpls.2016.00584
75. Henry A, Doucette W, Norton J, Bugbee B. Changes in crested wheatgrass root exudation caused by flood, drought, and nutrient stress. *J Environ Qual.* 2007;36(3):904-912. doi:10.2134/jeq2006.0425sc
76. Mee MT, Collins JJ, Church GM, Wang HH. Syntrophic exchange in synthetic microbial communities. *Proc Natl Acad Sci U S A.* 2014;111(20):E2149-E2156. doi:10.1073/pnas.1405641111
77. Morris BEL, Henneberger R, Huber H, Moissl-Eichinger C. Microbial syntrophy: Interaction for the common good. *FEMS Microbiol Rev.* 2013;37(3):384-406. doi:10.1111/1574-6976.12019
78. Peterson SB, Dunn AK, Klimowicz AK, Handelsman J. Peptidoglycan from *Bacillus cereus* mediates commensalism with rhizosphere bacteria from the Cytophaga-Flavobacterium group. *Appl Environ Microbiol.* 2006;72(8):5421-5427. doi:10.1128/AEM.02928-05
79. Besset-Manzoni Y, Rieusset L, Joly P, Comte G, Prigent-Combaret C. Exploiting rhizosphere microbial cooperation for developing sustainable agriculture strategies. *Environ Sci Pollut Res.* 2018;25(30):29953-29970. doi:10.1007/s11356-017-1152-2
80. Gu S, Wei Z, Shao Z, et al. Competition for iron drives phytopathogen control by natural rhizosphere microbiomes. *Nat Microbiol.* 2020;5(8):1002-1010. doi:10.1038/s41564-020-0719-8

81. Jousset A, Rochat L, Scheu S, Bonkowski M, Keel C. Predator-prey chemical warfare determines the expression of biocontrol genes by rhizosphere-associated *Pseudomonas fluorescens*. *Appl Environ Microbiol*. 2010;76(15):5263-5268. doi:10.1128/AEM.02941-09
82. Nandi M, Selin C, Brassinga AKC, et al. Pyrrolnitrin and hydrogen cyanide production by *Pseudomonas chlororaphis* strain PA23 exhibits nematicidal and repellent activity against *Caenorhabditis elegans*. *PLoS One*. 2015;10(4): e0123184. doi:10.1371/journal.pone.0123184
83. Raaijmakers JM, Mazzola M. Diversity and natural functions of antibiotics produced by beneficial and plant pathogenic bacteria. *Annu Rev Phytopathol*. 2012;50:403-424. doi:10.1146/annurev-phyto-081211-172908
84. Song C, Mazzola M, Cheng X, et al. Molecular and chemical dialogues in bacteria-protozoa interactions. *Sci Rep*. 2015;5:12837. doi:10.1038/srep12837
85. Vacheron J, Heiman CM, Keel C. Live cell dynamics of production, explosive release and killing activity of phage tail-like weapons for *Pseudomonas* kin exclusion. *Commun Biol*. 2021;4(1):87. doi:10.1038/s42003-020-01581-1
86. Mavrodi D V., Blankenfeldt W, Thomashow LS. Phenazine compounds in fluorescent *Pseudomonas* spp. biosynthesis and regulation . *Annu Rev Phytopathol*. 2006;44(1):417-445. doi:10.1146/annurev.phyto.44.013106.145710
87. Chin-A-Woeng TFC, Bloemberg G V, Lugtenberg BJJ. Phenazines and their role in biocontrol by *Pseudomonas* bacteria. *New Phytol*. 2003;157(3):503-523. doi:https://doi.org/10.1046/j.1469-8137.2003.00686.x
88. De Vleeschauwer D, Cornelis P, Höfte M. Redox-active pyocyanin secreted by

- Pseudomonas aeruginosa* 7NSK2 triggers systemic resistance to *Magnaporthe grisea* but enhances *Rhizoctonia solani* susceptibility in rice. *Mol Plant-Microbe Interact.* 2006;19(12):1406-1419. doi:10.1094/MPMI-19-1406
89. Thomashow LS, Weller DM. Role of a phenazine antibiotic from *Pseudomonas fluorescens* in biological control of *Gaeumannomyces graminis* var. *tritici*. *J Bacteriol.* 1988;170(8):3499-3508. doi:10.1128/jb.170.8.3499-3508.1988
90. Dar D, Thomashow LS, Weller DM, Newman DK. Global landscape of phenazine biosynthesis and biodegradation reveals species-specific colonization patterns in agricultural soils and crop microbiomes. *Elife.* 2020;9:e59726. doi:10.7554/ELIFE.59726
91. Mcrose DL, Newman DK. Redox-active antibiotics enhance phosphorus bioavailability. *Science.* 2021;371(6533):1033-1037. doi:10.1126/science.abd1515
92. Glasser NR, Kern SE, Newman DK. Phenazine redox cycling enhances anaerobic survival in *Pseudomonas aeruginosa* by facilitating generation of ATP and a proton-motive force. *Mol Microbiol.* 2014;92(2):399-412. doi:10.1111/mmi.12566
93. Dietrich LEP, Price-Whelan A, Petersen A, Whiteley M, Newman DK. The phenazine pyocyanin is a terminal signalling factor in the quorum sensing network of *Pseudomonas aeruginosa*. *Mol Microbiol.* 2006;61(5):1308-1321. doi:10.1111/j.1365-2958.2006.05306.x
94. Meirelles LA, Newman DK. Both toxic and beneficial effects of pyocyanin contribute to the lifecycle of *Pseudomonas aeruginosa*. *Mol Microbiol.*

- 2018;110(6):995-1010. doi:10.1111/mmi.14132
95. Eberl L. N-acyl homoserinelactone-mediated gene regulation in Gram-negative bacteria. *Syst Appl Microbiol*. 1999;22(4):493-506. doi:10.1016/S0723-2020(99)80001-0
96. Mukherjee S, Bassler BL. Bacterial quorum sensing in complex and dynamically changing environments. *Nat Rev Microbiol*. 2019;17(6):371-382. doi:10.1038/s41579-019-0186-5
97. Moore, ERB., Tindall, BJ, Martins Dos Santos, VAP., Pieper, DH, Ramos, JL., Palleroni, NJ. Nonmedical: Pseudomonas. In: Dworkin, M., Falkow, S., Rosenberg, E., Schleifer, KH., Stackebrandt, E. (eds) *The Prokaryotes*.646-703.doi:10.1007/0-387-30746-X_21
98. Yahr TL, Parsek MR. Pseudomonas aeruginosa. In: Dworkin M, Falkow S, Rosenberg E, Schleifer K-H, Stackebrandt E, eds. *The Prokaryotes: A Handbook on the Biology of Bacteria Volume 6: Proteobacteria: Gamma Subclass*. 2006:704-713. doi:10.1007/0-387-30746-X_22
99. Hesse C, Schulz F, Bull CT, et al. Genome-based evolutionary history of Pseudomonas spp. *Environ Microbiol*. 2018;20(6):2142-2159. doi:10.1111/1462-2920.14130
100. Zboralski A, Filion M. Genetic factors involved in rhizosphere colonization by phytobeneficial Pseudomonas spp. *Comput Struct Biotechnol J*. 2020;18:3539-3554. doi:10.1016/j.csbj.2020.11.025
101. Mavrodi DV., Mavrodi OV., Parejko JA, et al. Accumulation of the antibiotic phenazine-1-carboxylic acid in the rhizosphere of dryland cereals. *Appl Environ*

- Microbiol.* 2012;78(3):804-812. doi:10.1128/AEM.06784-11
102. USDA. Small grains 2021 summary. 2021:1-28.
https://www.nass.usda.gov/Publications/Todays_Reports/reports/smgr0921.pdf.
 103. Eberl L, Vandamme P. Members of the genus Burkholderia: good and bad guys. *F1000Research*. 2016;5. doi:10.12688/f1000research.8221.1
 104. Estrada-de los Santos P, Rojas-Rojas FU, Tapia-García EY, Vásquez-Murrieta MS, Hirsch AM. To split or not to split: an opinion on dividing the genus Burkholderia. *Ann Microbiol.* 2016;66(3):1303-1314. doi:10.1007/s13213-015-1183-1
 105. Sawana A, Adeolu M, Gupta RS. Molecular signatures and phylogenomic analysis of the genus burkholderia: proposal for division of this genus into the emended genus burkholderia containing pathogenic organisms and a new genus paraburkholderia gen. nov. harboring environmental species. *Front Genet.* 2014;5:429. doi:10.3389/fgene.2014.00429
 106. Sousa SA, Ramos CG, Leitão JH. Burkholderia cepacia complex: Emerging multihost pathogens equipped with a wide range of virulence factors and determinants. *Int J Microbiol.* 2011:607575. doi:10.1155/2011/607575
 107. Stopnisek N, Zuhlke D, Carlier A, et al. Molecular mechanisms underlying the close association between soil Burkholderia and fungi. *ISME J.* 2016;10(1):253-264. doi:10.1038/ismej.2015.73
 108. Yabuuchi E, Kosako Y, Oyaizu H, et al. Proposal of Burkholderia gen. nov. and transfer of seven species of the genus Pseudomonas homology group II to the new genus, with the type species Burkholderia cepacia (Palleroni and Holmes

1981) comb. nov. *Microbiol Immunol.* 1992;36(12):1251-1275.

doi:10.1111/j.1348-0421.1992.tb02129.x

109. Hendry S, Steinke S, Wittstein K, et al. Functional Analysis of Phenazine Biosynthesis Genes in Burkholderia spp. *Appl Environ Microbiol.* 2021;87(11): e02348-20. doi:10.1128/AEM.02348-20

CHAPTER II- TRANSCRIPTOMIC RESPONSES OF THE MODEL RHIZOSPHERE
BACTERIUM *PSEUDOMONAS SYNXANTHA* 2-79 TO BARLEY ROOT
EXUDATES

2.1 Abstract

Plants are metaorganisms that harbor numerous parasitic, commensal, and symbiotic microbes that form complex ecological communities comprising the “phytobiome” (a term describing the plant, the environment in which it resides, and the associated microorganisms). Most of the plant-associated microorganisms are concentrated in the rhizosphere, an interface between plant roots and soil influenced by root exudates. The rhizosphere microorganisms positively influence plant nutritional status, growth, and the ability to resist pathogens and abiotic stress. The comparative studies revealed distinct variations in bacterial diversity that correlate with the plant’s genotype, age, and response to biotic and abiotic stressors. It is thought that these changes in the rhizosphere microbiome are driven by organic rhizodeposits secreted into the soil by plant roots. However, the molecular details of these processes are still very much a black box.

We addressed this gap by focusing on responses of the model biocontrol rhizobacterium *Pseudomonas synxantha* 2-79 to the root exudates of barley (*Hordeum vulgare* L.). We generated root exudates from healthy barley plants and plants infected by the soilborne fungal pathogen *Rhizoctonia solani* AG-8 and profiled these exudates by targeted metabolomic analysis. We then added these exudates to 2-79 cultures and characterized microbial transcriptome responses to plant exometabolites by RNA-seq. Our results revealed that root exudates perturb hundreds of bacterial genes that function

in the uptake and catabolism of C and N sources, synthesis of antimicrobial secondary metabolites, and biofilm formation. These results reveal how rhizodeposition shapes the plant microbiome by recruiting organisms involved in growth promotion and disease control and how these microbial taxa adapt themselves in the competitive rhizosphere environment.

2.2 Introduction

All multicellular eukaryotes are considered holobionts, or organisms harboring diverse microbial communities that have a major role in key aspects of their host's biology.¹ These host-microbe interactions are not random and result from long-term coevolution often leading to associations in which the host and its microbiota collaborate in a mutually beneficial way.² One of the best-studied examples of such intimate and complex host-microbe interactions is represented by the plant microbiome. Plants harbor numerous parasitic, commensal, and symbiotic microbes that form complex ecological communities comprising the "phytobiome" (a term describing the plant, the environment in which it resides, and the associated microorganisms). The association between plants and microorganisms is ancient and thought to have originated over 400 million years ago.³ These interactions ultimately led to the emergence of diverse bacterial and fungal communities that reside within plant tissues (endosphere), on aerial plant surfaces (phyllosphere) and especially around plant roots (rhizosphere). The root-associated microorganisms are particularly abundant and collectively encompass the bulk of the plant microbiome. They positively influence plant nutritional status, growth, and the ability to resist pathogens and abiotic stress.⁴ Many of these beneficial effects are

systemic and involve signaling between the point of origin and other below- or aboveground parts of a plant.

In contrast to the carbon-limited bulk soil, the rhizosphere is a nitrogen-limited environment. By releasing rhizodeposits, plant roots recruit microorganisms that accelerate the decomposition of soil organic matter and improve the availability of nitrogen for plant uptake (the rhizosphere priming effect).⁵ The rhizosphere microbial communities are also enriched in N-cycling genes,⁶ and the role of bacterial diazotrophs and mycorrhizae in facilitating plant growth through the acquisition of nitrogen have been studied for decades. Another significant supply of nutrients is provided by arbuscular mycorrhizal (AM) fungi that form symbioses with an estimated 70–90% of plant species.⁷ The AM fungi are obligate biotrophs in the Glomeromycota that form extensive hyphal networks capable of mining ammonium, nitrate ions and phosphate from the soil and delivering these nutrients to the plant via intraradical mycelium.⁸ Many rhizosphere microorganisms actively modulate host phytohormone levels, which stimulates germination of seed and tubers, promotes stem and root growth, and alleviates the negative effects of abiotic stresses. Treatment of plants with strains producing auxins, cytokinins and/or gibberellins commonly results in better formation of root hairs, increased root growth and branching, and, as a result, in improved mineral and nutrient uptake.⁹

In addition to abiotic stressors, plants are attacked by various pests and pathogens including bacteria, fungi, oomycetes, and nematodes. Genetic resistance to most soilborne diseases is rare, and plants instead rely on their rhizosphere microbiome for protection from biotic stress. The defense mechanisms associated with rhizobacteria are

diverse and include the displacement of pathogens via competition for nutrients.¹⁰ Many rhizosphere microorganisms act as biological control agents by producing numerous polyketides, nonribosomal peptides, lytic enzymes and other classes of broad-spectrum antibacterial and antifungal compounds that directly inhibit the activity of plant pathogens.¹¹⁻¹⁵ Rhizosphere microorganisms also promote pathogen resistance through stimulation of induced systemic resistance (ISR), which enhances the plant defense responses against a broad range of pathogens.¹⁶

The term “rhizosphere” was first coined over a century ago by Lorenz Hiltner to describe the dynamic interface between plant roots and soil influenced by root exudates.¹⁷ This environment is characterized by temporal and spatial (sub-micrometer to supra-centimeter) gradients of pH, oxygen, redox potential, enzymes, water, nutrients, and plant exometabolites.¹⁸ The rhizosphere is characterized by a high level of microbial activity and can contain up to 10^{11} microbial cells per gram of plant root with over 30,000 estimated prokaryotic species.¹⁹ The comparison of rhizosphere communities across 30 angiosperm plant species that diverged 140 million years ago revealed a core microbiome dominated by Proteobacteria, Acidobacteria, Actinobacteria, Bacteroidetes, Verrucomicrobia and Firmicutes.²⁰ However, this and numerous other comparative studies reported distinct variations in bacterial diversity that correlate with the plant’s genotype, age, and response to biotic and abiotic stressors. It is thought that these changes in the rhizosphere microbiome are driven by organic rhizodeposits secreted into the soil by plant roots. These rhizodeposits are composed of border cells and numerous high-molecular-weight (polysaccharides, mucilage, proteins) and low-molecular-weight (carbohydrates, amino acids, organic acids, phenolics) compounds.²¹ These

exometabolites represent a significant source of carbon and nitrogen and are thought to attract microorganisms from the surrounding bulk soil, thereby shaping the rhizosphere communities. However, the molecular details of these processes are still very much a black box.

We addressed this important gap by focusing on responses of the model biocontrol rhizobacterium *Pseudomonas synxantha* 2-79 to root exudates of barley seedlings. We hypothesized that low-molecular-weight compounds exuded by barley roots modulate the expression of genes in 2-79 that are related to energy metabolism, production of secondary metabolites and colonization of plant surfaces. We tested this hypothesis by generating root exudates from healthy barley plants and plants infected by the soilborne fungal pathogen *R. solani* AG-8 and profiling these exudates by targeted metabolomic analysis. We then added these exudates to bacterial cultures and characterized transcriptome responses of 2-79 to plant exometabolites by RNA-seq. The results of these experiments provide a better understanding of how rhizodeposition shapes the plant microbiome and recruits microorganisms involved in growth promotion and disease control and how these microbial taxa adapt themselves in the competitive rhizosphere environment.

2.3 Materials and Methods

2.3.1 Microorganisms and culture conditions

Pseudomonas synxantha 2-79 was routinely cultured at 27°C in Luria-Bertani (LB) medium²² or King's B medium²³ and maintained as frozen glycerol stocks at -80°C. The RNA-seq experiments were performed in the MOPS minimal medium amended with 20 mM glucose.²⁴ The *R. solani* AG-8 isolate C1 was maintained at room temperature on

Potato Dextrose Agar (Difco) and stored on the same medium at 4°C. To inoculate barley seedlings, the pathogen was subcultured for one week on water agar.

2.3.2 Collection of barley root exudates

For the collection of root exudates, batches of 60 barley seeds (cv. Golden Promise) were soaked in water for 20 h and then surface-sterilized by immersing for 15 min in 25 mL of 1% AgNO₃ solution.²⁵ The sterilized seeds were rinsed five times each with sterile saline and deionized water and aseptically transferred to water agar plates for germination at 20°C in the dark. After 36-48 h, the germinated seeds were transferred into 10×10-cm square Petri dishes (having pre-made holes for the seedlings to grow) with Hoagland agar (2 seeds/plate).²⁶ Half of the plants were infected with *Rhizoctonia solani* AG-8 by placing agar plugs with actively growing fungal mycelium. The uninfected plants served as the healthy control group. The infection progress was followed by staining the plant roots as described by Perl-Treves et al.²⁷ Briefly, barley roots were carefully excised and treated for 1-2 min in 0.25% safranin red to stain the root meristem and vascular bundles. The samples were then placed for 1-2 min in aniline blue (0.5% aniline blue, 25% lactic acid, 50% glycerol), which preferentially stains fungal hyphae. The stained roots were de-stained briefly in a solution of 25% lactic acid/50% glycerol and examined under the microscope. All plates were sealed with Parafilm, covered with foil, and incubated vertically in a growth chamber at 16°C and a 12-h day/night cycle. After one week, the plants were transferred to sterile beakers (15 plants per beaker) containing 21 mL deionized water and gently rocked at 60 rpm to collect root exudates. After 3 h, the root exudates were collected, filter-sterilized and dispensed into conical

centrifuge tubes (10 mL each) for lyophilization at -50°C. The lyophilized samples were stored at -80°C for further use.

2.3.3 Metabolome profiling of root exudates

The lyophilized root exudates of the healthy and infected barley seedlings were sent for metabolome profiling to the Analytical Resources Core - Bioanalysis and Omics (ARC-BIO) at Colorado State University. Targeted quantitative analysis was performed for the following exometabolites: amino acids (asparagine, glutamine, glutamate, aspartate, phenylalanine, tryptophan, etc.), carbohydrates (arabinose, xylose, galactose, glucose, etc.), quaternary ammonium compounds (choline, carnitine, sarcosine, glycine betaine). We also aimed to detect and quantify several secondary metabolites such as 2,4-dihydroxy-7-methoxy-1,4-benzoxazin-3-one (DIMBOA), scopoletin, coumaric acid, ferulic acid, and cinnamic acid, that are known to modulate disease responses by priming resistance, inhibiting soilborne pathogens and/or attracting biocontrol organisms.²⁸⁻³²

The root exudates were extracted with aqueous methanol and analyzed using gas or liquid chromatography coupled mass spectrometry. Briefly, all samples were dissolved in ice-cold 80% methanol and spiked with appropriate internal standards. The mixtures were vortexed and incubated for 3 h at -20°C, followed by centrifugation at 17,000 × g for 15 min at 4°C. The supernatants were dried under nitrogen and a part of them were subjected to a two-step derivatization for GC-MS analysis. Metabolites were detected using a Trace 1310 GC coupled to a Thermo ISQ mass spectrometer (Thermo Fisher Scientific, Waltham, MA, USA). Samples (1 µL) were injected into a 30-m DB-5MS column (0.25 mm i.d., 0.25 µm film thickness) (Agilent) with a 1.2 mL min⁻¹ helium gas flow rate. GC inlet was held at 285°C. The oven program started at 80°C for 30 s,

followed by a ramp of $15^{\circ}\text{C min}^{-1}$ to 330°C , and an 8 min hold. The split ratio was set at 10, while the transfer line and ion source were held at 300 and 260°C , respectively. Masses between 50 - 650 m/z were scanned at 5 scans s^{-1} under electron impact ionization. The injector split ratio and oven temperature gradient varied with the assays.

The LC-MS/MS analysis were performed on an Acquity Classic UPLC coupled to a Xevo TQ-S triple quadrupole mass spectrometer (both from Waters, Milford, MA, USA). Chromatographic separations were carried out on an Acquity UPLC BEH Amide column (2.1×100 mm, $1.7 \mu\text{M}$) (Waters), operated at 40°C . Mobile phases consisted of (A) water with 10 mM ammonium formate and 0.1% formic acid, and (B) acetonitrile with 0.1% formic acid. The LC gradient was as follows, applied at a flowrate of 0.4 mL min^{-1} : time = 0 min, 99% B; time = 0.5 min, 99% B; time = 7 min, 5% B; time = 11 min, 5% B; time = 11.1 min, 90% B; time = 15 min, 90% B. Samples were maintained at 6°C in the autosampler, and the injection volume was set at $2 \mu\text{L}$. Mass detector was operated in ESI+ mode with the capillary voltage set to 0.7 kV and inter-channel delay set to 3 msec. Source temperature was 150°C and desolvation gas (nitrogen) temperature was 450°C . Desolvation gas flow and cone gas flow were 1000 L h^{-1} and 150 L h^{-1} respectively, and collision gas (argon) flow was 0.15 mL min^{-1} . The nebulizer pressure (nitrogen) was set to 7 Bar, and the MS acquisition functions were scheduled by retention time. Autodwell feature was set for each function and dwell time was calculated in the Masslynx software (Waters) to achieve >12 points-across-peak as the minimum data points per peak. Because of the expected wide concentration ranges of analytes, the collision energies were “de-optimized”, so that data could be collected in one injection.

GC-MS data was processed using Chromeleon 7.2.10 software (Thermo Fisher Scientific), while the LC-MS/MS data files were imported into Skyline package.³³ Each target analyte was visually inspected for retention time and peak area integration. Peak areas were extracted for target compounds detected in biological samples and normalized to the peak area of the appropriate internal standard or surrogate in each sample. Absolute quantitation was calculated using linear regression equations generated from calibration curves for each compound.

2.3.4 Effect of phosphate and root exudates on 2-79 growth and *phzA* gene expression

In 2-79, the production of phenazine-1-carboxylic acid (PCA) is regulated in response to environmental conditions and cell density. At lower population levels, the phenazine (*phz*) biosynthesis genes are activated by the phosphate deficit,³⁴ while at higher cell densities, the *phz* genes are strongly induced by AHL-mediated quorum sensing.³⁵ Hence, we performed a preliminary experiment to ensure that the RNA-seq culture conditions were conducive to the production of PCA by 2-79. We decided to use the MOPS minimal medium,²⁴ in which the phosphate levels can be varied without compromising the pH control. To determine the appropriate growth conditions for activation of the phenazine biosynthesis genes, we constructed a bioreporter, *P. synxantha* 2-79 Rif (pPROBE-TT-*phzA*), in which the *phzA* promoter is fused to *gfp* gene. The bioreporter strain was grown in the MOPS medium amended with two levels of phosphate (0.3 mM and 1 mM) with or without barley root exudates. The reporter plasmid was maintained by supplementing the cultures with 15 µg/mL tetracycline. The 20-fold concentrated root exudates were supplied by dissolving the lyophilized exudate

material directly in the growth medium. The bacteria were washed and inoculated in the MOPS medium at 5×10^7 CFU mL⁻¹ and the cultures were dispensed in black 96-well plates with clear bottom (Costar). Bacterial cultures without root exudates served as controls. The growth and phenazine gene expression were followed by taking hourly measurements of absorbance at 630 nm and fluorescence (excitation at 485 nm and emission at 528 nm) for a total of 48 hours. The absorbance values were converted to CFU mL⁻¹, and *gfp* fluorescence values were normalized per A₆₃₀. Readings taken with *P. synxantha* 2-79 without the *phzA::gfp* reporter were used to subtract the background fluorescence.

2.3.5 Transcriptome responses of 2-79 to barley root exudates

To characterize the transcriptome responses to barley exudates, 2-79 were grown overnight in MOPS - 2 mM phosphate, after which the cultures were washed and suspended in MOPS medium with 1 mM phosphate. The 20-fold concentrated solutions of root exudates were prepared by reconstituting the lyophilized material from healthy and infected plants in an appropriate volume of MOPS medium. These concentrated root exudates were filter-sterilized and mixed at 1:1 ratio with 2-79 cell suspension to achieve the density of 5×10^7 CFU mL⁻¹. Bacteria inoculated in the MOPS medium served as the control. The cultures were dispensed in CytoOne 96-well microtiter plates (USA Scientific) and incubated statically at 27°C till late-exponential phase (OD₆₃₀ of 0.7-0.8), after which the bacteria were harvested, stabilized in RNAProtect (QIAGEN, Germantown, MD, USA) and RNA was extracted with a RNeasy Protect Bacteria Mini Kit (QIAGEN). The extracted RNA was treated with TURBO DNase (Thermo Fisher Scientific). The RNA integrity was verified using a 2100 Bioanalyzer and an RNA 6000

Nano Kit (Agilent Technologies, Santa Clara, CA, USA) and all samples were shipped to Novogene (Sacramento, CA, USA). Four biological replicates of RNA per conditions were ribodepleted with a Ribo-Zero Plus rRNA Depletion Kit (Illumina, San Diego, CA, USA), stranded RNASeq libraries were prepared and sequenced in PE150 mode on a NovaSeq 6000 instrument (Illumina).

2.3.6 Bioinformatic analysis of expression data

The sequence reads were imported in KBase,³⁶ quality filtered with FastQC v.0.11.9 (<https://www.bioinformatics.babraham.ac.uk>) and aligned with HISAT2 v.2.1.0³⁷ to the complete 2-79 genome (GenBank accession number CP027755). Full-length transcripts were assembled with StringTie v2.1.5,³⁸ and differential expression analysis were carried out with DeSeq2 v.1.20.0.³⁹ Genes differentially expressed (i.e., absolute fold change >1.5 (log₂ scale), FDR < 0.05) between the control and experimental treatments were used for downstream analysis. The functional categorization of differentially expressed genes and gene enrichment analyses were performed using Blast2GO annotations⁴⁰ in OmicsBox (BioBam Bioinformatics, Cambridge, MA, USA).

2.4 Results and Discussion

2.4.1 An axenic culture system for infecting barley roots with *R. solani*

Surface-sterilized and germinated seeds of barley (cv. Golden Promise) were placed aseptically on Hoagland agar plates. Half of the plates were inoculated with *R. solani* AG-8 by placing an agar plug with fungal mycelium directly below the emerging plant roots. Within 2-3 days after inoculation, the fungal hyphae visibly spread from the inoculation plug, and after one week, the entire agar surface was covered by actively

growing fungal mycelium. The best infection rate was achieved with *R. solani* AG-8 pre-grown on water agar. Compared to the healthy control plants, the infected seedling grew slower and had shorter roots, some of which had darker lesions (Figure 2.1). The staining and microscopic analysis of the barley roots revealed a successful infection with the roots of infected plants covered with a dense network of *Rhizoctonia* hyphae (Figure 2.1). These results bear similarity to the *Rhizoctonia* root rot symptoms usually seen in barley fields, which eventually lead to the death of the crop, and lead to bare patches in the crop fields.⁴¹ The infection also results in water and nutrient stress to the plant, as the roots become compromised to translocate both moisture and nutrients.⁴²

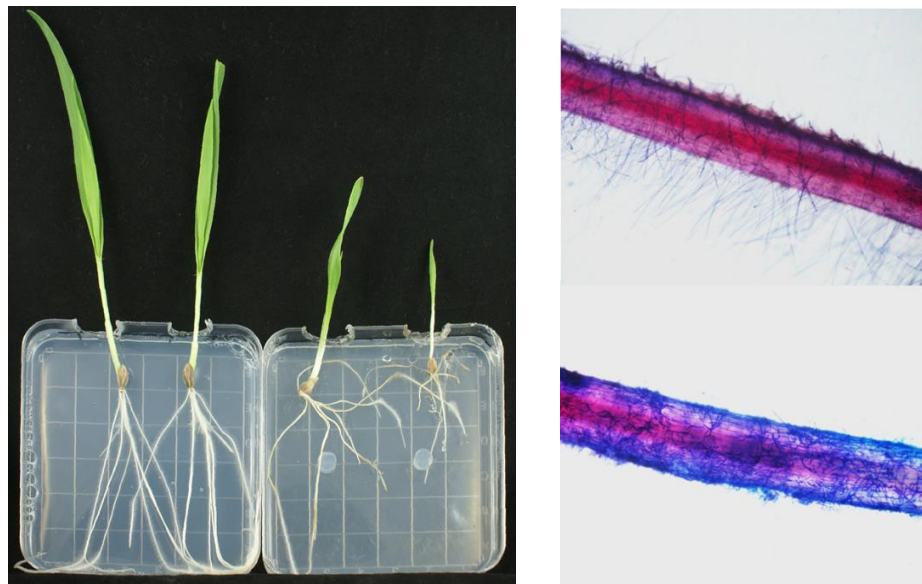


Figure 2.1 Axenic culture system used for collecting roots exudates from *Rhizoctonia*-infected barley. The left panel shows seedlings incubated on water agar with and without *R. solani* AG-8. The right panel shows a stained control root (top) and an infected root (bottom) covered with a network of *Rhizoctonia* hyphae.

2.4.2 Metabolome profiling of root exudates

We evaluated the effect of fungal infection on the rhizodeposition of barley by generating root exudates from the healthy control and *Rhizoctonia*-infected barley cv.

Golden Promise and performing their comparative metabolomic analysis. Our results demonstrated the presence of a diverse array of primary and secondary metabolites in both types of exudates (Figure 2.2). These exudates contained all amino acids with particularly high levels of asparagine and glutamine. Also were present different carbohydrates and organic acids, with noticeable amounts of fructose and malic acid, respectively. The exudates also contained several organic acids (especially malic, citric, and γ -aminobutyric acid, or GABA) and considerable amounts of quaternary ammonium compounds (QACs), especially choline and glycine betaine. The presence of the targeted secondary metabolites cinnamic acid, m-coumaric acid and ferulic acid was detected in both exudates. In contrast, 2,4-dihydroxy-7-methoxy-1,4-benzoxazin-3-one (DIMBOA) was not detected.

The fungal infection resulted in significantly lower amounts of some amino acids, such as valine, asparagine, and glutamine, whereas considerably higher amounts of phenylalanine, lysine, and arginine. Significantly lower levels of organic acids such as γ -aminobutyric acid (GABA) and succinic acid were also seen in the infected barley root exudates. The level of fructose was significantly decreased in infected root exudates, while the concentration of carnitine, although very low, was higher in the infected root exudates compared to the healthy control. Carnitine is synthesized endogenously in plants from the amino acids lysine and methionine,⁴³ and is involved in energy metabolism, hormonal actions and adaptation to stressful conditions. In barley seedlings, carnitine is known to alleviate the detrimental effects of salt and oxidative stress.⁴⁴ In the case of rhizobacteria, carnitine, along with other QACs, is known to be utilized as an osmolyte under water stress.⁴⁵ The decreased levels of exudation in fructose and some nitrogen-

rich amino acids can be attributed to the fact that plants tend to conserve these essential nutrients to decrease their pathogen susceptibility, and in turn, the rhizosphere soil may not be conducive for the pathogen to survive and infect the plant.⁴⁶

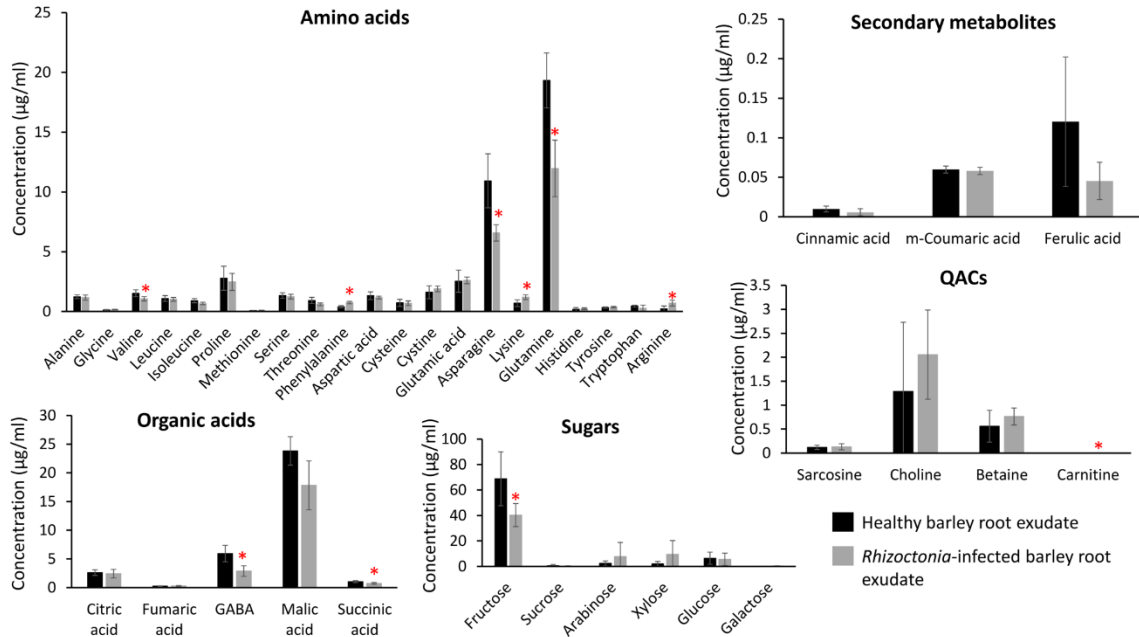


Figure 2.2 Concentrations (mean \pm SD) of primary and secondary metabolites and quaternary ammonium compounds (QACs) in exudates of healthy and *Rhizoctonia*-infected barley cv. *Golden Promise*.

Asterisks represent significant differences in metabolite concentrations as assessed by Student's T-test ($P < 0.05$).

We expected to see a significantly higher production of malic acid in the infected root exudates, as has been seen in *Arabidopsis thaliana* infected with the foliar pathogen *Pseudomonas syringae* DC3000, which selectively recruits beneficial *Bacillus* species in its rhizosphere.⁴⁷ However, such a trend was not observed in this study. We also found no significant difference in the concentrations of secondary metabolites, such as cinnamic acid and ferulic acid, in the infected barley root exudates. These phenylpropanoids function as plant defense compounds and contribute to the protection of barley from *Fusarium* infections.⁴⁸ This suggests that the root exudation profiles in barley might differ depending on the specific pathogen infection and its severity.

2.4.3 The effect of phosphate and root exudates on *phzA* gene expression

Since our research aimed at studying the transcriptomic responses of 2-79 to *Rhizoctonia*-infected barley root exudates, mainly pertaining to its biocontrol activities, we designed a preliminary experiment to determine the most favorable conditions of the expression of its phenazine biosynthesis genes. Our results revealed that 2-79 grew better in 1 mM compared to 0.3 mM phosphate and that the best growth was observed in cultures amended with root exudates (Figure 2.3).

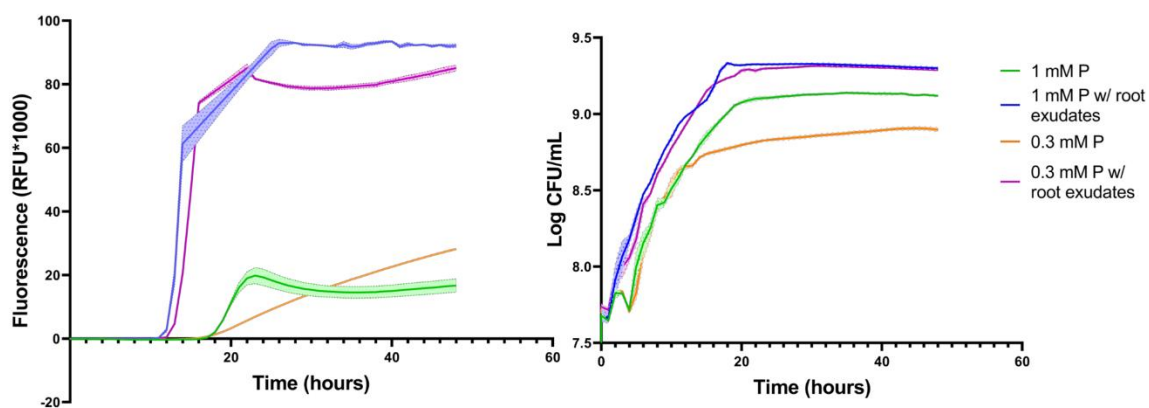


Figure 2.3 The bacterial growth and expression of the *phzA::gfp* reporter in 2-79 cultures at two levels of phosphate (1 mM or 0.3 mM) with and without root exudates.

The growth kinetics and *phzA* gene expression were determined by measuring absorbance (A630) and fluorescence (Ex 485/Em 528) with a Synergy HTX microplate reader (Biotek). Shading denotes standard deviations.

In contrast, the presence of *Rhizoctonia*-infected barley root exudates significantly increased the expression of phenazine biosynthesis, with the peak reporter fluorescence being higher under 1 mM phosphate. Based on these results, we decided to perform the RNA-seq experiment in the MOPS medium amended with 1 mM phosphate. These results align with previous studies showing that phenazine production pathways are regulated by signaling pathways that respond to phosphorus limitation. Redox-active phenazines help pseudomonads to scavenge phosphorus and help to sustain these organisms in phosphorus-limited environments.³⁴

2.4.4 Transcriptome responses of 2-79 to barley root exudates

Based on the results of the growth study, the 2-79 cultures were grown overnight in MOPS-2 mM phosphate medium, washed, and inoculated in the 1X MOPS-1 mM phosphate medium to achieve a cell density of 5×10^7 CFU mL⁻¹ (control treatment). The experimental treatments were amended with 20-fold concentrated root exudates of healthy and *Rhizoctonia*-infected barley plants. These cultures were grown statically at 27°C in 96-well plates and harvested at an OD₆₃₀ of 0.7-0.8 for RNA extraction. The transcriptome sequencing at Novogene generated a total of 236.2 million high-quality Illumina reads (~19.7 million reads per sample) that were aligned onto the 2-79 genome, assembled, and subjected to differential expression analysis with an FDR cutoff of 0.05 and an absolute log₂ fold change threshold of 1.5. The analysis revealed a total of 471 genes that were differentially expressed in response to root exudates (Figure 2.4). Among these, 179 and 66 genes, respectively, responded to the exudates of healthy or infected plants, while the expression of 229 genes was affected by both conditions.

Overall, we observed an induction of genes involved in the transport and catabolism of diverse carbohydrates, sugar alcohols, organic acids, and aromatic compounds. Pathways differentially expressed in response to exudates of both healthy and infected plants included a fructose-specific phosphotransferase system and genes for

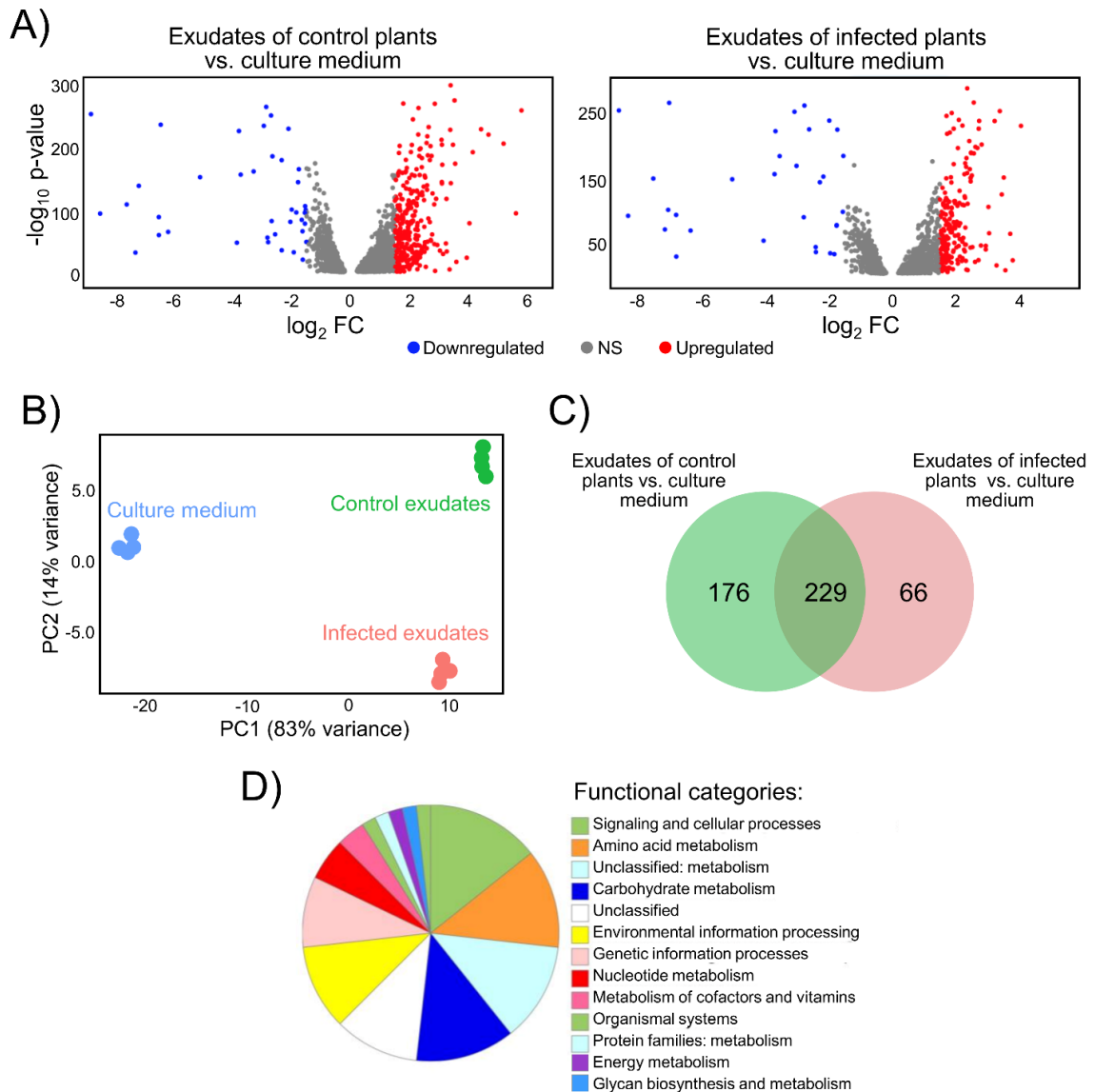


Figure 2.4 *Transcriptome responses of 2-79 to barley root exudates. (A) Volcano plots that show significantly up- and downregulated genes in red and blue. (B) Principal component analysis of biological replicates. (C) Venn diagram of differentially expressed genes (DEGs) that are unique and shared between treatments. (D) KEGG Orthology classification of proteins encoded by DEGs.*

the uptake and catabolism of arabinose and aminobenzoate. Additionally, the control exudates induced genes for the transport and/or catabolism of xylose, inositol, glycerol-3-phosphate, quinic acid, C4-dicarboxylic acids, GABA, quaternary ammonium compounds (QACs), and 3,4-dihydroxybenzoate (the β -ketoadipate pathway that converts

protocatechuate via 3-oxoadipate, succinyl-CoA and acetyl-CoA, which are processed by the TCA cycle).⁴⁹ In contrast, the exudates of infected plants activated uptake and catabolism of alkenesulfonates, polyols, and galactonate. The induction of some of these pathways agreed with the identification of corresponding substrates in root exudates (e.g., arabinose, fructose, xylose, malate, GABA, choline, sarcosine, betaine, and carnitine). These results agree with our earlier non-quantitative analysis of *Brachypodium*⁵⁰ root exudates, as well as with other studies, and suggest that root exudates make the plant rhizosphere a carbon-rich niche for plant-associated bacteria and that the utilization of these compounds forms a nutritional basis for the bacteria to colonize plant roots effectively.⁵¹

Another group of cellular pathways perturbed by root exudates function in metal ion homeostasis. Specifically, we observed a significant downregulation in bacterial genes involved in the metabolism of zinc, iron, and the synthesis of siderophores in cultures grown in both types of exudates. Iron is an essential micronutrient, and Strategy I plants respond to its deficiency by excreting protons that acidify the rhizosphere and reduce insoluble ferric iron to soluble Fe(II), which is taken up by a specific Fe transporter.⁵² In contrast, Strategy II plants that include barley and other graminaceous species acquire iron by secreting phytosiderophores.⁵³ These exometabolites are derivatives of mugineic acids that bind Fe(III) with a strong affinity, and the resultant iron-phytosiderophore complexes are then taken up by plant roots. Most rhizosphere bacteria, including *Pseudomonas* spp., also secrete iron-chelating metabolites, but at the same time capable of taking up exogenous siderophores, a strategy that helps to reduce energetic and nutrient costs.⁵⁴ A recent study demonstrated that *P. fluorescens* SBW25

responds to Fe deprivation in the rhizosphere by shutting down the synthesis of its own siderophores and consuming phytosiderophores secreted by the host plant.⁵⁵ Interestingly, phytosiderophores are also produced under Zn-limiting conditions and can chelate zinc.⁵⁶ It is plausible that the repression of iron and zinc acquisition genes in 2-79 treated by barley exudates is caused by the uptake of Fe and Zn in the form of phytosiderophore complexes.

It has been estimated that up to 80% of all bacteria and archaea live in biofilms, with planktonic cells occurring mostly during biofilm dispersal and the colonization of new habitats.⁵⁷ This estimate certainly applies to plant-associated microorganisms that colonize aerial, vascular and root tissues of their host by forming multicellular and multispecies surface-attached assemblies embedded in a self-produced matrix.⁵⁸ The presence of mucilage-embedded microcolonies on plant roots was first reported in the 1970s⁵⁹ and confirmed in numerous later studies that collectively revealed a close resemblance between the processes of rhizosphere colonization and biofilm formation. Bacterial biofilms are viewed as crucial contributors to many important animal and plant diseases since biofilm-residing pathogens efficiently colonize their hosts and are resilient to immune responses and antimicrobial agents. Similar ideas have been advanced in the field of rhizosphere research, where biofilms are considered an important trait contributing to the efficient colonization and persistence on root surfaces, and the formation of biofilms in response to root exudates, antimicrobials or stress factors was demonstrated for both beneficial and pathogenic rhizobacteria.⁶⁰⁻⁶⁶

Similar to biofilms formed in other environments, the colonization of plant root surfaces progresses via several stages that include reversible and irreversible attachment,

formation of microcolonies, maturation, and a dispersal process that generates new planktonic cells. Our results revealed induction of genes involved in the synthesis of fimbriae and type IVb pili, which are predicted to function in surface attachment and early stages of biofilm formation in 2-79 grown in both exudates (Figure 2.5).

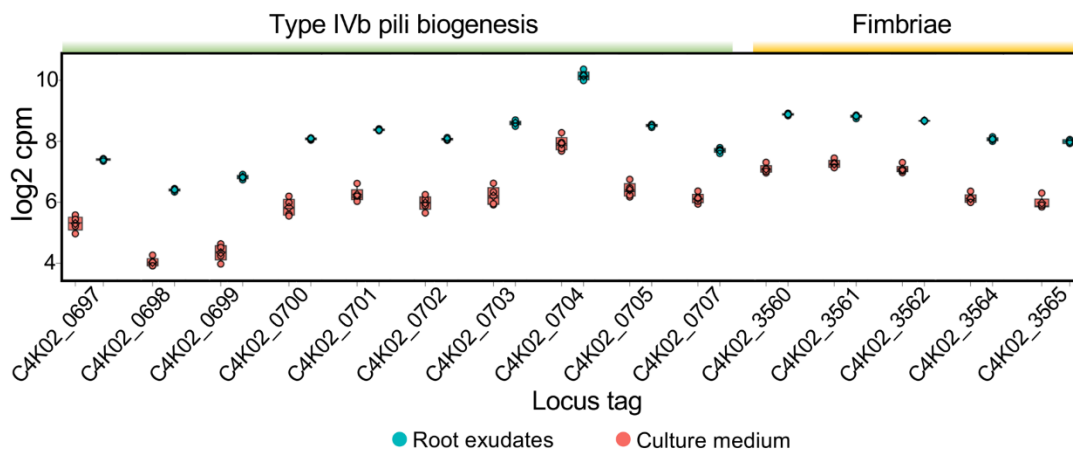


Figure 2.5 The response to root exudates involved induction of genes for the biogenesis of type IVb pili and fimbriae, which is consistent with surface attachment and transition to the biofilm growth mode.

We also observed the induction of a gene encoding a sensory box/GGDEF family protein.

Proteins carrying the GGDEF domain (named after the conserved central sequence pattern) function as diguanylate cyclases (DGC) and catalyze the condensation of two GTP molecules to form cyclic di-guanosine monophosphate (c-di-GMP).⁶⁷ In many bacteria, c-di-GMP acts as a second messenger that regulates a switch between the motile and sessile lifestyle, with low c-di-GMP levels associated with the planktonic phase and high levels correlating with surface-attached growth and biofilm formation.⁶⁸

Collectively, these results suggest that 2-79 cultures amended with root exudates were in the process of switching from flagella-based swimming to type IV pili-mediated motility and adhering to root surfaces with the help of adhesins, a pattern consistent with early

stages of biofilm formation.⁶⁹ These results are similar to the induction of genes related to extracellular matrix production in the plant growth-promoting bacterium *Bacillus amyloliquefaciens* SQR9 in the presence of maize root exudates.⁶⁶ Interestingly, we also found upregulation in denitrification-related genes and cytochrome c oxidase genes. In *Pseudomonas aeruginosa*, these enzymes assist in the growth in hypoxic and anoxic conditions. Cytochrome c oxidases lead to nitric oxide (NO) accumulation, which in turn results in the promotion of biofilm formation through cell elongation.⁷⁰

Finally, treatment of *P. synxantha* 2-79 with control root exudates resulted in the induction of genes involved in the biosynthesis of phenazine-1-carboxylic acid (PCA). PCA belongs to a large and diverse group of structurally-related secondary metabolites that act as extracellular electron shuttles and molecular signals that are crucial for the competitiveness of producing strains.⁷¹ In 2-79, PCA also contributes to the ability of this strain to suppress different plant-pathogenic fungi, including *R. solani* AG-8.¹⁵

Functional categorization of differentially expressed genes using Omicsbox revealed the membrane and cell periphery as the most abundant gene ontology (GO) term in the cellular component category. Ion binding and oxidoreductase activity were the most common GO term in the molecular function category. In contrast, the biological process category was dominated by the GO terms such as the metabolism of organic compounds, small molecules, and nitrogen compounds (Figure 2.6).

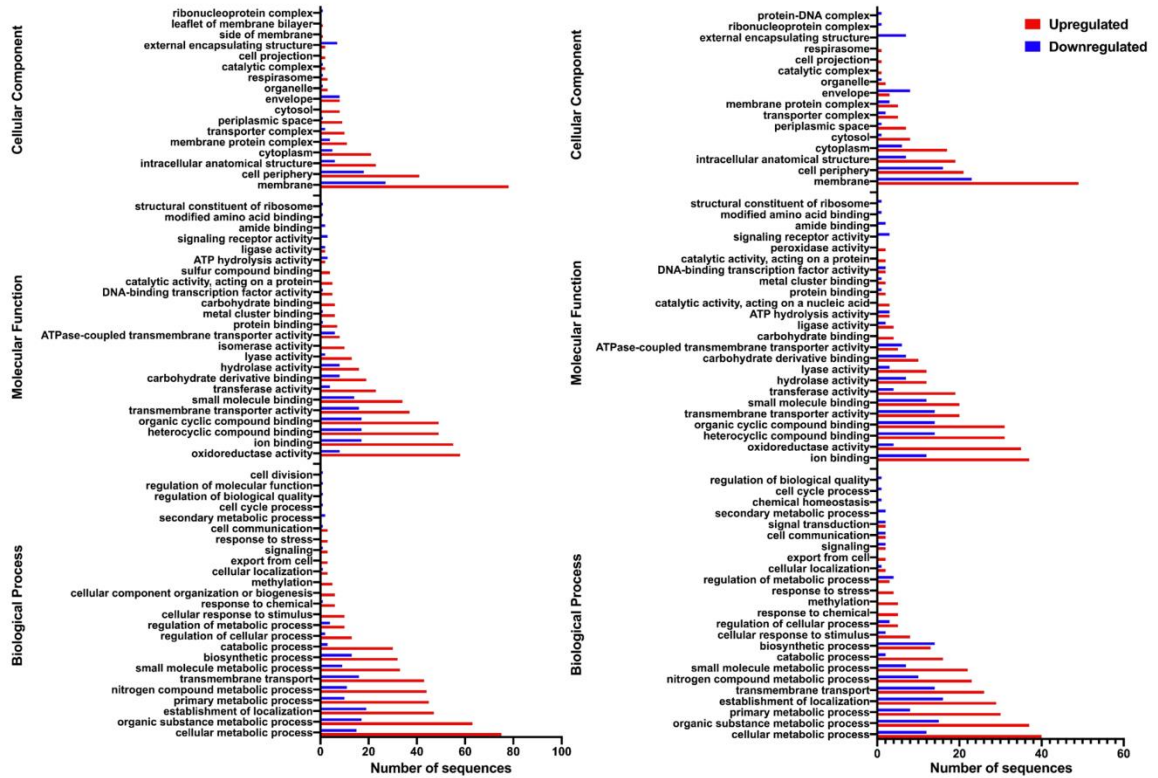


Figure 2.6 Gene ontology classification of differentially expressed genes of 2-79 in (left) healthy and (right) *Rhizoctonia*-infected root exudates compared to control conditions.

The terms were derived from 50 different functional groups (GO subcategory level 3).

These findings agree with the upregulation of 2-79 genes involved in the uptake and catabolism of diverse exometabolites from barley root exudates. The pathway enrichment analysis of upregulated DEGs (Fisher's exact test, $FDR < 0.05$) showed the overrepresentation of processes such as oxidoreductase activity and catabolic and transport processes. In contrast, GO terms associated with cellular processes, biological regulation, and organic substance metabolic processes were significantly underrepresented (Figure 2.7).

Finally, this study also aimed to create a controlled environment for studying plant root colonization by beneficial microorganisms for a better understanding of how they are recruited during pathogen infection. We hypothesized that *Rhizoctonia* infection would affect the chemical composition of barley root exudates and that, in turn, will modulate the expression of genes in 2-79 that are related to biocontrol and disease-suppression, including the phenazine biosynthesis genes. To test this hypothesis, we prepared exudates from control and *Rhizoctonia*-infected barley plants and compared their composition by targeted metabolomic profiling. These exudates were also added to bacterial cultures to compare transcriptomic responses of 2-79 to exometabolites secreted by healthy and diseased plant roots. This experimental system was chosen since the continuous cultivation of barley and dryland wheat at a cropping trial site in Ritzville, WA, led to the decline in *Rhizoctonia* root rot caused by *R. solani* AG-8.^{72,73} The analysis of rhizosphere communities from the *Rhizoctonia*-suppressive soil revealed the abundance of 2-79-like pseudomonads, that produce phenazines to compete against soil fungal pathogens.^{74,75}

Interestingly, phenazine biosynthesis genes were induced in cultures exposed to healthy root exudates but not in those treated with infected root exudates. This might have been due to the decrease in the several primary metabolites in the infected root exudates compared to the healthy ones and the possible concurrent uptake of the exudates by *Rhizoctonia*. On the other hand, the addition of infected exudates induced polyol transport genes, which might be caused by the secretion of polyols by *Rhizoctonia* in response to the plant environment. Polyols have osmoprotectant and antioxidant

properties and play a role in plant-pathogen interactions by protecting phytopathogens against osmotic and oxidative stress.^{76,77}

In conclusion, our results suggest that barley root exudates, like other plants, contain a diverse range of important carbon and nitrogen sources that modulate several uptake and catabolism genes, as well as biofilm formation genes in 2-79. These findings reveal diverse mechanisms involved in the adaptation of microorganisms to plant rhizosphere and demonstrate how rhizodeposition shapes the plant microbiome and recruits taxa involved in growth promotion and disease control and how these microbial taxa adapt themselves in the competitive rhizosphere environment. These results will aid in future studies of soil disease suppression and induction of systemic response in crop plants.

2.5 References

1. Miller WB. The eukaryotic microbiome: Origins and implications for fetal and neonatal life. *Front Pediatr.* 2016;4. doi:10.3389/fped.2016.00096
2. Koskella B, Bergelson J. The study of host-microbiome (co)evolution across levels of selection. *Philos Trans R Soc B Biol Sci.* 2020;375(1808):20190604. doi:10.1098/rstb.2019.0604
3. Krings M, Taylor TN, Hass H, Kerp H, Dotzler N, Hermsen EJ. Fungal endophytes in a 400-million-yr-old land plant: Infection pathways, spatial distribution, and host responses. *New Phytol.* 2007;174(3):648-657. doi:10.1111/j.1469-8137.2007.02008.x
4. Trivedi P, Leach JE, Tringe SG, Sa T, Singh BK. Plant-microbiome interactions: from community assembly to plant health. *Nat Rev Microbiol.* 2020;18(11):607-

621. doi:10.1038/s41579-020-0412-1
5. Henneron L, Kardol P, Wardle DA, Cros C, Fontaine S. Rhizosphere control of soil nitrogen cycling: a key component of plant economic strategies. *New Phytol.* 2020;228(4):1269-1282. doi:10.1111/nph.16760
 6. Ling N, Wang T, Kuzyakov Y. Rhizosphere bacteriome structure and functions. *Nat Commun.* 2022;13(1):836. doi:10.1038/s41467-022-28448-9
 7. Fitter AH, Moyersoen B. Evolutionary trends in root-microbe symbioses. *Philos Trans R Soc B Biol Sci.* 1996;351(1345):1367-1375. doi:10.1098/rstb.1996.0120
 8. Hodge A, Fitter AH. Substantial nitrogen acquisition by arbuscular mycorrhizal fungi from organic material has implications for N cycling. *Proc Natl Acad Sci U S A.* 2010;107(31):13754-13759. doi:10.1073/pnas.1005874107
 9. Glick BR. *Plant Growth-Promoting Bacteria : Mechanisms and Applications.* 2012;2012:963401. doi: 10.6064/2012/963401
 10. Mendes R, Garbeva P, Raaijmakers JM. The rhizosphere microbiome: Significance of plant beneficial, plant pathogenic, and human pathogenic microorganisms. *FEMS Microbiol Rev.* 2013;37(5):634-663. doi:10.1111/1574-6976.12028
 11. Mazurier S, Corberand T, Lemanceau P, Raaijmakers JM. Phenazine antibiotics produced by fluorescent pseudomonads contribute to natural soil suppressiveness to Fusarium wilt. *ISME J.* 2009;3(8):977-991. doi:10.1038/ismej.2009.33
 12. Mojgani N. Bacteriocin-producing rhizosphere bacteria and their potential as a biocontrol agent. In: *Rhizotrophs: Plant Growth Promotion to Bioremediation.* 2017;2:165-181. doi:10.1007/978-981-10-4862-3_8

13. Raaijmakers JM, De Bruijn I, De Kock MJD. Cyclic lipopeptide production by plant-associated *Pseudomonas* spp.: Diversity, activity, biosynthesis, and regulation. *Mol Plant-Microbe Interact.* 2006;19(7):699-710. doi:10.1094/MPMI-19-0699
14. Raaijmakers JM, Weller DM. Natural plant protection by 2,4-diacetylphloroglucinol-producing *Pseudomonas* spp. in take-all decline soils. *Mol Plant-Microbe Interact.* 1998;11(2). doi:10.1094/MPMI.1998.11.2.144
15. Thomashow LS, Weller DM. Role of a phenazine antibiotic from *Pseudomonas fluorescens* in biological control of *Gaeumannomyces graminis* var. *tritici*. *J Bacteriol.* 1988;170(8):3499-3508. doi:10.1128/jb.170.8.3499-3508.1988
16. Pieterse CMJ, Zamioudis C, Berendsen RL, Weller DM, Van Wees SCM, Bakker PAHM. Induced systemic resistance by beneficial microbes. *Annu Rev Phytopathol.* 2014;52:347-375. doi:10.1146/annurev-phyto-082712-102340
17. Hartmann A, Rothballer M, Schmid M. Lorenz Hiltner, a pioneer in rhizosphere microbial ecology and soil bacteriology research. In: *Plant and Soil.* 2008;312:7-14. doi:10.1007/s11104-007-9514-z
18. Kuzyakov Y, Razavi BS. Rhizosphere size and shape: Temporal dynamics and spatial stationarity. *Soil Biol Biochem.* 2019;135:343-360. doi:10.1016/j.soilbio.2019.05.011
19. White LJ, Ge X, Brözel VS, Subramanian S. Root isoflavonoids and hairy root transformation influence key bacterial taxa in the soybean rhizosphere. *Environ Microbiol.* 2017;19(4):1391-1406. doi:10.1111/1462-2920.13602
20. Fitzpatrick CR, Copeland J, Wang PW, Guttman DS, Kotanen PM, Johnson MTJ.

- Assembly and ecological function of the root microbiome across angiosperm plant species. *Proc Natl Acad Sci U S A*. 2018;115(6):E1157-E1165.
doi:10.1073/pnas.1717617115
21. Kuzyakov Y, Xu X. Competition between roots and microorganisms for nitrogen: Mechanisms and ecological relevance. *New Phytol*. 2013;198(3):656-669.
doi:10.1111/nph.12235
 22. Green, R M, Sambrook J. *Molecular Cloning: A Laboratory Manual*, 4th edition. *Cold Spring Harb Lab Press*. 2012;33(1).
 23. King EO, Ward MK, Raney DE. Two simple media for the demonstration of pyocyanin and fluorescein. *J Lab Clin Med*. 1954;44(2):301-307.
 24. LaBauve AE, Wargo MJ. Growth and laboratory maintenance of *Pseudomonas aeruginosa*. *Curr Protoc Microbiol*. 2012; Chapter 6:Unit-6E.1.
doi:10.1002/9780471729259.mc06e01s25
 25. Munkager V, Vestergård M, Priemé A, et al. AgNO₃ sterilizes grains of barley (*Hordeum vulgare*) without inhibiting germination—a necessary tool for plant–microbiome research. *Plants*. 2020;9(3):372. doi:10.3390/plants9030372
 26. Hoagland DR, Arnon DI. The water-culture method for growing plants without soil. *Circ Calif Agric Exp Stn*. 1950;347(2):32.
 27. Perl-Treves R, Foley RC, Chen W, Singh KB. Early induction of the Arabidopsis GSTF8 promoter by specific strains of the fungal pathogen *Rhizoctonia solani*. *Mol Plant-Microbe Interact*. 2004;17(1):70-80. doi:10.1094/MPMI.2004.17.1.70
 28. Ding X, Yang M, Huang H, et al. Priming maize resistance by its neighbors: Activating 1,4-benzoxazine-3-ones synthesis and defense gene expression to

- alleviate leaf disease. *Front Plant Sci.* 2015;6:830. doi:10.3389/fpls.2015.00830
29. Massalha H, Korenblum E, Tholl D, Aharoni A. Small molecules below-ground: the role of specialized metabolites in the rhizosphere. *Plant J.* 2017;90(4):788-807. doi:10.1111/tpj.13543
30. Neal AL, Ahmad S, Gordon-Weeks R, Ton J. Benzoxazinoids in root exudates of maize attract *Pseudomonas putida* to the rhizosphere. *PLoS One.* 2012;7(4):e35498. doi:10.1371/journal.pone.0035498
31. Stringlis IA, Yu K, Feussner K, et al. MYB72-dependent coumarin exudation shapes root microbiome assembly to promote plant health. *Proc Natl Acad Sci U S A.* 2018;115(22):E5213-E5222. doi:10.1073/pnas.1722335115
32. Zhang H, Yang Y, Mei X, et al. Phenolic acids released in maize rhizosphere during maize-soybean intercropping inhibit *Phytophthora* blight of soybean. *Front Plant Sci.* 2020;11:886. doi:10.3389/fpls.2020.00886
33. MacLean B, Tomazela DM, Shulman N, et al. Skyline: An open source document editor for creating and analyzing targeted proteomics experiments. *Bioinformatics.* 2010;26(7):966-968. doi:10.1093/bioinformatics/btq054
34. Mcrose DL, Newman DK. Redox-active antibiotics enhance phosphorus bioavailability. *Science.* 2021;371(6533):1033-1037. doi:10.1126/science.abd1515
35. Khan SR, Mavrodi D V, Jog GJ, Suga H, Thomashow LS, Farrand SK. Activation of the *phz* operon of *Pseudomonas fluorescens* 2-79 requires the LuxR homolog PhzR, N-(3-OH-Hexanoyl)-L-homoserine lactone produced by the LuxI homolog PhzI, and a cis-acting *phz* box. *J Bacteriol.* 2005;187(18):6517-6527.

doi:10.1128/JB.187.18.6517-6527.2005

36. Arkin AP, Cottingham RW, Henry CS, et al. KBase: The United States Department of Energy Systems Biology Knowledgebase. *Nat Biotechnol.* 2018;36(7):566-569. doi:10.1038/nbt.4163
37. Kim D, Paggi JM, Park C, Bennett C, Salzberg SL. Graph-based genome alignment and genotyping with HISAT2 and HISAT-genotype. *Nat Biotechnol.* 2019;37(8):907-915. doi:10.1038/s41587-019-0201-4
38. Pertea M, Pertea GM, Antonescu CM, Chang T-C, Mendell JT, Salzberg SL. StringTie enables improved reconstruction of a transcriptome from RNA-seq reads. *Nat Biotechnol.* 2015;33(3):290-295. doi:10.1038/nbt.3122
39. Love MI, Huber W, Anders S. Moderated estimation of fold change and dispersion for RNA-seq data with DESeq2. *Genome Biol.* 2014;15(12):550. doi:10.1186/s13059-014-0550-8
40. Götz S, García-Gómez JM, Terol J, et al. High-throughput functional annotation and data mining with the Blast2GO suite. *Nucleic Acids Res.* 2008;36(10):3420-3435. doi:10.1093/nar/gkn176
41. Paulitz TC, Smith JD, Kidwell KK. Virulence of *Rhizoctonia oryzae* on wheat and barley cultivars from the Pacific Northwest. *Plant Dis.* 2003;87(1):51-55. doi:10.1094/PDIS.2003.87.1.51
42. Hüberli D. Tips and Tactics: *Rhizoctonia*. *Grain Res Dev Corp.* 2016. https://grdc.com.au/__data/assets/pdf_file/0018/170343/grdc_tips_and_tactics_rhizoctonia_western_web.pdf
43. Rippa S, Zhao Y, Merlier F, Charrier A, Perrin Y. The carnitine biosynthetic

- pathway in *Arabidopsis thaliana* shares similar features with the pathway of mammals and fungi. *Plant Physiol Biochem.* 2012;60:109-114.
doi:10.1016/j.plaphy.2012.08.001
44. Oney-Birol S. Exogenous L-carnitine promotes plant growth and cell division by mitigating genotoxic damage of salt stress. *Sci Rep.* 2019;9(1):17229.
doi:10.1038/s41598-019-53542-2
45. Khan N, Ali S, Tariq H, et al. Water conservation and plant survival strategies of rhizobacteria under drought stress. *Agronomy.* 2020;10(11):1683.
doi:10.3390/agronomy10111683
46. Huang H, Nguyen Thi Thu T, He X, et al. Increase of fungal pathogenicity and role of plant glutamine in nitrogen-induced susceptibility (NIS) to rice blast. *Front Plant Sci.* 2017;8:265. doi:10.3389/fpls.2017.00265
47. Rudrappa T, Czymbek KJ, Paré PW, Bais HP. Root-secreted malic acid recruits beneficial soil bacteria. *Plant Physiol.* 2008;148(3):1547-1556.
doi:10.1104/pp.108.127613
48. Lanoue A, Burlat V, Henkes GJ, Koch I, Schurr U, Röse USR. De novo biosynthesis of defense root exudates in response to *Fusarium* attack in barley. *New Phytol.* 2010;185(2):577-588. doi:10.1111/j.1469-8137.2009.03066.x
49. Guzik U, Hupert-Kocurek K, Wojcieszysk D. Intradiol dioxygenases — the key enzymes in xenobiotics degradation. In: *Biodegradation of Hazardous and Special Products*; 2013. doi:10.5772/56205
50. Mavrodi O V., McWilliams JR, Peter JO, et al. Root exudates alter the expression of diverse metabolic, transport, regulatory, and stress response genes in

- rhizosphere *Pseudomonas*. *Front Microbiol.* 2021;12.
doi:10.3389/fmicb.2021.651282
51. Mark GL, Dow JM, Kiely PD, et al. Transcriptome profiling of bacterial responses to root exudates identifies genes involved in microbe-plant interactions. *Proc Natl Acad Sci U S A.* 2005;102(48):17454-17459.
doi:10.1073/pnas.0506407102
52. Hell R, Stephan UW. Iron uptake, trafficking and homeostasis in plants. *Planta.* 2003;216(4):541-551. doi:10.1007/s00425-002-0920-4
53. Bocchini M, Bartucca ML, Ciancaleoni S, et al. Iron deficiency in barley plants: Phytosiderophore release, iron translocation, and DNA methylation. *Front Plant Sci.* 2015;6:514. doi:10.3389/fpls.2015.00514
54. Hider RC, Kong X. Chemistry and biology of siderophores. *Nat Prod Rep.* 2010;27(5):637-657. doi:10.1039/b906679a
55. Boiteau RM, Markillie LM, Hoyt DW, et al. Metabolic interactions between *Brachypodium* and *Pseudomonas fluorescens* under controlled iron-limited conditions. *mSystems.* 2021;6(1):e00580-20. doi:10.1128/msystems.00580-20
56. Schenkeveld WDC, Oburger E, Gruber B, et al. Metal mobilization from soils by phytosiderophores – experiment and equilibrium modeling. *Plant Soil.* 2014;383(1-2):59-71. doi:10.1007/s11104-014-2128-3
57. Flemming HC, Wuertz S. Bacteria and archaea on Earth and their abundance in biofilms. *Nat Rev Microbiol.* 2019;17(4):247-260. doi:10.1038/s41579-019-0158-9
58. Danhorn T, Fuqua C. Biofilm formation by plant-associated bacteria. *Annu Rev*

- Microbiol.* 2007;61:401-422. doi:10.1146/annurev.micro.61.080706.093316
59. Rovira AD, Newman EI, Bowen HJ, Campbell R. Quantitative assessment of the rhizoplane microflora by direct microscopy. *Soil Biol Biochem.* 1974;6(4):211-216. doi:10.1016/0038-0717(74)90053-4
60. Bais HP, Fall R, Vivanco JM. Biocontrol of *Bacillus subtilis* against infection of *Arabidopsis* roots by *Pseudomonas syringae* is facilitated by biofilm formation and surfactin production. *Plant Physiol.* 2004;134(1):3017-319. doi:10.1104/pp.103.028712
61. Espinosa-Urgel M, Kolter R, Ramos JL. Root colonization by *Pseudomonas putida*: Love at first sight. *Microbiology.* 2002;148(2):341-343. doi:10.1099/00221287-148-2-341
62. Haggag WM, Timmusk S. Colonization of peanut roots by biofilm-forming *Paenibacillus polymyxa* initiates biocontrol against crown rot disease. *J Appl Microbiol.* 2008;104(4):961-969. doi:10.1111/j.1365-2672.2007.03611.x
63. Heindl JE, Wang Y, Heckel BC, Mohari B, Feirer N, Fuqua C. Mechanisms and regulation of surface interactions and biofilm formation in *Agrobacterium*. *Front Plant Sci.* 2014;5:176. doi:10.3389/fpls.2014.00176
64. Selin C, Habibian R, Poritsanos N, Athukorala SNP, Fernando D, De Kievit TR. Phenazines are not essential for *Pseudomonas chlororaphis* PA23 biocontrol of *Sclerotinia sclerotiorum*, but do play a role in biofilm formation. *FEMS Microbiol Ecol.* 2010;71(1):73-83. doi:10.1111/j.1574-6941.2009.00792.x
65. Timmusk S, Grantcharova N, Wagner EGH. *Paenibacillus polymyxa* invades plant roots and forms biofilms. *Appl Environ Microbiol.* 2005;71(11):7292-7300.

doi:10.1128/AEM.71.11.7292-7300.2005

66. Zhang N, Yang D, Wang D, et al. Whole transcriptomic analysis of the plant-beneficial rhizobacterium *Bacillus amyloliquefaciens* SQR9 during enhanced biofilm formation regulated by maize root exudates. *BMC Genomics*. 2015;16(1):685. doi:10.1186/s12864-015-1825-5
67. Dahlstrom KM, O'Toole GA. A Symphony of cyclases: Specificity in diguanylate cyclase signaling. *Annu Rev Microbiol*. 2017;71:179-195. doi:10.1146/annurev-micro-090816-093325
68. Jenal U, Reinders A, Lori C. Cyclic di-GMP: second messenger extraordinaire. *Nat Rev Microbiol*. 2017;15(5):271-284. doi:10.1038/nrmicro.2016.190
69. Morris CE, Monier JM. The Ecological Significance of Biofilm Formation by Plant-Associated Bacteria. *Annu Rev Phytopathol*. 2003;41:429-453. doi:10.1146/annurev.phyto.41.022103.134521
70. Hamada M, Toyofuku M, Miyano T, Nomura N. cbb3-type cytochrome c oxidases, aerobic respiratory enzymes, impact the anaerobic life of *Pseudomonas aeruginosa* PAO1. *J Bacteriol*. 2014;196(22):3881-3889. doi:10.1128/JB.01978-14
71. Okegbe C, Fields BL, Cole SJ, et al. Electron-shuttling antibiotics structure bacterial communities by modulating cellular levels of c-di-GMP. *Proc Natl Acad Sci U S A*. 2017;114(26):E5236-E5245. doi:10.1073/pnas.1700264114
72. Schillinger WF, Paulitz TC. Reduction of Rhizoctonia bare patch in wheat with barley rotations. *Plant Dis*. 2006;90(3):302-306. doi:10.1094/PD-90-0302
73. Yin C, Hulbert SH, Schroeder KL, et al. Role of bacterial communities in the

natural suppression of *Rhizoctonia solani* bare patch disease of wheat (*Triticum aestivum* L.). *Appl Environ Microbiol.* 2013;79(23):7428-7438.

doi:10.1128/AEM.01610-13

74. Jaaffar AKM, Parejko JA, Paulitz TC, Weller DM, Thomashow LS. Sensitivity of *Rhizoctonia* isolates to phenazine-1-carboxylic acid and biological control by phenazine-producing *Pseudomonas* spp. *Phytopathology.* 2017;107(6):692-703. doi:10.1094/PHYTO-07-16-0257-R
75. Schlatter D, Kinkel L, Thomashow L, Weller D, Paulitz T. Disease suppressive soils: New insights from the soil microbiome. *Phytopathology.* 2017;107(11):1284-1297. doi:10.1094/PHYTO-03-17-0111-RVW
76. Meena M, Prasad V, Zehra A, Gupta VK, Upadhyay RS. Mannitol metabolism during pathogenic fungal-host interactions under stressed conditions. *Front Microbiol.* 2015;6:1019. doi:10.3389/fmicb.2015.01019
77. Ramirez ML, Chulze SN, Magan N. Impact of osmotic and matric water stress on germination, growth, mycelial water potentials and endogenous accumulation of sugars and sugar alcohols in *Fusarium graminearum*. *Mycologia.* 2004;96(3):470-478. doi:10.1080/15572536.2005.11832946

CHAPTER III- EFFECT OF WATER STRESS ON ROOT EXUDATION AND ITS
ROLE IN THE ALTERATION OF GENE EXPRESSION AND PHYSIOLOGY OF
THE MODEL RHIZOSPHERE BACTERIUM *PSEUDOMONAS SYNXANTHA* 2-79

3.1 Abstract

Drought is an abiotic stress factor that affects agriculture on a global scale. Plants employ various mechanisms to adapt to water-stressed conditions, including nurturing distinct microbial communities that modulate phytohormone levels and produce water-sequestering biofilms. *Pseudomonas synxantha* 2-79 is a beneficial strain isolated from the rhizosphere of dryland wheat grown in central Washington State. This organism protects dryland cereals from soilborne fungal pathogens and thrives in arid soils. The molecular mechanisms that allow 2-79 to maintain physiological activity and tight mutualistic interactions with its plant hosts in dry soils remain obscure. Previous research in our lab revealed that plant root exudates contain quaternary ammonium compounds (QACs), which function as efficient microbial osmoprotectants. The 2-79 genome encodes several membrane transporters, which are critical for the rhizosphere competence and allow this organism to take up exogenous QACs. Externally supplied root exudates and QACs protect 2-79 from water stress. In this study, we produced root exudates from wheat cv. Tara grown under water-replete and water-stressed conditions. Metabolome profiling revealed that roots of water-stressed plants exude significantly higher amounts of QACs. To characterize the effect of exometabolites produced by water-stressed plants on rhizobacteria, we cultured 2-79 in the presence of wheat root exudates. We then analyzed changes in the expression of 2-79 genes by RNA-seq. The differential gene expression analysis identified 154 and 56 genes that responded,

respectively, to water-stressed and control root exudates. Among genes upregulated in response to water-stressed exudates were those encoding enzymes for the catabolism of QACs (sarcosine oxidase, glycine-betaine demethylase). These results provide insight into the effects of drought on the rhizosphere microbiome and demonstrate that plant root exudates play a major role in the survival of root-associated microorganisms in water-deprived conditions.

3.2 Introduction

40% of the total land area in the world is occupied by arid and semi-arid regions which are collectively inhabited by over two billion people.^{1,2} These regions deal with frequent fluctuations in temperatures and rainfall and are highly vulnerable to global climate change. The dryland soils are characterized by low biological activity and low fertility due to the deficit of moisture, nutrients, and organic matter.³ Despite these challenges, the livelihood of most people living in these drylands depends on natural resource-based activities, such as herding and the production of legumes, cereals, vegetables, and forages.⁴ The economic importance of dryland farming will continue to grow due to the projected rise in the number of people living in water-scarce areas accompanied by a sharp increase in food demand by 2050.⁵ This increasing challenge to food security and requirement of improved productivity and sustainability of dryland farming will likely need a combination of advanced agronomic practices, implementation of climate-resilient crops and development of innovative microbiome technologies for improved nutrient cycling, disease management, and better stress resilience.^{6,7}

Plants employ a variety of morpho-physiological adaptations to prevent themselves from drought, that result in stomatal closure, increased water uptake due to

changes in the root architecture, and tissue-specific modulation of hormonal signaling to adjust osmotic processes.⁸ Plants also recruit beneficial rhizosphere microorganisms that positively influence plant fitness in response to stressors associated with global climate change (e.g., drought, salt, temperature, and soil pollution) by modulating stress hormones, producing plant growth-promoting factors, maintaining the host's nutritional status, and by suppressing pathogenic stressors.^{9,10} Recent studies demonstrated that soil moisture shapes the belowground plant microbiome and that the drought-adapted rhizobiome confers water stress tolerance.¹¹⁻¹⁵ It is generally accepted that the foundation for the differential affinity of rhizobacteria towards host plants is built upon the interaction of microorganisms and with complex secretions, lysates, and mucilages exuded by plant roots.¹⁶ However, in contrast to the well-studied mechanisms of drought tolerance in plants, the physiological and molecular events behind the recruitment of beneficial rhizobacteria and their adaptation to low water-content habitats remain poorly understood.

This study explored microbial responses to the water-stressed rhizosphere by focusing on molecular interactions between wheat and *Pseudomonas synxantha* 2-79, a strain that exemplifies a defined group of beneficial rhizobacteria that are specifically associated with wheat grown in arid parts of the Pacific Northwest. Our previous studies revealed an abundance of 2-79 like bacteria in the rhizosphere of wheat grown in parts of the central and eastern Washington, which receive annual precipitation as low as 150-300 mm.¹⁷⁻¹⁹ These bacteria produce the broad-spectrum antibiotic phenazine-1-carboxylic acid (PCA) and control *Rhizoctonia solani* AG-8, a ubiquitous soilborne fungal pathogen that represents major yield constraints in wheat grown in this extreme climatic region.²⁰

Interestingly, the population density of the 2-79 like pseudomonads was inversely related to annual precipitation or irrigation suggesting a unique adaptation to the rhizosphere of dryland wheat.^{21,22}

Microorganisms employ diverse physiological defensive mechanisms to cope with deleterious effects of water stress. One type of such widespread survival strategies involve the accumulation of neutral metabolites, referred to as compatible solutes, osmolytes or osmoprotectants that help to maintain homeostasis in hyperosmotic environments such as arid or saline soils.^{23,24} Common microbial osmoprotectants include sugars (trehalose), polyols (mannitol), amino acids (proline), amino acid derivatives (N-acetylglutaminylglutamine amide, or NAGGN), and quaternary ammonium compounds (QACs) like choline, glycine betaine and carnitine.²⁵ Bacteria can synthesize compatible solutes de novo or uptake them from the environment for osmoprotection or catabolism.^{26,27} Compatible solutes not only aid in maintaining the osmolarity of bacterial cells, thereby resisting dehydration, but also provide resistance against other temperature stress,²⁸ thus increasing the ability of bacteria to proliferate in adverse ecological niches.

We have recently investigated genome-wide transcriptomic responses to root exudates in several well-characterized rhizosphere pseudomonads, including *P. synxantha* 2-79.²⁹ Our results revealed that exometabolites secreted by plant roots perturb numerous microbial genes encoding diverse enzymes, transporters, as well as regulatory, stress response, and conserved hypothetical proteins. Interestingly, some of the differentially genes were predicted to function in the uptake and catabolism of quaternary ammonium compounds (QACs) prompting us to investigate the contribution of these pathways to the adaptation of microorganisms to the water-stressed rhizosphere lifestyle.

In this study, we generated root exudates from wheat, the primary host of *P. synxantha* 2-79, grown under both water-replete and water-stressed conditions and performed their metabolomic profiling. We demonstrated that water-stressed root exudates contain elevated levels of choline and glycine betaine and protect 2-79 from osmotic stress. The exposure of 2-79 to these exudates was accompanied by the upregulation of QAC uptake and catabolism genes, which helped us determine the importance of these genes in the adaptation of 2-79 in water-stressed conditions.

3.3 Materials and Methods

3.3.1 Bacterial strains and culture conditions

Pseudomonas synxantha 2-79 was routinely cultured at 27°C in Luria-Bertani (LB) medium³⁰ or King's medium B³¹ and maintained as frozen glycerol stocks at -80°C. The RNA-seq and bacterial osmoprotection assays were performed in the full- or half-strength 21C minimal medium containing per 1 L: 1.0 g NH₄Cl, 3.5 g Na₂HPO₄×2H₂O, 2.8 g KH₂PO₄, and 20 ml of the Huntner's microelement solution.^{32,33} Carbon source was supplemented with 10 mM glucose or a mix of 10 mM glucose and 20 mM pyruvate.^{26,27}

3.3.2 Collection of wheat root exudates

Seeds of hard red spring wheat (cultivar Tara) were surface sterilized with chlorine gas.³⁴ Briefly, the seeds were dispensed in 50-mL conical centrifuge tubes and placed into an airtight glass desiccator containing a beaker with 100 mL of fresh commercial chlorine bleach mixed with 3 mL of concentrated HCl. The desiccator was sealed and placed in a fume hood for 16 h. The germination rate was monitored by placing the sterilized seeds on moistened germination paper and incubating at 20°C for 48 h. To collect root exudates, sterile germinated seeds were placed into 1 L wide-mouth

glass jars containing glass beads and distilled water. The jars were transferred into an environmental chamber (Percival Scientific, Perry, IA, USA) and incubated at 20°C for 6 d.²⁹ After that, a subset of the plants were subjected to water stress by submerging their roots for 24 h into 0.3 M NaCl. The control plants were treated with distilled water. After the incubation, all seedlings were collected, and their roots were rinsed in several changes of distilled water. The root exudates were collected by placing the rinsed plant roots for 3 h into conical flasks containing 25 mL of distilled water. The root exudates were collected, lyophilized, and shipped for metabolomic profiling to the Analytical Resources Core - Bioanalysis and Omics (ARC-BIO) at Colorado State University.

3.3.3 Metabolomic profiling of root exudates

The root exudates were extracted with aqueous methanol and analyzed using gas or liquid chromatography coupled mass spectrometry. Briefly, all samples were dissolved in ice-cold 80% methanol and spiked with appropriate internal standards. The mixtures were vortexed and incubated for 3 h at -20°C, followed by centrifugation at 17,000 × g for 15 min at 4°C. The supernatants were dried under nitrogen and subjected to a two-step derivatization for GC-MS analysis. Metabolites were detected using a Trace 1310 GC coupled to a Thermo ISQ mass spectrometer (Thermo Fisher Scientific, Waltham, MA, USA). Samples (1 µL) were injected into a 30-m TG-5MS column (0.25 mm i.d., 0.25 µm film thickness) (Thermo Fisher Scientific) with a 1.2 mL min⁻¹ helium gas flow rate. GC inlet was maintained at 285°C. The oven program consisted of 80°C for 30 s, followed by a ramp of 15°C min⁻¹ to 330°C, and an 8 min hold. The split ratio was set at 10, while the transfer line and ion source were held at 300 and 260°C, respectively. Masses between 50-650 m/z were scanned at 5 scans sec⁻¹ under electron impact

ionization. The injector split ratio and oven temperature gradient were adjusted depending on the assay.

The LC-MS/MS analysis were performed on an Acquity Classic UPLC coupled to a Xevo TQ-S triple quadrupole mass spectrometer (both from Waters, Milford, MA, USA). Chromatographic separations were carried out on an Acquity UPLC BEH Amide column (2.1 x 100 mm, 1.7 μ M) (Waters) operated at 30°C. Mobile phases consisted of (A) water with 10 mM ammonium formate and 0.1% formic acid, and (B) acetonitrile with 0.1% formic acid. The following gradient was applied at a flowrate of 0.4 mL min⁻¹: time = 0 min, 99% B; time = 0.5 min, 99% B; time = 7 min, 5% B; time = 11 min, 5% B; time = 11.5 min, 99% B; time = 15 min, 99% B. Samples were maintained at 6°C in the autosampler, and the injection volume was set at 3 μ L. Mass detector was operated in ESI-mode with the capillary voltage set to 0.7 kV and inter-channel delay set to 3 msec. Source temperature was 150°C and desolvation gas (nitrogen) temperature was 450°C. Desolvation gas flow was 1000 L h⁻¹, cone gas flow was 150 L h⁻¹, and collision gas (argon) flow was 0.15 mL min⁻¹. The nebulizer pressure (nitrogen) was set to 7 Bar, and the MS acquisition functions were scheduled by retention time. Autodwell feature was set for each function and dwell time was calculated in the Masslynx software (Waters) to achieve >12 points-across-peak as the minimum data points per peak. Because of the expected wide concentration ranges of analytes, each sample was injected 3-4 times with different dilutions.

GC-MS data was processed using Chromeleon 7.2.10 software (Thermo Fisher Scientific), while the LC-MS/MS data files were imported into Skyline package (MacLean et al., 2010). Each target analyte was visually inspected for retention time and

peak area integration. Peak areas were extracted for target compounds detected in biological samples and normalized to the peak area of the appropriate internal standard or surrogate in each sample. Absolute quantitation was performed using linear regression equations obtained from calibration curves generated for each compound.

3.3.4 Bacterial osmoprotection assays

2-79 was cultured overnight on ½-21C glucose-pyruvate agar, after which the cells were collected, washed, suspended in the same liquid medium at 10^6 CFU mL⁻¹, and the osmotic stress was imposed through the addition of NaCl. Bacteria grown in the medium served as the control. The osmoprotective properties of root exudates were tested by amending the growth medium with 10-fold concentrated root exudates dissolved in ½-21C. The ability of root exudates to rescue the growth of water-stressed 2-79 was compared to 1 mM glycine betaine. All cultures were incubated statically in CytoOne 96-well microtiter plates (USA Scientific) for 48 h at 27°C, and the growth was monitored by measuring absorbance at 600 nm with Synergy HTX microplate reader (BioTek). Each treatment had 4 replicates and the entire experiment was repeated twice. Differences between treatments were analyzed by ANOVA or Kruskal-Wallis test ($P < 0.05$) in JMP v.14 (SAS Institute, Cary, NC, USA).

3.3.5 RNA extraction and processing

To profile transcriptome responses of 2-79 to wheat root exudates, the bacteria were grown overnight on 21C-glucose plates, after which the cells were scraped off, washed, and suspended in liquid 21C-glucose medium. The 10-fold concentrated solutions of root exudates were prepared by reconstituting the lyophilized material from water-replete and water-stressed plants in an appropriate volume of 21C. These

concentrated root exudates were filter-sterilized and mixed at 1:1 ratio with 2-79 cell suspension to achieve the density of 10^7 CFU mL⁻¹. Bacteria inoculated in the 21C-glucose medium served as the control. The cultures were dispensed in CytoOne 96-well microtiter plates (USA Scientific, Ocala, FL, USA) and incubated statically at 27°C till mid-exponential phase (OD₆₃₀ of 0.5-0.6), after which the bacteria were harvested, stabilized in RNAprotect (QIAGEN, Germantown, MD, USA) and extracted with a RNeasy Protect Bacteria Mini Kit (QIAGEN). The extracted RNA was treated with TURBO DNase (Thermo Fisher Scientific) and quantified using a QuantiFluor RNA kit (Promega Co., Madison, WI, USA). The RNA integrity was verified using a 2100 Bioanalyzer and an RNA 6000 Nano Kit (Agilent Technologies, Santa Clara, CA, USA) and all samples were shipped to Novogene (Sacramento, CA, USA). Four biological replicates of RNA per conditions were ribodepleted with a Ribo-Zero Plus rRNA Depletion Kit (Illumina, San Diego, CA, USA), stranded RNASeq libraries were prepared and sequenced in PE150 mode on a NovaSeq 6000 instrument (Illumina).

3.3.6 Transcriptomic and gene expression studies

The sequenced reads were imported in KBase (Arkin et al., 2018),³⁵ quality filtered with FastQC v.0.11.5 (<https://www.bioinformatics.babraham.ac.uk>) and aligned with HISAT2 v.2.1.0³⁶ to the complete 2-79 genome (GenBank accession number CP027755). Full-length transcripts were assembled with StringTie v.1.3.3,³⁷ and differential expression analysis was carried out with DeSeq2 v.1.20.0.³⁸ Genes differentially expressed (i.e., absolute fold change >1 (log₂ scale), FRD < 0.01) between the control and experimental treatments were used for downstream analysis. The functional categorization of differentially expressed genes and gene enrichment analyses

were performed using Blast2GO annotations³⁹ in OmicsBox (BioBam Bioinformatics, Cambridge, MA, USA). Raw RNA-seq reads were also analyzed for the presence of small non-coding RNAs. Briefly, the reads were aligned to the 2-79 genome with Bowtie2⁴⁰ and the output SAM files were converted to BAM format and merged and indexed with SAMtools.⁴¹ The merged BAM files were further converted to BED format using the BEDTools suite⁴² and regions of high expression (sequencing depth ≥ 250) were filtered with the Integrative Genomics Viewer (IGV).⁴³ A BEDgraph file of the 2-79 genome was filtered to only include the gene annotations and intersected with the expression data in BEDtools to identify the expressed intergenic regions ≥ 40 nt in length. The resultant sequences were compared to the known small RNAs of *Pseudomonas* species.⁴⁴⁻⁴⁶ The taxonomic distribution of selected metabolic pathways were analyzed with Annotree⁴⁷ using the following cutoff parameters: % identity > 30 , e-value < 0.00001 , % subject alignment > 70 , and % query alignment > 70 .

3.3.7 RT-qPCR assays

Extracted RNA was converted to cDNA using First Strand cDNA Synthesis Kit (New England Biolabs) and used in the RT-qPCR assays performed with the Luna Universal qPCR Master Mix (New England Biolabs) and primer sets targeting the QAC catabolism genes *gbcA* (*gbcAf* 5'-CTGCCGCACTCCTGGAACCAC-3', *gbcAr* 5'-GCGTCCTTGTGCACGATCCACT-3'), *dgcA* (*dgcAf* 5'-GCCAACGTCATCCC GAACATGAGC-3', *dgcAr* 5'-CAGCACCGGAACCTTGACCACT-3'), and *soxB* (*soxBf* 5'-ATCGAATCCCACCCGCTGCAA-3', *soxBr* 5'-CCGATCACCAGG TCGCCCTT-3'). The expression of target genes was normalized to that of the housekeeping gene *rpoD* amplified with primers *rpoDf* (5'-TCGTGGCAACAA

GCAGGCAATCG-3') and rpoDr (5'-CGCGCTCAACCAGGCCTTCGAAC-3'). The assay was performed using a CFX96 Real-Time PCR Detection System and CFX Maestro software (Bio-Rad Laboratories, USA).

3.4 Results and Discussion

3.4.1 Water stress significantly alters the composition of wheat root exudates

To evaluate the effect of water stress on rhizodeposition, we generated root exudates from water-replete (control) and osmotically stressed wheat cv. Tara and performed their comparative metabolomic profiling. The instrumental analysis demonstrated the presence of diverse amino acids, carbohydrates, and organic acids (Figure 3.1). Both types of exudates contained all common amino acids (except cysteine)

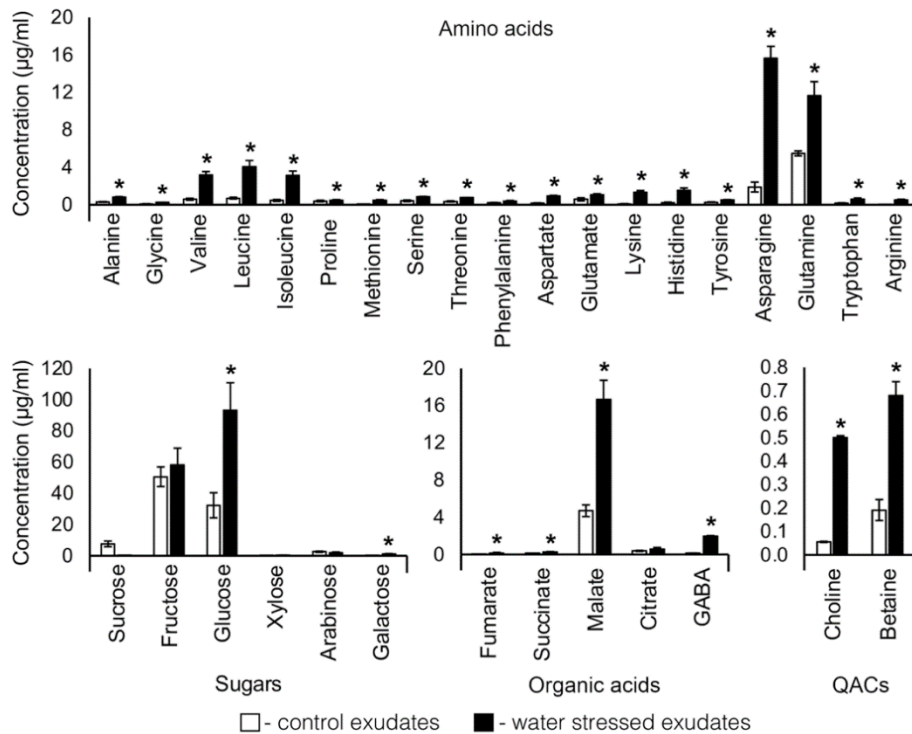


Figure 3.1 Concentrations (mean \pm SD) of primary metabolites and quaternary ammonium compounds (QACs) in exudates of water-replete and water-stressed spring wheat cv. Tara.

Asterisks represent significant differences in metabolite concentrations as assessed by Student's T-test ($P < 0.05$).

with particularly high levels of asparagine and glutamine. The exudates also contained significant amounts of quaternary ammonium compounds (QACs), especially choline and glycine betaine. Carnitine and sarcosine were detected but not quantified because both compounds coeluted with interfering substances. The quantitative analysis revealed that water stress significantly alters the levels of multiple metabolites. The water-stressed plants secreted elevated amounts of several amino acids (asparagine, glutamine, leucine, isoleucine, and valine), glucose, malate, succinate, fumarate, and γ -aminobutyric acid (GABA). Most notably, the stress resulted in significantly higher concentrations of choline and glycine betaine that function as key osmoprotectants in higher plants and diverse groups of microorganisms. This confirmed that the secretion of plant root exudates is largely controlled by environmental stimuli.⁴⁸

3.4.2 Root exudates rescue the growth of 2-79 under water stress

We evaluated the protective effect of metabolites secreted by plant roots on rhizobacteria by supplementing osmotically stressed cultures of 2-79 with wheat root exudates. The results of this experiment revealed that the potent growth inhibition caused by 0.3 M NaCl could be reversed by 1.0 mM glycine betaine, a well-studied microbial osmoprotectant. Interestingly, root exudates exerted an equally strong protective effect and closely matched glycine betaine by restoring the growth of water-stressed 2-79 by ~90% at 48 hours (Figure 3.2). These findings suggest that the belowground chemical crosstalk between the plant-associated microorganisms and their host plays an essential role in the ability of both partners to adapt and cope with abiotic and biotic stresses of survival in arid conditions.

3.4.3 Transcriptome responses of 2-79 to wheat root exudates

The RNA-seq experiment with *P. synxantha* 2-79 grown in the control conditions and the presence of water-replete and water-stressed root exudates generated 235.3 million high-quality Illumina sequencing reads (~19.6 million reads per sample) that were mapped to the complete genome of this strain. The statistical analysis with an FDR cutoff of 0.01 and an absolute log₂ fold change threshold of 1.0 revealed a total of 166 genes that were differentially expressed in response to wheat root exudates (Figure 3.3). These genes encoded multiple transporters of the ABC and RND superfamilies, diverse transcription factors, hypothetical proteins, as well as numerous enzymes involved in central and peripheral metabolism. Among 149 genes differentially expressed in response to water-stressed root exudates were those involved in the catabolism of carbohydrates (including components of the fructose-specific phosphotransferase (PTS) system), myo-inositol and amino acids. Also was observed a significant upregulation of a gene encoding an extracytoplasmic function (ECF) sigma factor of RNA polymerase, which suggests an activation of cell envelope-related stress response in response to root exudates.⁴⁹

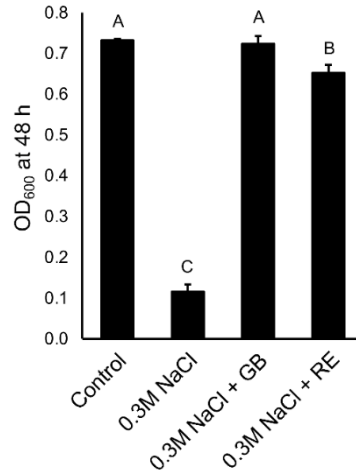


Figure 3.2 Root exudates of water-stressed wheat cv. Tara are rich in QACs and protect 2-79 from osmotic stress.

The bacteria were cultured for 48 h in the low osmoticum $\frac{1}{2}$ -21C-glucose-pyruvate medium, and the osmotic stress was imposed by 0.3M NaCl. The growth medium was amended with 1 mM glycine betaine (GB) or 10X concentrated root exudates (RE). Error bars show standard deviation. Different letters indicate treatments that are significantly different from the control according to Wilcoxon signed-rank test ($P < 0.05$).

These findings were further supported by the functional categorization of the differentially expressed genes, which revealed the integral component of the membrane as the most highly represented gene ontology (GO) term in the cellular component category (Figure 3.4). Cation or anion binding were the most common GO terms in the

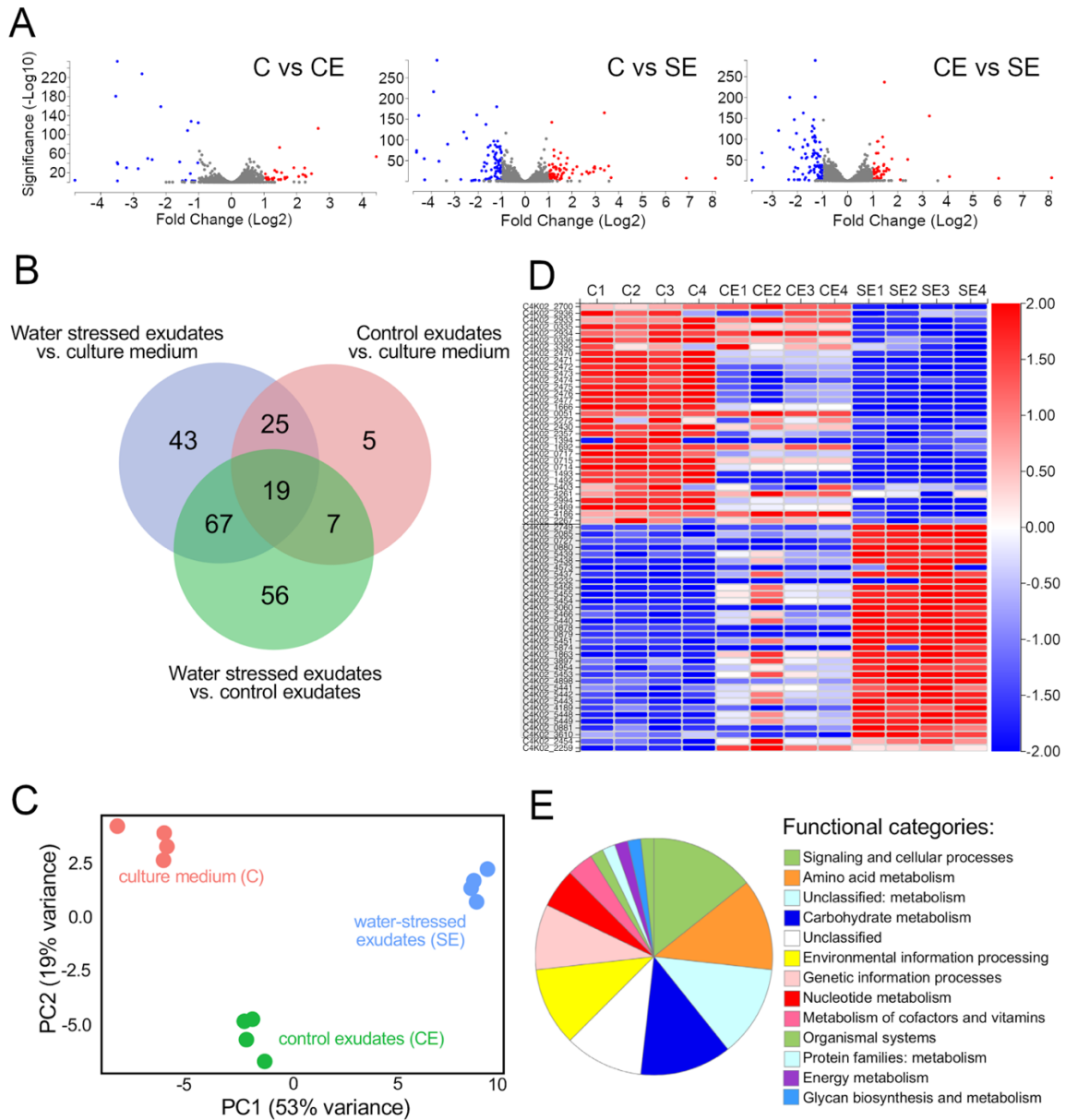


Figure 3.3 *Transcriptome responses of 2-79 to wheat root exudates.* (A) *Volcano plots that show significantly up- and downregulated genes in red and blue (C, culture medium; CE, control exudates; SE, water-stressed exudates).* (B) *Venn diagram of differentially expressed genes (DEGs) that are unique and shared between treatments.* (C) *Principal component analysis of biological replicates.* (D) *Changes in expression of selected differentially expressed genes.* (E) *KEGG Orthology classification of proteins encoded by DEGs.*

molecular function category, while GO terms like transport, cellular aromatic compound and organonitrogen compound metabolic processes dominated the biological process

category. The GO term enrichment analysis of differentially expressed genes using revealed a significant overrepresentation (Fisher's exact test, FDR adjusted P-value of 0.05) of sarcosine oxidase activity in 2-79 exposed the water-stressed root exudates versus control grown in the 1/2-21C medium.

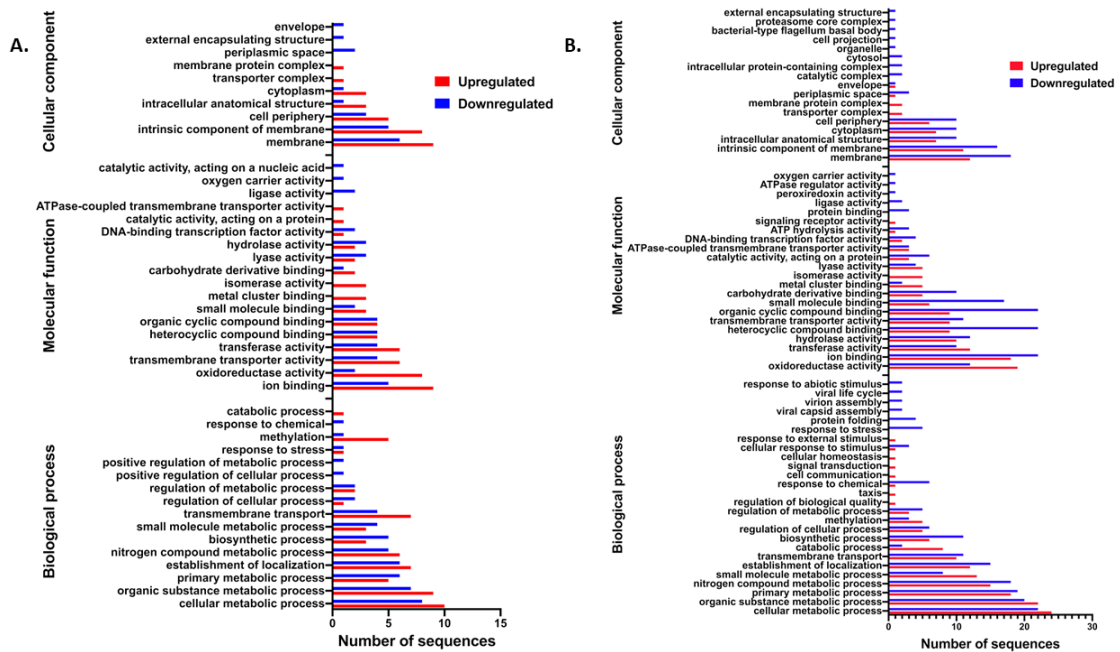


Figure 3.4 Gene ontology classification of 2-79 DEGs in (A) water-replete and (B) water-stressed root exudates compared to control conditions.

The GO terms were derived from 50 different functional groups (GO subcategory level 3).

Another functional category of pathways perturbed by root exudates included diverse small noncoding RNAs. We observed high levels of expression of transfer-messenger RNA (tmRNA) that function in the recycling of stalled ribosomes.⁵⁰ The expression of *phrS* and P27 small RNAs suggests that exposure to root exudates may affect the quorum sensing signaling of 2-79,^{51,52} while the expression of Hfq-associated sRNAs *crcZ*, P30 and P26 points at the involvement of catabolite repression.^{46,52-54} We also observed high levels of expression in 150 unannotated intergenic regions, which may indicate the presence of new sRNA genes or riboswitches. To the best of our knowledge,

this work is the first study that has examined the effect of root exudates on the expression of small noncoding RNAs in rhizosphere species of *Pseudomonas*.

Rhizobacteria cope with the detrimental effects of water stress by secreting hydrating biofilms matrices and accumulating osmoprotectants, a group of neutrally charged small molecules that balance osmotic pressure and stabilize cellular components.²⁵ Fluorescent pseudomonads use a range of such osmoprotectants, including N-acetyl-glutaminyglutamine amide (NAGGN), trehalose, glutamate, mannitol and quaternary ammonium compounds (QACs).⁵⁵⁻⁵⁹ Under water replete conditions, *Pseudomonas* spp. catabolize the QACs like choline, glycine betaine (GB), sarcosine and carnitine as C and N sources. In contrast, under water stress, they convert choline to glycine betaine (GB), which is then accumulated for osmoprotection. Curiously, pseudomonads lack the ability to synthesize QACs *de novo* but have evolved an extensive array of transporters and enzymes for the uptake and metabolism of these compounds.⁵⁶ This paradox is explained by the widespread presence of GB and its precursor, choline, in animals and plants that serve as host organisms for many *Pseudomonas* spp.^{60,61} In pseudomonads, the physiological importance of QACs was studied in the opportunistic human pathogens *P. aeruginosa* and foliar plant pathogen *P. syringae*,^{56,57} but their role in rhizosphere settings remains poorly understood.

The results of our study revealed that water stress significantly alters the composition of root exudates and that stressed plants secrete elevated amounts of QACs. In agreement with these changes, 2-79 responds to water-stressed exudates by upregulating key QAC catabolism genes that encode glycine betaine demethylase, dimethylglycine demethylase and sarcosine oxidase (Figure 3.5). These changes in the

expression of *gbcA*, *dgcA* and *soxB* were confirmed by the RT-qPCR analysis of 2-79 grown in the presence of exudates of water-replete and water-stressed plants.

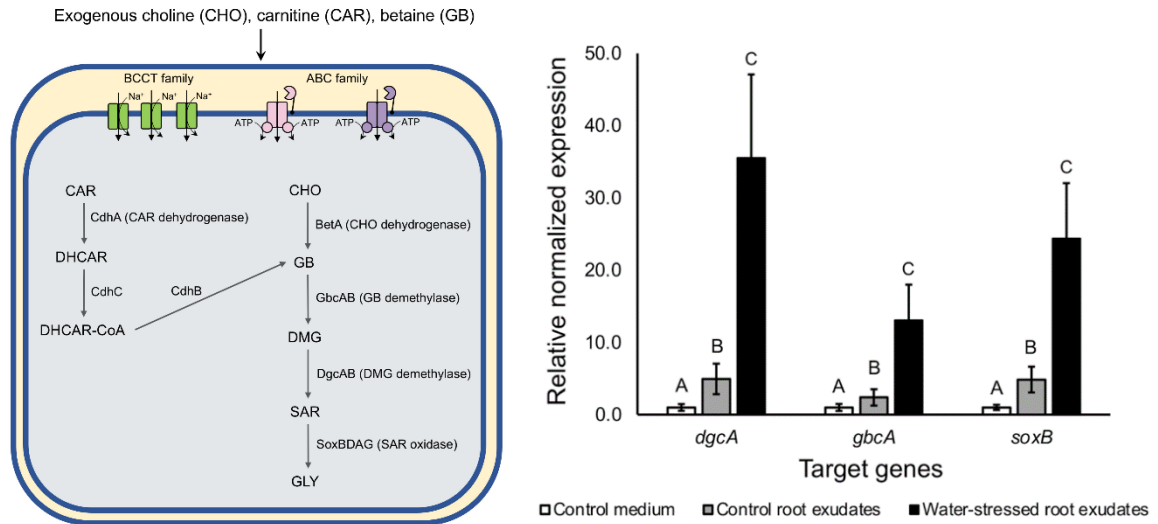


Figure 3.5 The summary of *P. synxantha* 2-79 genes predicted to function in the uptake and catabolism of QACs (left), and relative expression of key QAC catabolism genes in response to culture medium, water replete and water-stressed root exudates as analyzed by RT-qPCR (right).

DHCAR; 3-dehydro carnitine, DHCAR-CoA, 3-dehydrocarnitine-CoA; DMG, dimethylglycine; SAR, sarcosine; GLY, glycine. Bars with different letters denote significant differences in gene expression as analyzed by ANOVA followed by Tukey-Kramer's HSD test (P<0.05).

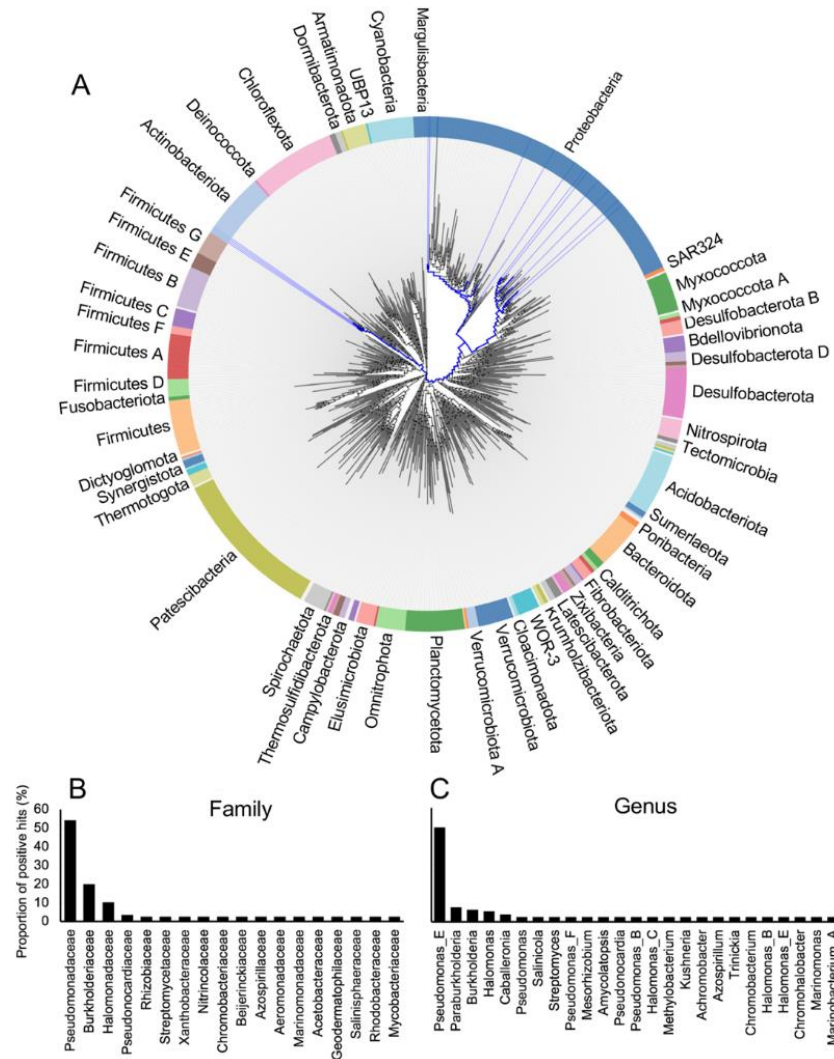


Figure 3.6 The distribution of QAC catabolism pathways across different bacterial phyla (A) and the proportion of bacterial families (B) and genera (C) carrying *betAB*, *gbcAB*, *dgcAB*, and *soxBDAG* genes.

The analysis was conducted in AnnoTree using the following cutoff parameters: % identity > 30, e-value < 0.00001, % subject alignment >70, and % query alignment >70.

Additional studies conducted by the Mavrodi lab demonstrated that 2-79 uses GB and choline as carbon sources and as osmoprotectants. In contrast, sarcosine serves only as a C source, while carnitine is not catabolized but provides protection from water stress (data not shown). Importantly, a 2-79 mutant devoid of all QAC transporter genes was less competitive in the rhizosphere colonization than the wild-type strain. Collectively,

these results suggest a mechanism through which roots of dryland wheat grown in the arid parts of the Inland Pacific Northwest recruit and support high populations of 2-79-like pseudomonads, which in exchange protect their host plants from soilborne fungal pathogens by producing phenazine-1-carboxylic acid. Interestingly, the comparison of sequenced bacterial genomes revealed that the QAC catabolizing genes are not limited to pseudomonads and also present in other Gammaproteobacteria (*Halomonas*), Betaproteobacteria (*Burkholderia*), and even Actinobacteria (*Streptomyces*) (Figure 3.6). The ubiquitous presence of these pathways suggests that the ability to take up and metabolize plant-derived QACs is a microbial trait vital for the adaptation to soil- and plant-associated habitats.

3.5 References

1. FAO. *Carbon Sequestration in Dryland Soils*. Vol 35.; 2004.
2. Hoover DL, Bestelmeyer B, Grimm NB, et al. Traversing the wasteland: A framework for assessing ecological threats to drylands. *Bioscience*. 2020;70(1):35-47. doi:10.1093/biosci/biz126
3. Reynolds JF, Stafford Smith DM, Lambin EF, et al. Ecology: Global desertification: Building a science for dryland development. *Science*. 2007;316(5826):847-851. doi:10.1126/science.1131634
4. Rodriguez D, de Voil P, Power B. Modelling dryland agricultural systems. In: *Innovations in Dryland Agriculture*.2017:239-256. doi:10.1007/978-3-319-47928-6_9
5. Vos R, Bellù LG. Global trends and challenges to food and agriculture into the 21st century. *Sustain Food Agric*. 2019:11-30. doi:10.1016/b978-0-12-812134-

4.00002-9

6. Rivero RM, Mittler R, Blumwald E, Zandalinas SI. Developing climate-resilient crops: improving plant tolerance to stress combination. *Plant J.* 2022;109(2):373-389. doi:10.1111/tpj.15483
7. D'Hondt K, Kostic T, McDowell R, et al. Microbiome innovations for a sustainable future. *Nat Microbiol.* 2021;6(2):138-142. doi:10.1038/s41564-020-00857-w
8. Gupta A, Rico-Medina A, Caño-Delgado AI. The physiology of plant responses to drought. *Science.* 2020;368(6488):266-269. doi:10.1126/science.aaz7614
9. Rubin RL, van Groenigen KJ, Hungate BA. Plant growth promoting rhizobacteria are more effective under drought: a meta-analysis. *Plant Soil.* 2017;416(1-2):309-323. doi:10.1007/s11104-017-3199-8
10. Shah A, Nazari M, Antar M, et al. PGPR in agriculture: A sustainable approach to increasing climate change resilience. *Front Sustain Food Syst.* 2021;5. doi:10.3389/fsufs.2021.667546
11. Naylor D, Coleman-Derr D. Drought stress and root-associated bacterial communities. *Front Plant Sci.* 2018;8:2223. doi:10.3389/fpls.2017.02223
12. Naylor D, Degraaf S, Purdom E, Coleman-Derr D. Drought and host selection influence bacterial community dynamics in the grass root microbiome. *ISME J.* 2017;11(12):2691-2704. doi:10.1038/ismej.2017.118
13. Santos-Medellín C, Edwards J, Liechty Z, Nguyen B, Sundaresan V. Drought stress results in a compartment-specific restructuring of the rice root-associated microbiomes. *mBio.* 2017;8(4):e00764-17. doi:10.1128/mBio.00764-17

14. Lau JA, Lennon JT. Rapid responses of soil microorganisms improve plant fitness in novel environments. *Proc Natl Acad Sci U S A*. 2012;109(35):14058-14062. doi:10.1073/pnas.1202319109
15. Jochum MD, McWilliams KL, Pierson EA, Jo YK. Host-mediated microbiome engineering (HMME) of drought tolerance in the wheat rhizosphere. *PLoS One*. 2019;14(12):e0225933. doi:10.1371/journal.pone.0225933
16. Sasse J, Martinoia E, Northen T. Feed your friends: Do plant exudates shape the root microbiome? *Trends Plant Sci*. 2018;23(1):25-41. doi:10.1016/j.tplants.2017.09.003
17. Mavrodi DV., Mavrodi OV., Parejko JA, et al. Accumulation of the antibiotic phenazine-1-carboxylic acid in the rhizosphere of dryland cereals. *Appl Environ Microbiol*. 2012;78(3):804-812. doi:10.1128/AEM.06784-11
18. Dar D, Thomashow LS, Weller DM, Newman DK. Global landscape of phenazine biosynthesis and biodegradation reveals species-specific colonization patterns in agricultural soils and crop microbiomes. *Elife*. 2020;9:e59726. doi:10.7554/ELIFE.59726
19. Parejko JA, Mavrodi DV., Mavrodi OV., Weller DM, Thomashow LS. Population structure and diversity of phenazine-1-carboxylic acid producing fluorescent *Pseudomonas* spp. from dryland cereal fields of central Washington state (USA). *Microb Ecol*. 2012;64(1):226-241. doi:10.1007/s00248-012-0015-0
20. Jaaffar AKM, Parejko JA, Paulitz TC, Weller DM, Thomashow LS. Sensitivity of *Rhizoctonia* isolates to phenazine-1-carboxylic acid and biological control by phenazine-producing *Pseudomonas* spp. *Phytopathology*. 2017;107(6):692-703.

doi:10.1094/PHYTO-07-16-0257-R

21. Mavrodi OV., Mavrodi DV., Parejko JA, Thomashow LS, Weller DM. Irrigation differentially impacts populations of indigenous antibiotic-producing *Pseudomonas* spp. In the rhizosphere of wheat. *Appl Environ Microbiol.* 2012;78(9):3214-3220. doi:10.1128/AEM.07968-11
22. Mavrodi DV., Mavrodi OV., Elbourne LDH, et al. Long-term irrigation affects the dynamics and activity of the wheat rhizosphere microbiome. *Front Plant Sci.* 2018;9:345. doi:10.3389/fpls.2018.00345
23. Yancey PH, Clark ME, Hand SC, Bowlus RD, Somero GN. Living with water stress: Evolution of osmolyte systems. *Science.* 1982;217(4566):1214-1222. doi:10.1126/science.7112124
24. Empadinhas N, Da Costa MS. Osmoadaptation mechanisms in prokaryotes: Distribution of compatible solutes. *Int Microbiol.* 2008;11(3):151-161. doi:10.2436/20.1501.01.55
25. Miller KJ, Wood JM. Osmoadaptation by rhizosphere bacteria. *Annu Rev Microbiol.* 1996;50:101-136. doi:10.1146/annurev.micro.50.1.101
26. Chen C, Beattie GA. Characterization of the osmoprotectant transporter OpuC from *Pseudomonas syringae* and demonstration that cystathionine-beta-synthase domains are required for its osmoregulatory function. *J Bacteriol.* 2007;189(19):6901-6912. doi:10.1128/JB.00763-07
27. Chen C, Li S, McKeever DR, Beattie GA. The widespread plant-colonizing bacterial species *Pseudomonas syringae* detects and exploits an extracellular pool of choline in hosts. *Plant J.* 2013;75(6):891-902. doi:10.1111/tpj.12262

28. Hoffmann T, Bremer E. Protection of *Bacillus subtilis* against cold stress via compatible-solute acquisition. *J Bacteriol.* 2011;193(7):1552-1562.
doi:10.1128/JB.01319-10
29. Mavrodi OV., McWilliams JR, Peter JO, et al. Root exudates alter the expression of diverse metabolic, transport, regulatory, and stress response genes in rhizosphere *Pseudomonas*. *Front Microbiol.* 2021;12:651282.
doi:10.3389/fmicb.2021.651282
30. Green, R M, Sambrook J. Molecular cloning: A laboratory manual, 4th edition. *Cold Spring Harb Lab Press.* 2012;33(1).
31. King EO, Ward MK, Raney DE. Two simple media for the demonstration of pyocyanin and fluorescein. *J Lab Clin Med.* 1954;44(2):301-307.
32. Halverson LJ, Firestone MK. Differential effects of permeating and nonpermeating solutes on the fatty acid composition of *Pseudomonas putida*. *Appl Environ Microbiol.* 2000;66(6):2414-2421. doi:10.1128/AEM.66.6.2414-2421.2000
33. Smibert R, Krieg N. Phenotypic characterization. In: Gerhard P, Murray RG, Wood WA and Krieg NR, eds., *Methods for General and Molecular Bacteriology*, American Society of Microbiology:611-654.
34. Lindsey 3rd BE, Rivero L, Calhoun CS, Grotewold E, Brkljacic J. Standardized method for high-throughput sterilization of *Arabidopsis* seeds. *J Vis Exp.* 2017;(128):56587. doi:10.3791/56587
35. Arkin AP, Cottingham RW, Henry CS, et al. KBase: The United States Department of Energy Systems Biology Knowledgebase. *Nat Biotechnol.*

- 2018;36(7):566-569. doi:10.1038/nbt.4163
36. Kim D, Paggi JM, Park C, Bennett C, Salzberg SL. Graph-based genome alignment and genotyping with HISAT2 and HISAT-genotype. *Nat Biotechnol.* 2019;37(8):907-915. doi:10.1038/s41587-019-0201-4
 37. Pertea M, Pertea GM, Antonescu CM, Chang T-C, Mendell JT, Salzberg SL. StringTie enables improved reconstruction of a transcriptome from RNA-seq reads. *Nat Biotechnol.* 2015;33(3):290-295. doi:10.1038/nbt.3122
 38. Love MI, Huber W, Anders S. Moderated estimation of fold change and dispersion for RNA-seq data with DESeq2. *Genome Biol.* 2014;15(12):550. doi:10.1186/s13059-014-0550-8
 39. Götz S, García-Gómez JM, Terol J, et al. High-throughput functional annotation and data mining with the Blast2GO suite. *Nucleic Acids Res.* 2008;36(10):3420-3435. doi:10.1093/nar/gkn176
 40. Langmead B, Salzberg SL. Fast gapped-read alignment with Bowtie 2. *Nat Methods.* 2012;9(4):357-359. doi:10.1038/nmeth.1923
 41. Li H, Handsaker B, Wysoker A, et al. The sequence alignment/map format and SAMtools. *Bioinformatics.* 2009;25(16):2078-2079. doi:10.1093/bioinformatics/btp352
 42. Quinlan AR, Hall IM. BEDTools: a flexible suite of utilities for comparing genomic features. *Bioinformatics.* 2010;26(6):841-842. doi:10.1093/bioinformatics/btq033
 43. Thorvaldsdóttir H, Robinson JT, Mesirov JP. Integrative Genomics Viewer (IGV): high-performance genomics data visualization and exploration. *Brief*

- Bioinform.* 2013;14(2):178-192. doi:10.1093/bib/bbs017
44. Gómez-Lozano M, Marvig RL, Molin S, Long KS. Genome-wide identification of novel small RNAs in *Pseudomonas aeruginosa*. *Environ Microbiol.* 2012;14(8):2006-2016. doi:10.1111/j.1462-2920.2012.02759.x
 45. Gómez-Lozano M, Marvig RL, Molina-Santiago C, Tribelli PM, Ramos JL, Molin S. Diversity of small RNAs expressed in *Pseudomonas* species. *Environ Microbiol Rep.* 2015;7(2):227-236. doi:10.1111/1758-2229.12233
 46. Sonnleitner E, Abdou L, Haas D. Small RNA as global regulator of carbon catabolite repression in *Pseudomonas aeruginosa*. *Proc Natl Acad Sci U S A.* 2009;106(51):21866-21871. doi:10.1073/pnas.pnas.0910308106
 47. Mendler K, Chen H, Parks DH, Lobb B, Hug LA, Doxey AC. AnnoTree: visualization and exploration of a functionally annotated microbial tree of life. *Nucleic Acids Res.* 2019;47(9):4442-4448. doi:10.1093/nar/gkz246
 48. Berendsen RL, Pieterse CMJ, Bakker PAHM. The rhizosphere microbiome and plant health. *Trends Plant Sci.* 2012;17(8):478-486. doi:10.1016/j.tplants.2012.04.001
 49. Otero-Asman JR, Wettstadt S, Bernal P, Llamas MA. Diversity of extracytoplasmic function sigma (σ ECF) factor-dependent signaling in *Pseudomonas*. *Mol Microbiol.* 2019;112(2):356-373. doi:10.1111/mmi.14331
 50. Wu S. Characterization of tmRNA function and regulation in *Pseudomonas aeruginosa*. [Doctoral dissertation]. Auburn, AL: Auburn University; 2013.
 51. Chen R, Wei X, Li Z, et al. Identification of a small RNA that directly controls the translation of the quorum sensing signal synthase gene *rhlI* in *Pseudomonas*

- aeruginosa. *Environ Microbiol.* 2019;21(8):2933-2947. doi:10.1111/1462-2920.14686
52. Sonnleitner E, Gonzalez N, Sorger-Domenigg T, et al. The small RNA PhrS stimulates synthesis of the *Pseudomonas aeruginosa* quinolone signal. *Mol Microbiol.* 2011;80(4):868-885. doi:https://doi.org/10.1111/j.1365-2958.2011.07620.x
53. Chihara K, Bischler T, Barquist L, et al. Conditional Hfq association with small noncoding RNAs in *Pseudomonas aeruginosa* revealed through comparative UV cross-linking immunoprecipitation followed by high-throughput sequencing. *mSystems.* 2019;4(6):e00590-19. doi:10.1128/mSystems.00590-19
54. Pusic P, Tata M, Wolfinger MT, Sonnleitner E, Häussler S, Bläsi U. Cross-regulation by CrcZ RNA controls anoxic biofilm formation in *Pseudomonas aeruginosa*. *Sci Rep.* 2016;6(1):39621. doi:10.1038/srep39621
55. Galvão TC, De Lorenzo V, Cánovas D. Uncoupling of choline-O-sulphate utilization from osmoprotection in *Pseudomonas putida*. *Mol Microbiol.* 2006;62(6):1643-1654. doi:10.1111/j.1365-2958.2006.05488.x
56. Wargo MJ. Homeostasis and catabolism of choline and glycine betaine: Lessons from *Pseudomonas aeruginosa*. *Appl Environ Microbiol.* 2013;79(7):2112-2120. doi:10.1128/AEM.03565-12
57. Chen C, Beattie GA. *Pseudomonas syringae* BetT is a low-affinity choline transporter that is responsible for superior osmoprotection by choline over glycine betaine. *J Bacteriol.* 2008;190(8):2717-2725. doi:10.1128/JB.01585-07
58. Freeman BC, Chen C, Yu X, Nielsen L, Peterson K, Beattie GA. Physiological

- and transcriptional responses to osmotic stress of two *Pseudomonas syringae* strains that differ in epiphytic fitness and osmotolerance. *J Bacteriol.* 2013;195(20):4742-4752. doi:10.1128/JB.00787-13
59. Kurz M, Buren AY, Seip B, Lindow SE, Gross H. Genome-driven investigation of compatible solute biosynthesis pathways of *pseudomonas syringae* pv. *syringae* and their contribution to water stress tolerance. *Appl Environ Microbiol.* 2010;76(16):5452-5462. doi:10.1128/AEM.00686-10
60. McNeil SD, Nuccio ML, Hanson AD. Betaines and related osmoprotectants. Targets for metabolic engineering of stress resistance. *Plant Physiol.* 1999;120(4):945-950. doi:10.1104/pp.120.4.945
61. Storey R, Wyn Jones RG. Betaine and choline levels in plants and their relationship to NaCl stress. *Plant Sci Lett.* 1975;4(3):161-168. doi:10.1016/0304-4211(75)90090-5

CHAPTER IV- GENES INVOLVED IN THE REGULATION OF BIOSYNTHESIS
AND RESISTANCE TO REDOX-ACTIVE PHENAZINES IN THE MODEL SOIL
BACTERIUM BURKHOLDERIA LATA 383

4.1 Abstract

Burkholderia are Gram-negative bacteria that include saprophytes, nitrogen-fixers, and species associated with nosocomial infections. Our recent studies demonstrated that multiple species in the *B. cepacia*, *B. pseudomallei*, and *B. glumae/B. gladioli* clades carry genes for the synthesis of phenazines. Phenazines are colored, structurally diverse, microbial secondary compounds with a common nitrogen-containing tricyclic core. They act as molecular signals and extracellular electron shuttles that contribute to the competitiveness of the producer organisms in their natural habitats. They also undergo redox cycling to generate reactive oxygen species that suppress other organisms. The study of phenazines has mostly been confined to the model opportunistic pathogen *Pseudomonas aeruginosa* and many aspects of phenazine biology in other groups of bacteria remain poorly understood. In this study, we identified genes involved in the production, regulation, and resistance to phenazines in *B. lata* 383, a member of the *B. cepacia* complex. We subjected this strain to a transposon mutagenesis screen and characterized transcriptomes of phenazine and quorum sensing (QS) mutants of strain 383. Our results indicate that QS regulates phenazine production in *Burkholderia* and that this cell-cell communication also controls a number of other phenotypic traits in these bacteria. Finally, we analyzed transcriptome responses to phenazine methosulfate in *B. lata* 383 and two closely related phenazine-non-producing *Burkholderia* strains. Our result revealed that *Burkholderia* spp. cope with phenazine toxicity by upregulating

pathways involved in oxidative stress response, iron-sulfur cluster biogenesis and multidrug efflux.

4.2 Introduction

The plant rhizosphere is a carbon-rich niche and home to diverse microorganisms that interact with the plant host and among themselves. These interactions can be antagonistic, cooperative, or neutral.¹ These mechanisms play a major role in shaping the rhizosphere microbiome. Microbes compete among themselves mainly for nutrients and, in the process, produce different types of secondary metabolites, including numerous antimicrobial compounds.² These naturally-occurring antimicrobials are chemically diverse and range from broad-spectrum antibiotics to ribosomally synthesized substances known as bacteriocins,^{3,4} that specifically target a particular group of competitor microbes. The antimicrobial compounds also include numerous redox-active metabolites (RAMs) that promote multiple benefits in the producer, such as acquiring nutrients, controlling redox homeostasis, and supporting survival in anoxic conditions.^{5,6} These molecules are often toxic as they react with oxygen and lead to the formation of reactive oxygen species, thus putting selective pressure on surrounding microbes.^{7,8} RAMs can promote both resistance and tolerance in the producer microorganism,^{5,9} but in many cases, the molecular mechanisms involved in the secretion of these molecules and the resistance machinery of the producer organism remain unclear.

Microbial phenazines encompass a family of colored RAMs with a common nitrogen-containing tricyclic ring structure. Many phenazines were discovered in the 1950s and were originally described as microbial pigments.^{10,11} However, later studies revealed that phenazines contribute to the virulence and competitiveness of

microorganisms by acting as toxins, antibiotics, and antifungal agents.^{12,13} They act as extracellular electron shuttles and promote nutrient acquisition, biofilm formation, and survival in hypoxic conditions. The phenazine tricyclic is synthesized from chorismic acid by a set of conserved “core” enzymes encoded by the *phzA/BCDEFG* operon.¹⁴ The end product of the “core” pathway is phenazine-1-carboxylic acid (PCA) or phenazine-1,6-dicarboxylic acid (PDC), which in many bacteria converted to species-specific phenazine metabolites through the action of auxiliary modifying enzymes.¹⁵ Although the phenazine enzymology is well understood, our knowledge of the regulation of biosynthesis is limited to *Pseudomonas* spp. where the *phz* genes are governed by a complex interplay between quorum sensing, nutrient levels and environmental conditions.



Figure 4.1 Pigmentation associated with the synthesis of 4,9-dihydrophenazine-1,6-dicarboxylic acid dimethylester (left) and color gradient (right) observed in standing cultures of *B. lata* 383, presumably due to reduction of phenazines.

A recent study in our lab revealed the widespread presence of phenazine biosynthesis genes in different clades of *Burkholderia* spp., including strains of *B. cepacia*, *B. pseudomallei*, and *B. glumae/B. gladioli* clades.¹⁶ We further demonstrated the importance of phenazine production for the formation of *Burkholderia* biofilms. *Burkholderia*, like their *Pseudomonas* counterparts, encompass a large and diverse group of saprophytes, economically important pathogens, and plant commensals.¹⁷ However, in contrast to the model opportunistic human pathogen *Pseudomonas aeruginosa*, our

understanding of the biological function of phenazines in *Burkholderia* and the regulation of their biosynthesis and resistance remains limited.

We have addressed this gap in knowledge by focusing on the regulatory and resistance aspects of phenazine synthesis in *B. lata* 383, a soil isolate that belongs to the taxon K group of the *Burkholderia cepacia* (Bcc) species complex. This group, besides *B. lata*, includes strains of *Burkholderia contaminans*.¹⁸ Both species have been isolated from numerous environmental sources (including plant tissues and rhizosphere) and clinical samples associated with opportunistic infections in humans.^{19,20} Among strains of the taxon K group, nosocomial infections are linked primarily to the emerging cystic fibrosis pathogen *B. contaminans*. However, there also have been reports of healthcare-associated outbreaks connected with *B. lata*.²¹ Hence, it is imperative that the role of phenazines in the ecological fitness of this economically important bacteria is deciphered. Based on the biological activity and diverse functions of microbial phenazines, we hypothesized that *Burkholderia* carry an extensive set of genes involved in the regulation of biosynthesis and efflux of these redox-active metabolites. To test this hypothesis, we performed a transposon mutagenesis screen and comparative transcriptomic profiling of *B. lata* 383, its isogenic mutants and closely related phenazine-nonproducing *Burkholderia* strains.

4.3 Materials and Methods

4.3.1 Microorganisms and culture conditions

Burkholderia lata 383, *B. cepacia* ATCC 25416, and *B. cenocepacia* K56-2 were routinely cultured at 30°C in Luria-Bertani (LB) medium²² or King's medium B (KMB).²³ *Escherichia coli* was grown at 37°C in the LB medium. Antibiotic supplements

were used at the following concentrations: trimethoprim, 50 or 100 $\mu\text{g mL}^{-1}$; chloramphenicol, 35 or 180 $\mu\text{g mL}^{-1}$; polymyxin B, 15 $\mu\text{g mL}^{-1}$; and kanamycin, 50 $\mu\text{g mL}^{-1}$. All strains were maintained as frozen glycerol stocks at -80°C .

4.3.2 Transposon mutagenesis of *B. lata* 383

The *B. lata* 383 genome was subjected to random mutagenesis with the pTnMod-OTp' plasposon.²⁴ The plasposon was introduced into the strain using triparental mating between the *B. lata* 383 recipient, *E. coli* JM109/pTnMod-OTp' donor, and *E. coli* HB101/pRK2013 helper strains.²⁵ The donor and helper strains were grown overnight at 37°C on LB agar amended with trimethoprim and kanamycin respectively. The recipient *B. lata* strain was grown on LB plates at 30°C . The bacterial cells were scraped, adjusted in LB to 10^7 CFU mL^{-1} , and grown to the mid-exponential phase ($\text{OD}_{600}\sim 0.4-0.6$), after which 3 mL of each culture was harvested by centrifugation at 1,400 rpm for 10 min. The cell pellets were then washed and resuspended in 0.5 mL (*E. coli*) or 1.5 mL (*B. lata*) of LB supplemented with 10 mM MgSO_4 . Equal volumes of each cell suspension were combined, and 100 μL of the mixture was spot-plated on LB- MgSO_4 agar. The mating was performed at 30°C for 24 h, after which the biomass was scraped off and suspended in 1 mL LB broth and plated on LB agar amended with 100 $\mu\text{g mL}^{-1}$ of trimethoprim and 15 $\mu\text{g mL}^{-1}$ of polymyxin B (to kill the *E. coli* donor and helper cells). Appropriate negative controls on this selection plate were made on the day of mating to account for the effectiveness of the antibiotic selection. The plates were incubated at 30°C for 40 h.

Individual trimethoprim-resistant colonies were picked using sterile 10 μL pipette tips and inoculated into 96-well microtiter plates (LightLabs, USA) containing 100 μL KMB broth in each well. Wells inoculated with the wild-type *B. lata* 383 and its isogenic

phenazine-deficient *phzA* mutant¹⁶ served as positive and negative controls. The inoculated microplates were incubated at 30°C for 72 h and screened for the loss of pigmentation associated with phenazine production. The non-pigmented clones were inoculated in test tubes with KMB broth, and the loss of pigmentation was verified after incubation with shaking at 30°C for 24 h. The confirmed mutants and all microtiter plates generated in the transposon screen were stored at -80°C after adding glycerol.

4.3.3 Mapping of transposon insertion sites in pigment-deficient mutants

Mapping of the transposon insertion sites was conducted using the arbitrarily primed PCR approach of Manoil.²⁶ Briefly, DNA from pigment-deficient mutants was first amplified by PCR with the transposon-specific forward primer TnMod_Primer1 (5'-AGGCTCAGTGCAAATTTATCC-3') and the degenerate reverse primer TnMod_Primer2b (5'-GGCCACGCGTCGACTAGTACNNNNNNNNNNACGCC-3'). The amplified fragments were subjected to a second round of PCR with primers TnMod_Primer3 (5'-TTGAACGTGTGGCCTAAGCGAGC-3') and TnMod_Primer4 (5'-GGCCACGCGTCGACTAGTAC-3'). The amplicons were purified using a GeneJet PCR Purification kit (Thermo Fisher) and the transposon insertion junctions were sequenced using the TnMod_Primer3 at Eurofins Genomics, USA. The sequences were mapped to the *B. lata* 383 genome using the DIAMOND blast server at the Burkholderia Genome Database.²⁷

4.3.4 Comparison of phenazine gene expression in pigment-deficient mutants

The effect of transposon insertions in non-pigmented mutants on the expression of phenazine biosynthesis genes was evaluated by qPCR. Briefly, the strains were inoculated in KMB at 10⁷ CFU mL⁻¹ and grown with 220 rpm shaking at 30°C until the

onset of visible purple pigmentation in the wild-type control (~20-22 h). Approximately 5×10^8 cells were harvested, and RNA was extracted with the RNeasy Mini Kit (QIAGEN). The RNA was treated with Turbo DNase (Thermo Fisher) and cleaned using the Zymo Clean and Concentrator Kit (Zymo). The purified RNA was then used in qRT-PCR with *phzE*-specific primers phzE-F (5'-CGCGGCTTCAAGACACACG-3'), phzE-R (5'-AGCGCGGTATCGGCATCA-3') and the phzE-P probe (5'-FAM-TGCGACGAGCACGAAACGGT-BHQ1-3'). The amplifications were performed with the TaqPath 1-Step RT-qPCR Master Mix (Thermo Fisher), and fold changes were calculated by the $2^{-\Delta\Delta ct}$ method using the CFX Maestro software (Bio-Rad). Samples untreated with reverse transcriptase served as a control for the absence of contaminating genomic DNA. RNA samples extracted from wild-type *B. lata* 383 and its *phzA* mutant served as controls.

4.3.5 Construction of *B. lata* isogenic mutants and complementation

Genome regions flanking the *cepI* gene were amplified using the following primer sets: cepI1 (5'-CAGGGTTTTCCAGTCACGACCCGCGCATGACTTCACCTT-3'), cepI2 (5'-CGACGCAGATGTTACTCACTTACCAACCAAGCTGCTCGACG-3'), cepI3 (5'-TAAGTGAGT AACATCTGCGTCGACGTTTGCCGCACTAGGAAT-3') and cepI4 (5'-GGATAACAATTTACACAG GAGAATCCGGCGGTAGGGCTC-3'). The PCR was performed with Q5 High Fidelity DNA polymerase (New England Biolabs, USA) and the amplicons were purified using the GeneJet PCR purification kit (Thermo Fisher). The amplicons were cloned into a linearized gene replacement vector pDONRpEx18Tp-sceI-*pheS*²⁸ using the 2X HiFi DNA Assembly Master Mix (New England Biolabs). This vector harbors a mutated *pheS* gene which kills the wild-type *B. lata* in the presence of

0.1% p-chlorophenylalanine. Single crossover mutants were patched on M9 medium²⁹ amended with 20 mM glucose and incubated for 2 days at 30°C. These clones were then transferred on M9-glucose and 0.1% p-chlorophenylalanine to select the double crossover mutants. The selected mutants were further confirmed for the loss of trimethoprim resistance due to vector backbone loss by growing them on parallelly on LB with and without trimethoprim. These confirmed mutants were checked by PCR for the desired deletions using primers *cepI1* and Stop (5'-CGACGCAGATGTTACTCACTTA-3') as well as for the absence of the plasmid genes with primers *dhfr_F* (5'-TAATATTGAAAAGGAAGAGTATGGGTCAAAGTAGCGATGAAGC-3') and *dhfr_R* (5'-AACTTGGTCTGACAGTTAGGCCACACGTTCAAGTGC-3').

To complement the isogenic mutant, the full-length *cepI* was amplified with primer sets *cepIup* (5'-GGATAACAATTTACACAGGAAAAGCACAGATCCGAGGACAC-3') and *cepIlow* (5'-CAGGGTTTTCCCAGTCACGACCGGTTCAGCGGCGATGGC-3'). The amplification was performed with Q5 High Fidelity DNA polymerase (New England Biolabs), and the purified amplicon was cloned into a linearized pBBR1MCS plasmid vector using the 2X HiFi DNA Assembly Master Mix (New England Biolabs). The plasmid was purified and, after confirmation of its integrity, electroporated into the *B. lata cepI* mutant. Briefly, the overnight culture of the mutant was washed and reconstituted using cold 10% glycerol. Eighty microliters of cells were mixed with 100 ng of plasmid and electroporated in a 2-mm gap cuvette at 1.8 kV pulse voltage, resistance 600 Ohms and capacitance 10 µF. After electroporation, cells were revived by growing for 2 h in LB medium. The plasmid-bearing complemented mutants will be selected and maintained on LB amended with chloramphenicol. A mutant

complemented with an empty vector was also created in a similar manner to serve as a control in downstream experiments.

4.3.6 Phenotypic assays

The effect of quorum sensing on phenazine pigmentation was assessed by growing the wild-type *B. lata* 383 strain, its quorum sensing mutants, and their complements in KMB broth for 20-22 h with shaking at 220 rpm. The effects of quorum sensing on the overall fitness of the bacteria were studied using motility, biofilm, siderophore and exoprotease formation assays. For the exoproteases and siderophore formation assays, overnight cultures of the strains were adjusted to 10^8 CFU mL⁻¹. The adjusted cultures were spotted on Chrome Azurol S (CAS) agar³⁰ and skim milk agar³¹ to visualize, respectively, the production of siderophores and exoprotease. The plates were incubated at 30°C for 72 h after which the zone of the iron sequestration for the siderophore assay and milk protein degradation for the exoproteases assay were measured. For the motility assay, we looked at the swimming motility of the strains on M8 plates supplemented with 0.2% glucose, 0.5% casamino acid, 1mM MgSO₄, and 0.3% agar³². Sterile pipette tips were dipped in the overnight cultures of the strains, and stabbed into the center of the agar plates, making sure that they do not touch the base of the plates. The plates were incubated upright at 30°C for 36 h, after which the colony diameters were measured.

The formation of static biofilms was evaluated by staining surface-attached bacteria with crystal violet.³³ Briefly, overnight KMB cultures were adjusted to 10^8 CFU mL⁻¹ and 100-μL aliquots of the adjusted cultures were dispensed in a PVC microtiter plate (Corning Costar, Tewksbury, MA, USA). The plate was incubated at 30°C for 48 h,

after which the liquid was discarded, and the plate was washed to remove planktonic cells. The biofilms were stained with 125 μ L of 0.1% crystal violet solution for 30 min, after which the stain was discarded, and the plate was washed thoroughly. Finally, 125 μ L of 30% acetic acid was added to each well to dissolve the stain for 15 min. The solubilized stain was transferred to a new microtiter plate (CytoOne, USA) and quantified by measuring absorbance at 550 nm.

4.3.7 Transcriptomic responses of *B. lata* 383 mutants

Genome-wide gene expression patterns of wild-type *B. lata* 383, its isogenic phenazine biosynthesis (*phzA::Tp^r*) and quorum sensing (Δ *cepI*) mutant were compared. Three replicate cultures of each strain were grown in KMB broth till the wild-type cultures started the production of visible phenazine pigmentation. Approximately 5×10^8 cells were harvested and used for RNA extraction with the RNeasy Mini Kit (QIAGEN). The RNA was treated with DNase, concentrated with the Zymo Clean and Concentrator Kit (Zymo), checked for their integrity using the RNA 6000 Nano Kit (Agilent) and shipped for sequencing to Novogene (Sacramento, CA, USA). The RNA samples were ribodepleted with a Ribo-Zero Plus rRNA Depletion Kit (Illumina, San Diego, CA, USA) and stranded RNASeq libraries were prepared and sequenced in PE150 mode on a NovaSeq 6000 instrument (Illumina). The RNA-seq reads were imported in KBase,³⁴ and aligned with HISAT2 v.2.1.0³⁵ to the complete *B. lata* 383 genome (GenBank accession number GCA_000012945.1). Full-length transcripts were assembled with StringTie v.2.1.5,³⁶ and differential expression analysis will be carried out with DeSeq2 v.1.20.0.³⁷ Genes differentially expressed (i.e., absolute fold change >2 (\log_2 scale), FRD < 0.05) between the wild-type and the mutant strains were used for downstream analysis. The

functional categorization of differentially expressed genes and gene enrichment analyses were performed using Blast2GO annotations³⁸ in OmicsBox (BioBam Bioinformatics, Cambridge, MA, USA).

4.3.8 Effect of phenazine metabolites on *Burkholderia* transcriptome

To characterize the response of *Burkholderia* to external phenazines *B. lata* 383, *B. cepacia* ATCC 25416 and *B. cenocepacia* K56-2 were treated with phenazine methosulfate (PMS). The latter two strains are plant and animal pathogens respectively, that do not produce phenazines. The overnight broth cultures of the three strains grown at 30°C with 220 rpm shaking were adjusted to 5×10^7 CFU mL⁻¹ in 96-well microtiter plates and incubated at 30°C till mid exponential phase (OD₆₀₀~0.5-0.6). Half of the cultures were treated with 100 µM PMS dissolved in deionized water. The other half received an equal volume of deionized water and served as controls. All cultures were incubated at 30°C for another hour, after which the cells were harvested, and RNA was extracted using the RNeasy Mini Kit (QIAGEN). The RNA processing and transcript sequencing were performed essentially as described in 4.3.7. The RNA-seq reads were imported in KBase,³⁴ and correspondingly aligned with HISAT2 v.2.1.0³⁵ to the complete *B. lata* 383 genome (GenBank accession number GCA_000012945.1), *B. cepacia* ATCC 25416 genome (GenBank accession number GCA_003546465.1) and *B. cenocepacia* K56-2 genome (GenBank accession number GCA_000981305.1). Full-length transcripts were assembled with StringTie v.2.1.5,³⁶ and differential expression analysis will be carried out with DeSeq2 v.1.20.0.³⁷ Genes differentially expressed (i.e., absolute fold change >1.5 (log₂ scale), FRD < 0.05) between the control and the PMS-treated samples were used for downstream analysis. The functional categorization of differentially

expressed genes and gene enrichment analyses were performed using Blast2GO annotations³⁸ in OmicsBox (BioBam Bioinformatics). We validated the RNA-seq results with qRT-PCR with primers mexE-F (5'-CCGCGACCAGGATGCTTTG-3'), mexE-R (5'-TCGATGATCCGCTCGCCAT-3'), and probe mexE-P (5'-FAM-TCACCGACCAGGACCGCAAGT-BHQ1-3') that target the RND-9 efflux genes of *B. lata* 383.

4.4 Results and Discussion

4.4.1 Phenazine synthesis in *B. lata* 383 involves diverse regulatory and metabolic pathways

The transposon mutagenesis screen of ~15,000 mutants yielded 27 non-pigmented clones mapped to functionally diverse genes (Table 4.1). We recovered mutations in several genes of the shikimic acid pathway, such as shikimate kinase (*aroK*), shikimate-5-dehydrogenase (*aroE*) and 3-phosphoshikimate 1-carboxyvinyltransferase (EPSP synthase, *aroA*), which collectively convert phosphoenolpyruvate to the immediate phenazine precursor, chorismic acid.^{39,40} Mutations were found in *pcmI*, which encodes one a phenazine biosynthesis enzyme predicted to convert phenazine-1,6-dicarboxylic acid methylester to dimethyl 4,9-dihydroxy-1,6-phenazinedicarboxylic acid.¹⁶ We discovered several mutations in a LysR-type transcriptional regulator, which might regulate D-lactate dehydrogenase involved in pyruvate production,⁴¹ and a yet uncharacterized membrane kinase from a 2-component signal transduction system. We also recovered a mutation in a toluene ABC transporter ATP binding protein, which might function in the transport of thiamine pyrophosphate,⁴² which is an essential cofactor in pyruvate decarboxylation.⁴³ In *P. aeruginosa*, a putative toluene ABC

transporter was linked to the production of pyomelanin, a pigment that contribute to the persistence of the microbial community in cystic fibrosis and urinary tract infections.⁴⁴ Thus, it is evident that pyruvate production leads to the formation of chorismate, and the subsequent conversion of chorismate is the key phenazine biosynthesis pathway in *Burkholderia*.

Finally, we identified multiple transposon hits within the quorum sensing circuit comprised of the homoserine lactone synthase CepI and the LuxR-type transcriptional regulator CepR. We recovered mutations within *cepR* and a hypothetical gene in *cepI-cepR* intergenic region.⁴⁵ We also constructed an isogenic mutant by deleting the *cepI* gene that functions in the synthesis of diffusible N-octanoyl L-homoserine lactone (C8-AHL). This mutant was non-pigmented as well, and the pigmentation was restored after complementation with a pBBR1MCS plasmid carrying a functional copy of the *cepI* gene (Figure 4.2).

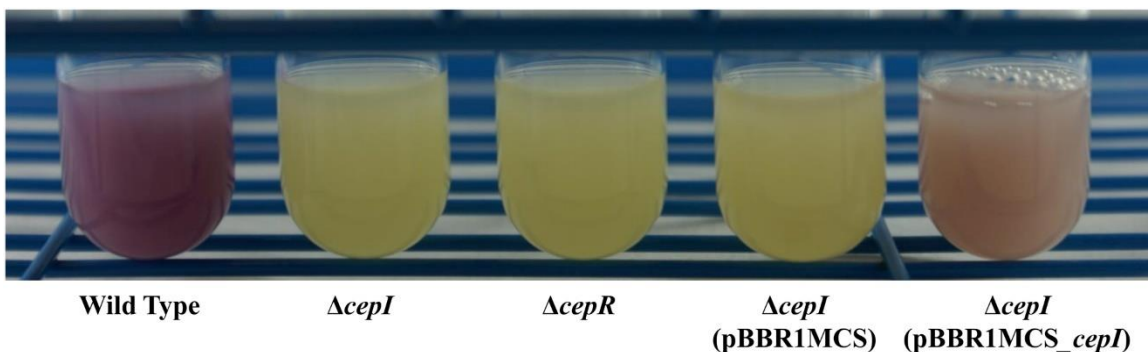


Figure 4.2 *The loss of phenazine pigmentation in ΔcepI and cepR::Tn5 quorum sensing mutants and its restoration in the ΔcepI strain complemented with a pBBR1MCS plasmid carrying functional cepI gene.*

Table 4.1 Summary of *B. lata* 383 genes with mutations associated with the loss of phenazine pigmentation.

Mutant	Locus Tag	Predicted function	Chromosome	Localization	Mutant type	Pathway
0D11	BCEP18194_RS26245	LysE type translocator (amino acid exporter protein)	2	Cytoplasmic membrane	Transposon	Amino acid transport
13F11	BCEP18194_RS07655	toluene ABC transporter ATP binding protein	1	Unknown	Transposon	Possible thiamine pyrophosphate synthesis
39E10	BCEP18194_RS02740	membrane protein (2- component sensor kinase)	3	Cytoplasmic membrane	Transposon	Signaling
9G11	BCEP18194_RS09260	NAD kinase	1	Cytoplasmic	Transposon	NAD metabolism

Table 4.1 (continued).

3G11	BCEP18194_RS10895	3-phosphoshikimate 1-carboxyvinyltransferase	1	Unknown	Transposon	Chorismate synthesis via shikimic acid pathway
10G11	BCEP18194_RS34555	glutathione S-transferase	2	Unknown	Transposon	Protein binding
$\Delta cepI$	BCEP18194_RS28040	acyl-homoserine-lactone synthase	2	Cytoplasmic	Allelic replacement	Quorum sensing
10E11	BCEP18194_RS28050	<i>cepR</i> (LuxR family transcriptional regulator)	2	Cytoplasmic	Transposon	Quorum sensing
64G6	BCEP18194_RS28300	3-phenylpropionate dioxygenase	2	Cytoplasmic	Transposon	Iron-sulfur cluster binding
27B12	BCEP18194_RS09670	LysR-type transcriptional regulator	1	Cytoplasmic	Transposon	Regulator of D-lactate dehydrogenase
10A8	BCEP18194_RS18045	triosephosphate isomerase	1	Cytoplasmic	Transposon	Glycolysis

Table 4.1 (continued).

126B3	BCEP18194_RS30615	phenazine biosynthesis <i>gene pcmI</i>	2	Unknown	Transposon	Phenazine synthesis
$\Delta phzA$	BCEP18194_RS30620	phenazine biosynthesis <i>gene phzA</i>	2	Cytoplasmic	Allelic replacement	Phenazine synthesis
139E3	BCEP18194_RS08585	shikimate 5- dehydrogenase AroE	1	Cytoplasmic	Transposon	Chorismate synthesis via shikimic acid pathway
58C4	BCEP18194_RS20340	1-acyl-sn-glycerol-3- phosphate acyltransferase	1	Cytoplasmic membrane	Transposon	Phosphatidic acid synthesis for membrane lipids

4.4.2 Phenazine gene expression in *Burkholderia* mutants

We measured phenazine gene expression in the *Burkholderia* mutants by RT-qPCR targeting the *phzE*, which encodes a core phenazine biosynthesis enzyme. Our results confirmed that in most transposon mutants, the loss of pigmentation was accompanied by a complete or markedly reduced transcription of the phenazine operon (Figure 4.3).

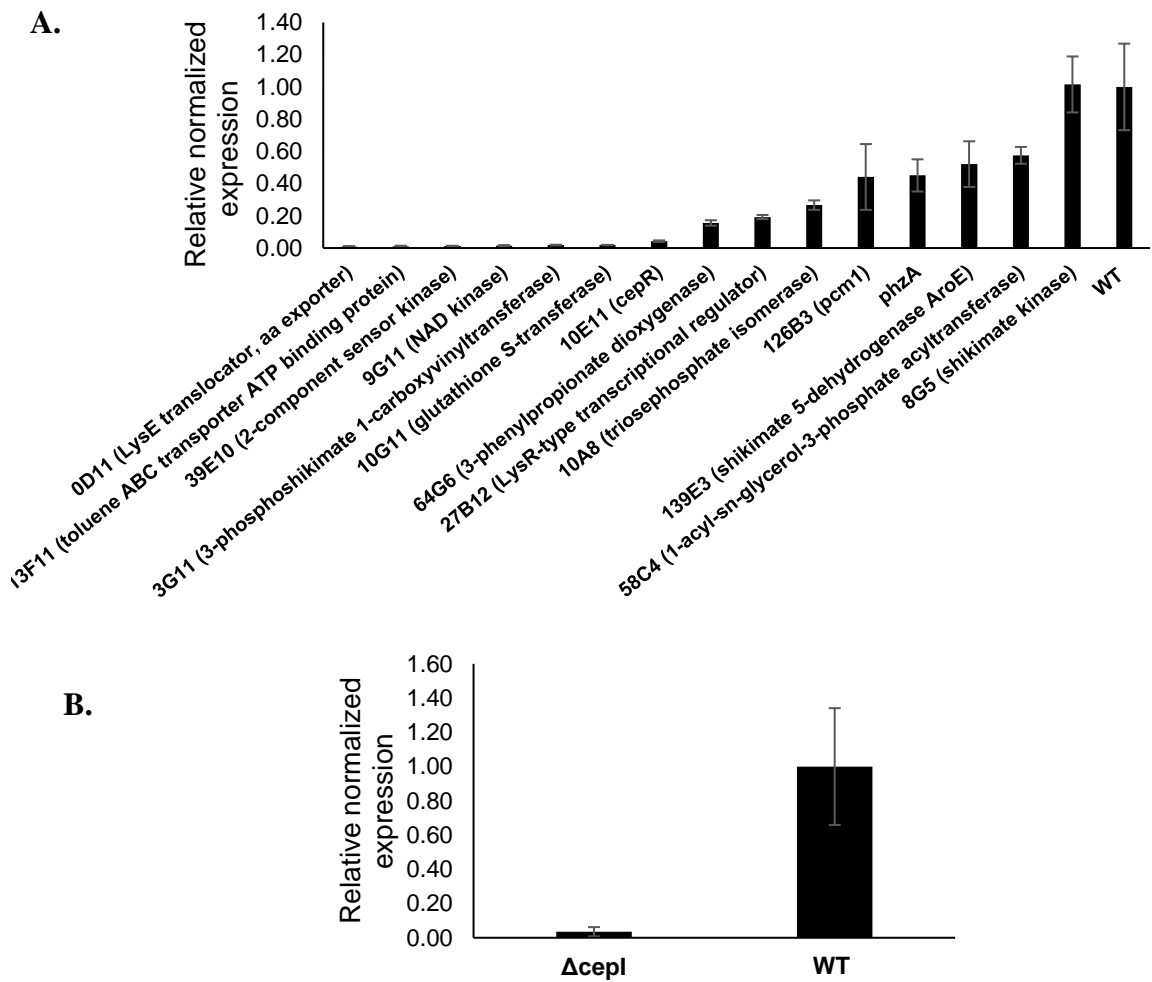


Figure 4.3 The expression of the core phenazine biosynthesis gene *phzE* in (A) selected non-pigmented transposon mutants and (B) Δ cepI knockout mutant of *B. lata* 383.

Error bars represent standard errors of means from three replicates for each sample.

4.4.3 The effect of quorum sensing on the physiology of *B. lata* 383

We tested the effects of quorum sensing on the motility, biofilm formation, and production of exoproteases and siderophores by *B. lata* 383. Our results revealed that the quorum sensing mutants were significantly affected in their ability to form biofilms and secrete siderophores and exoprotease (Figure 4.4). While the biofilm formation and

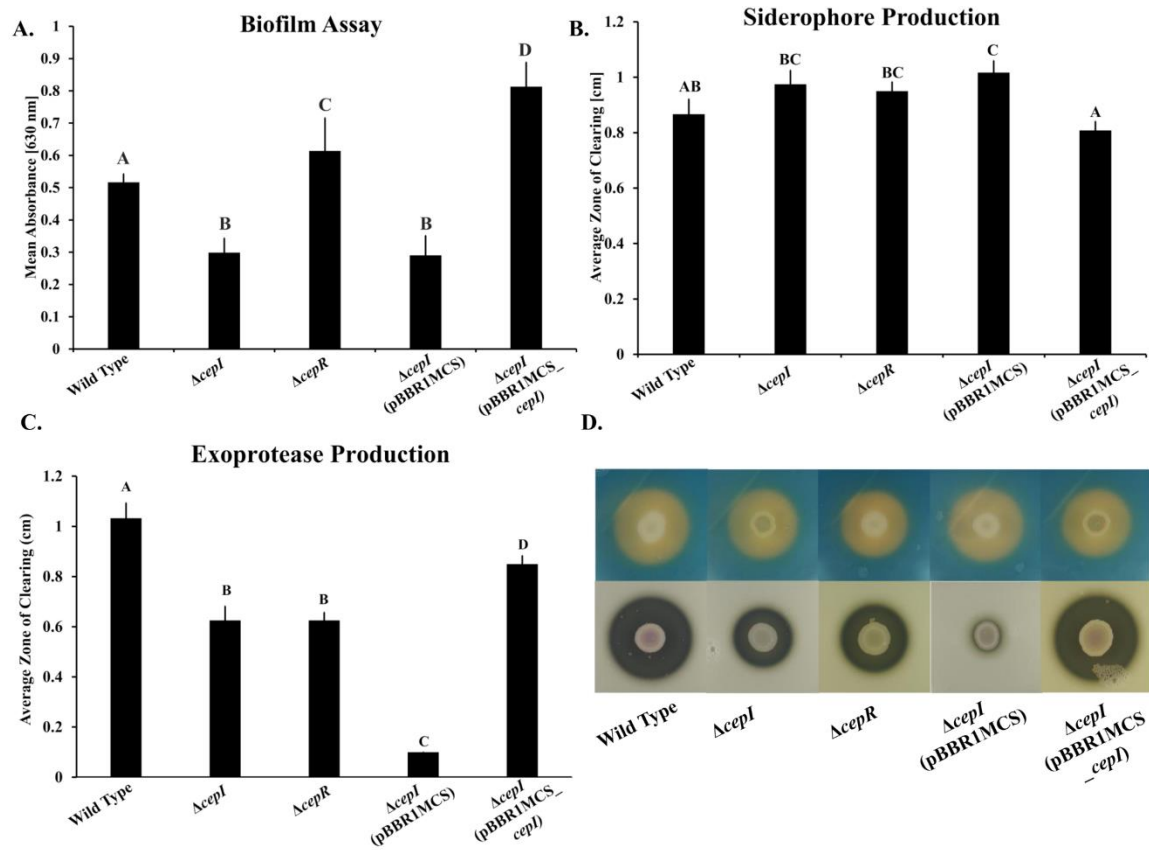


Figure 4.4 Phenotypic assays with *B. lata* 383 and quorum sensing mutants. (A) Biofilm assays demonstrate significant differences amongst treatments; (B) Siderophore assay and (C) Exoprotease assay showing zones of clearing significantly different in mutants; (D) Zone of clearing in (top) siderophore assay and (bottom) exoprotease assay of wild-type and mutant *B. lata* 383.

Different letters indicate significant differences ($P < 0.05$) between treatments.

production of exoprotease were reduced significantly in the mutants, the siderophore production increased. However, we did not find significant differences in the swimming

or swarming motility of the bacteria. Our results agree with studies of the human pathogen *B. cepacia* H111⁴⁶ and a rhizosphere biocontrol strain *B. ambifaria*,⁴⁷ where AHL-mediated quorum sensing was implicated in biofilm formation, production of siderophores and exoprotease. This indicates that quorum sensing plays a very significant role in the ecological fitness of *Burkholderia*, both in the rhizosphere and human environments. However, this is the first study to demonstrate that phenazine production in *Burkholderia* is regulated in response to cell density, similar to the opportunistic human pathogen *P. aeruginosa* and strains of the *P. fluorescens* species complex.⁴⁸

4.4.4 Transcriptomic responses of *B. lata* 383 and mutants

We further characterized the effect of mutations in *cepI* and *phzA* genes on transcriptome responses of *B. lata* 383. The transcriptome sequencing generated 213.8 million high-quality reads (~23.8 million reads per sample), which were mapped to the complete 383 genome. Statistical analysis with an FDR cutoff of 0.05 and an absolute log₂ fold change threshold of 2.0 identified 195 and 23 differentially expressed genes in the *cepI* and *phzA* mutants, respectively (Figure 4.5). Genes differentially expressed in the *phzA* mutant represented a subset of quorum sensing genes and functioned in the synthesis of phenazines and catabolism of aromatic compounds (Figure 4.5B). Among the latter were genes of the *aph* pathway that uses a multi-component phenol hydroxylase to convert phenol into catechol, which then undergoes the aromatic ring meta-cleavage by the catechol-2,3-dioxygenase and ultimately yields TCA intermediates.⁴⁹ Phenazines compete for the pool of chorismic acid with several metabolic pathways that form intermediates (e.g., anthranilate, salicylate), which can be converted to catechol. It is plausible that disruption of phenazine biosynthesis in *cepI* and *phzA* mutants causes an

accumulation of such intermediates and leads to the observed induction of the *aph* pathway. In addition to these changes, the quorum sensing mutant exhibited a significant downregulation in genes for the synthesis of the secondary metabolite pyrrolnitrin, which has antifungal properties and protects bacteria from predation by bacterivorous nematodes.^{50,51} This finding was in agreement with studies in other *Burkholderia* species that demonstrated the control of pyrrolnitrin production by quorum sensing.^{47,52}

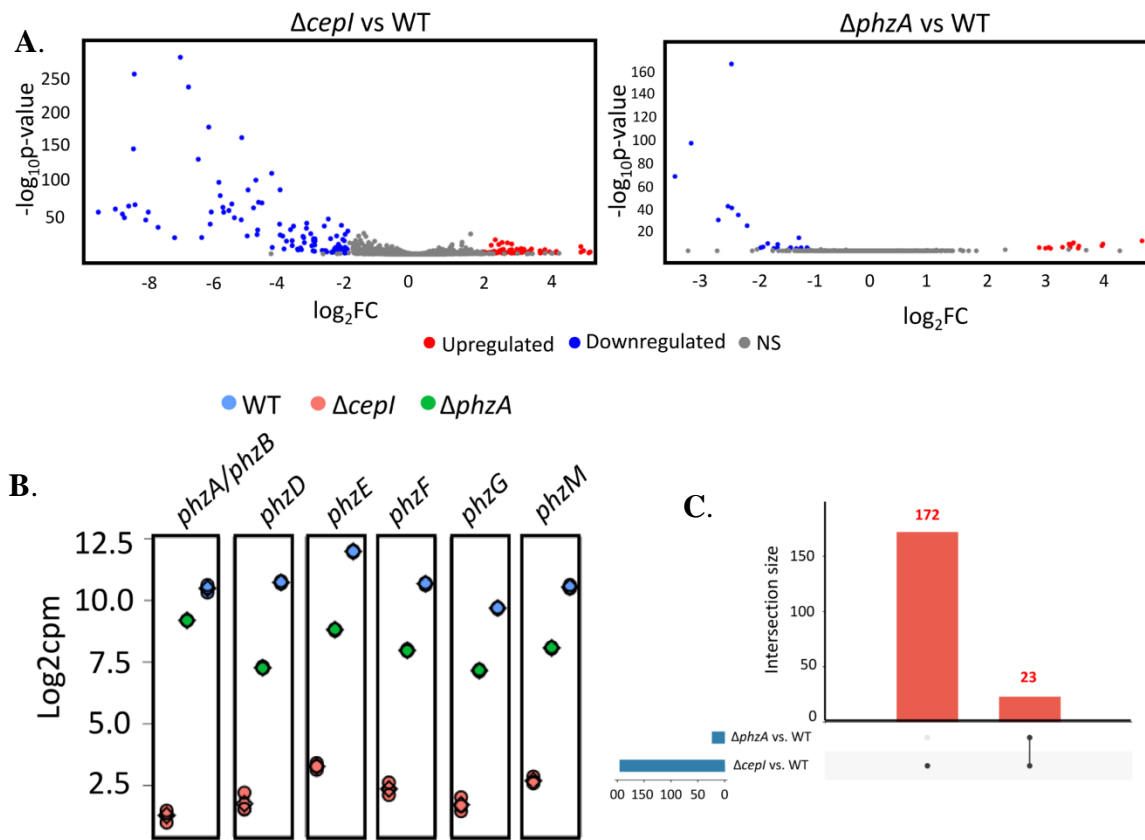


Figure 4.5 The effect of *phzA* and *cepI* mutations on the *B. lata* transcriptome. (A) Volcano plots of genes significantly up- and downregulated in both mutants in comparison to the wild-type strain (WT). (B) The significant downregulation of phenazine synthesis genes in the quorum-sensing mutant. (C) Differentially expressed genes that are shared and unique to the *phzA* and *cepI* mutants.

The functional categorization of the differentially expressed genes in *cepI* and *phzA* mutants identified the membrane and intracellular anatomic structure as the most

highly represented GO terms in the cellular component category, while oxidoreductase activity and heterocyclic compound binding were among the most abundant GO terms in the molecular function category. The biological processes were dominated by GO terms related to metabolic processes. Interestingly, several downregulated genes in the *cepI* mutant were categorized as bacterial flagellar development, possibly contributing to the mutant's deficiency in forming static biofilms (Figure 4.6).

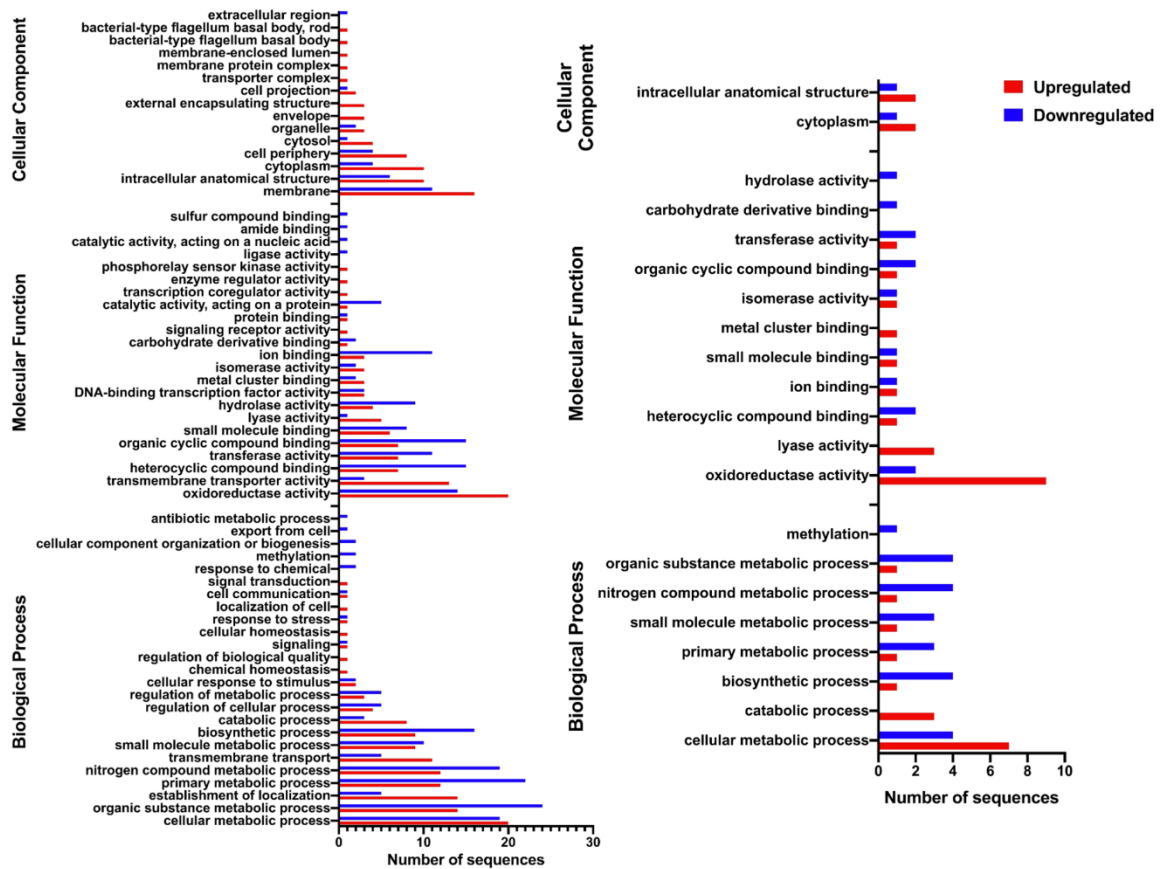


Figure 4.6 Gene ontology classification of differentially expressed genes of *B. lata* 383 in the (left) *cepI* and (right) *phzA* mutants compared to the wild-type strain.

The terms were derived from 50 different functional groups (GO subcategory level 3).

4.4.5 Effect of phenazine on *Burkholderia* transcriptome

Redox-active phenazines act as broad-range antibiotics and toxins because of their ability to divert electron flow and increase the production of reactive oxygen species, such as O_2^- and H_2O_2 .⁵³ The molecular mechanisms that prevent self-poisoning were characterized in a limited range of phenazine producers. Most of our knowledge is based on the opportunistic human pathogen *P. aeruginosa* that neutralizes phenazine toxicity by actively excreting with RND-type multidrug efflux pumps.⁵⁴ Our understanding of how other phenazine-producing species respond to and survive in the presence of these redox-active metabolites remains limited. We addressed this gap by analyzing transcriptomic responses to phenazine methosulfate (PMS) in *B. lata* 383 and two closely related phenazine-nonproducing strains, *B. cepacia* ATCC 25416 and *B. cenocepacia* K56-2. The transcriptome sequencing generated approximately 420 million high-quality reads (approximately 23.3 million reads per sample). The reads were aligned to the respective *Burkholderia* genomes and statistically analyzed for differentially expressed genes using an FDR cutoff of 0.05 and an absolute \log_2 fold change threshold of 1.5. The analysis revealed 101 differentially expressed genes in *B. lata* 383, 94 in *B. cepacia* ATCC 25416 and 38 in *B. cenocepacia* K56-2 compared to their respective control conditions (Figure 4.7). Among these, 23 genes were shared among all three strains (Table 4.2).

The analysis yielded three distinct categories of induced pathways that matched their counterparts described in *P. aeruginosa* and *B. multivorans*.^{55,56} The first group of genes operates in oxidative stress response and functions to detoxify H_2O_2 . These genes

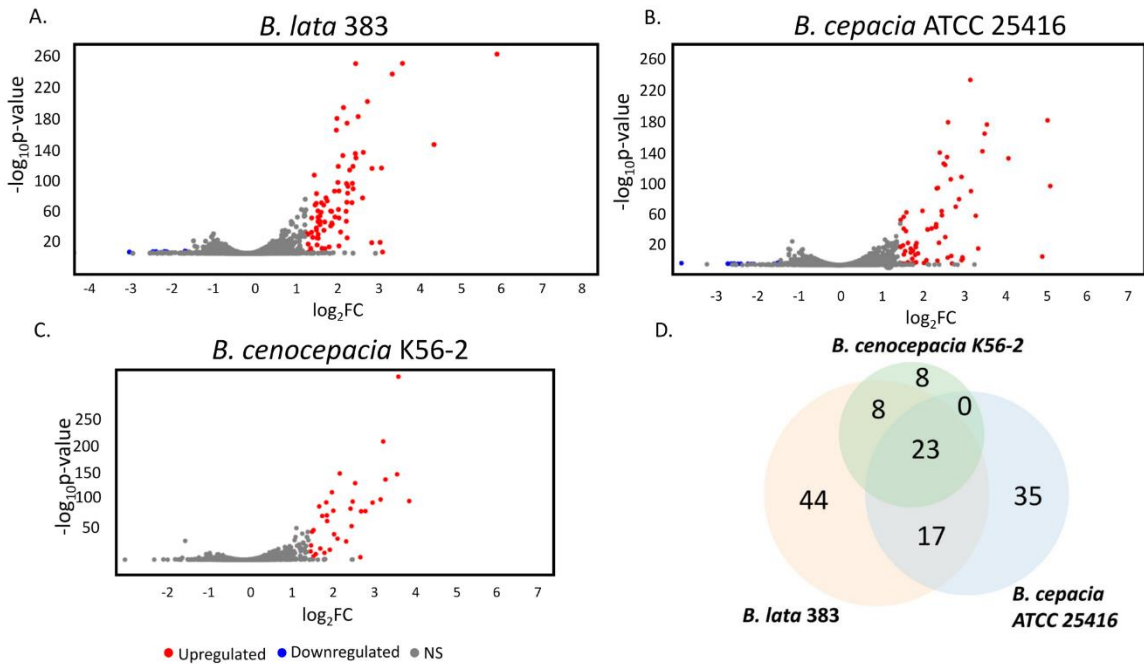


Figure 4.7 Volcano plots showing significantly up- and downregulated genes in phenazine methosulfate-treated (A) *B. lata* 383, (B) *B. cepacia* ATCC 25416, and (C) *B. cenocepacia* K56-2 compared to control conditions; (D) Venn diagram showing shared and unique differentially expressed genes in the three strains.

encode alkyl hydroperoxide reductases, catalases, peroxidases and rubrerythrin, a nonheme iron protein involved in oxidative stress defense in anaerobic microorganisms.^{57,58} The second group of genes is predicted to function in the efflux of phenazines and includes the redox-sensitive transcription regulator SoxR and the redox-regulated efflux pump RND-9 of the RND (Resistance-Nodulation- Division) superfamily. Also was observed the induction of several transporters of the major facilitator superfamily (MFS). A follow-up qPCR experiment confirmed a sharp upregulation of the RND-9 genes in *B. lata* 383 cultures treated with phenazine methosulfate compared to the untreated control (Figure 4.8).

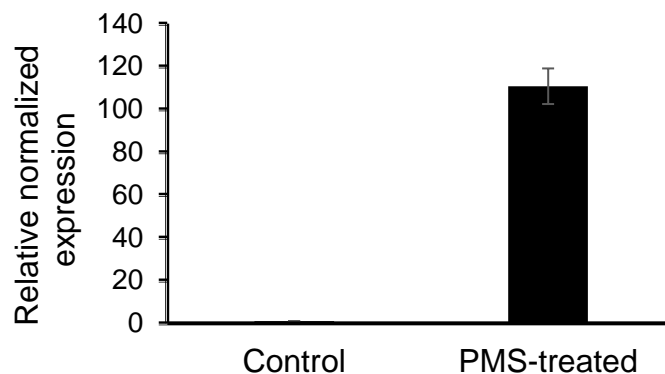


Figure 4.8 *The RND-9 efflux pump genes are strongly upregulated in response to treatment of B. lata 383 with phenazine methosulfate (PMS).*

The third category of *Burkholderia* genes induced by PMS is predicted to function in the biogenesis of Fe-S clusters. This may signify a defensive response to the damage of these prosthetic groups by phenazines or by the accumulation of phenazine-mediated reactive oxygen species.⁵⁶ Other notable pathways upregulated in the studied strains by PMS include putative chromate transporters, antibiotic biosynthesis monooxygenase and a homodimeric pyruvate dehydrogenase encoded by a gene downstream of the RND-9 locus.

The functional categorization of the differentially expressed genes in both *B. lata* 383 and *B. cepacia* ATCC 25416 revealed the intracellular anatomic structure, cytoplasm, cytosol, and cell periphery as the most highly represented GO terms in the cellular component category, while the molecular function category was dominated by GO terms such as oxidoreductase activity, ion binding, and heterocyclic compound binding. The biological process category was mostly dominated by GO terms representing metabolic processes. Several genes upregulated in both cultures were categorized as cellular detoxification and

homeostasis, which correlate to the defensive responses of the bacteria due to PMS exposure (Figure 4.9A, B).

Table 4.2 Shared differentially expressed genes and their predicted functions in *Burkholderia* strains exposed to phenazine methosulfate.^a

Predicted function	<i>B. lata</i> 383		<i>B. cepacia</i> ATCC 25416		<i>B. cenocepacia</i> K56-2	
	Feature ID ^b	log ₂ Fold change	Feature ID ^b	log ₂ Fold change	Feature ID ^b	log ₂ Fold change
Iron-sulfur cluster biosynthesis						
Fe-S cluster assembly protein IscX	BCEP18194_RS17240	2.66	DM41_RS01645	2.85	WQ49_RS28670	2.06
ISC system 2Fe-2S type ferredoxin	BCEP18194_RS17245	2.41	DM41_RS01650	2.59	WQ49_RS28665	1.9
Fe-S protein assembly chaperone HscA	BCEP18194_RS17250	2.25	DM41_RS01655	2.04	WQ49_RS28660	1.72
Fe-S protein assembly co-chaperone HscB	BCEP18194_RS17255	2.2	DM41_RS01660	2.39	WQ49_RS28655	1.88
iron-sulfur cluster assembly protein IscA	BCEP18194_RS17260	2.42	DM41_RS01665	2.42	WQ49_RS28650	2.01
Fe-S cluster assembly scaffold IscU	BCEP18194_RS17265	2.29	DM41_RS01670	2.46	WQ49_RS28645	1.79
IscS subfamily cysteine desulfurase	BCEP18194_RS17270	2.73	DM41_RS01675	2.66	WQ49_RS28640	1.9

Table 4.2 (continued).

Fe-S cluster assembly transcriptional regulator IscR	BCEP18194_RS17275	3.65	DM41_RS01680	3.62	WQ49_RS28635	2.54
IscS subfamily cysteine desulfurase	BCEP18194_RS34795	3.14	DM41_RS33125	2.73	WQ49_RS28640	1.9
Chromate efflux						
chromate transporter	BCEP18194_RS21935	2.21	DM41_RS06515	1.58	WQ49_RS24050	2.67
chromate transporter	BCEP18194_RS21940	2.49	DM41_RS06520	1.86	WQ49_RS24045	2.43
Oxidoreductases						
2-hydroxyacid dehydrogenase	BCEP18194_RS25310	2.52	DM41_RS31520	2.64	WQ49_RS07580	2.19
SDR family oxidoreductase	BCEP18194_RS27775	2.31	DM41_RS39875	1.89	WQ49_RS05400	2.14
pyruvate dehydrogenase (acetyl-transferring), homodimeric type	BCEP18194_RS27800	4.12	DM41_RS39850	3.51	WQ49_RS05375	3.52
Redox-active regulation						
redox-sensitive transcriptional activator SoxR	BCEP18194_RS27780	2.58	DM41_RS39870	2.51	WQ49_RS05395	2.04
Multidrug efflux pumps and transporters						
efflux RND transporter periplasmic adaptor subunit	BCEP18194_RS27785	6.4	DM41_RS39865	4.89	WQ49_RS05390	7.58

Table 4.2 (continued).

efflux RND transporter permease subunit	BCEP18194_RS27790	6.19	DM41_RS39860	4.58	WQ49_RS05385	7.71
efflux transporter outer membrane subunit	BCEP18194_RS27795	5.94	DM41_RS39855	4.45	WQ49_RS05380	7.17
MFS transporter	BCEP18194_RS29415	5.38	DM41_RS38485	3.23	WQ49_RS04210	5.78
Oxidative stress response						
peroxiredoxin	BCEP18194_RS32515	6.29	DM41_RS35360	6.74	WQ49_RS15395	1.53
alkyl hydroperoxide reductase subunit F	BCEP18194_RS32520	6.85	DM41_RS35355	7.24	WQ49_RS15400	2.33
catalase	BCEP18194_RS33710	8.18	DM41_RS23580	7.44	WQ49_RS16810	2.46
Others						
serine hydrolase	BCEP18194_RS36115	2.92	DM41_RS31735	3.21	WQ49_RS18900	1.54

^aThe shared differentially expressed genes were identified by BLASTp with the cutoff parameters of E-value < 1e-06, minimum percent identity > 40%, and minimum percent coverage > 65%

^bFeature IDs indicate NCBI RefSeq locus tags

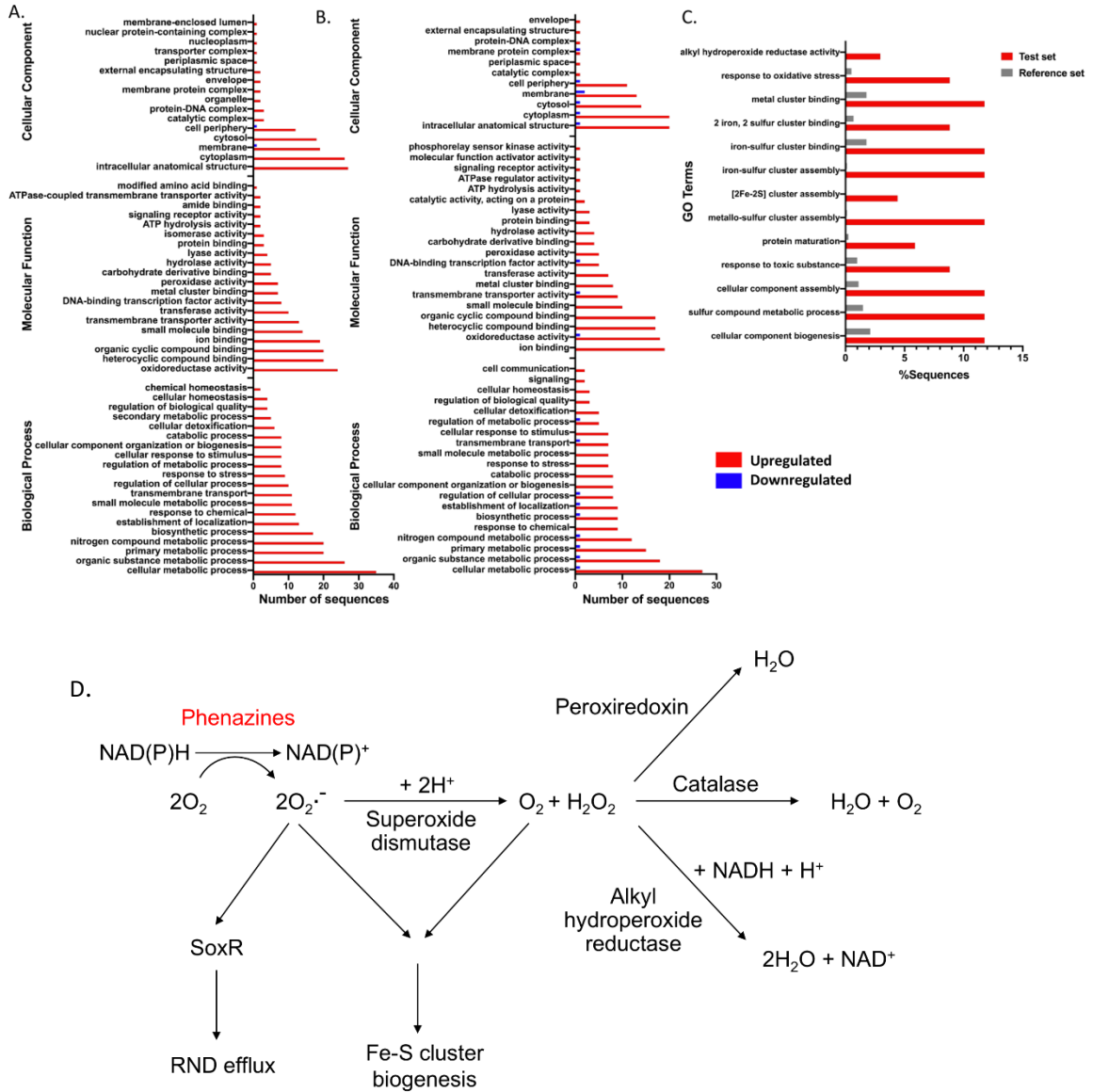


Figure 4.9 Gene ontology classification of differentially expressed genes of phenazine methosulfate-treated (A) *B. lata* 383 and (B) *B. cepacia* ATCC 25416 compared to control conditions; (C) GO term enrichment analysis of upregulated genes in phenazine methosulfate-treated *B. cepacia* ATCC 25416 compared to control conditions. (D) A representation of defense responses in *Burkholderia* cells triggered by phenazine exposure.

The terms were derived from 50 different functional groups (GO subcategory level 3). The enrichment analysis was performed using Fisher's exact test (false discovery rate-adjusted P value of ≤ 0.05).

The DEGs for K56-2 did not map to any known GO terms, hence the functional categorization could not be done, although we expect it to yield similar results. Finally,

the pathway enrichment analysis of upregulated DEGs (Fisher's exact test, FDR < 0.05) in *B. cepacia* ATCC 25416 showed the overrepresentation of processes such as oxidative stress response, iron-sulfur cluster binding and response to toxic substances (Figure 4.9C). Although the enrichment analysis for the other strains was not significant, it is certain that the phenazine methosulfate exposure triggers an oxidative stress response in these bacteria, which then leads to the induction of efflux pumps that are likely to export the toxic phenazines.

To conclude, our study identified that *Burkholderia* spp. possess a diverse set of genes that function in the biosynthesis of phenazines, cell density-dependent regulation of this process and inherent tolerance to these redox-active metabolites. The involvement of RND efflux suggests that the accumulation of phenazines in natural habitats may contribute to the continuous emergence and evolution of resistance toward clinical drugs and antibiotics.⁶ Our future studies will explore the phenazine-mediated tolerance of antibiotics in *B. lata* 383, which will have broader implications on the potential use of this strain as a biocontrol agent in agriculture, as well as in determining possible therapeutic remedies for closely related opportunistic pathogens of the *Burkholderia cepacia* species complex (Bcc).

4.5 References

1. Chepserson J, Moleleki LN. Rhizosphere bacterial interactions and impact on plant health. *Curr Opin Microbiol.* 2023;73:102297.
doi:<https://doi.org/10.1016/j.mib.2023.102297>
2. Granato ET, Meiller-Legrand TA, Foster KR. The evolution and ecology of bacterial warfare. *Curr Biol.* 2019;29(11):R521-R537.

doi:10.1016/j.cub.2019.04.024

3. Holtsmark I, Eijsink VGH, Brurberg MB. Bacteriocins from plant pathogenic bacteria. *FEMS Microbiol Lett.* 2008;280(1):1-7. doi:10.1111/j.1574-6968.2007.01010.x
4. Alvarez-Sieiro P, Montalbán-López M, Mu D, Kuipers OP. Bacteriocins of lactic acid bacteria: extending the family. *Appl Microbiol Biotechnol.* 2016;100(7):2939-2951. doi:10.1007/s00253-016-7343-9
5. Perry EK, Meirelles LA, Newman DK. From the soil to the clinic: the impact of microbial secondary metabolites on antibiotic tolerance and resistance. *Nat Rev Microbiol.* 2022;20(3):129-142. doi:10.1038/s41579-021-00620-w
6. Meirelles LA, Perry EK, Bergkessel M, Newman DK. Bacterial defenses against a natural antibiotic promote collateral resilience to clinical antibiotics. *PLoS Biol.* 2021;19(3):e3001093. doi:10.1371/journal.pbio.3001093
7. Singh AK, Shin JH, Lee KL, Imlay JA, Roe JH. Comparative study of SoxR activation by redox-active compounds. *Mol Microbiol.* 2013;90(5):983-996. doi:10.1111/mmi.12410
8. Imlay JA. The molecular mechanisms and physiological consequences of oxidative stress: lessons from a model bacterium. *Nat Rev Microbiol.* 2013;11(7):443-454. doi:10.1038/nrmicro3032
9. Meirelles LA, Newman DK. Redox-active secondary metabolites act as interspecies modulators of antibiotic resilience. *BioRxiv.* 2021.
10. Bell SC, Turner JM. Iodinin biosynthesis by a pseudomonad. *Biochem Soc Trans.* 1973;1(3):751-753. doi:10.1042/bst0010751

11. Korth H, Roemer A, Budzikiewicz H, Pulverer G. 4,9 Dihydroxyphenazine 1,6 dicarboxylic acid dimethylester and the “missing link” in phenazine biosynthesis. *J Gen Microbiol.* 1978;104(2):299-303. doi:10.1099/00221287-104-2-299
12. Lau GW, Ran H, Kong F, Hassett DJ, Mavrodi D. Pseudomonas aeruginosa pyocyanin is critical for lung infection in mice. *Infect Immun.* 2004;72(7):4275-4278. doi:10.1128/IAI.72.7.4275-4278.2004
13. Mahajan-Miklos S, Tan MW, Rahme LG, Ausubel FM. Molecular mechanisms of bacterial virulence elucidated using a Pseudomonas aeruginosa-Caenorhabditis elegans pathogenesis model. *Cell.* 1999;96(1):47-56. doi:10.1016/S0092-8674(00)80958-7
14. Guttenberger N, Blankenfeldt W, Breinbauer R. Recent developments in the isolation, biological function, biosynthesis, and synthesis of phenazine natural products. *Bioorganic Med Chem.* 2017;25(22):6149-6166. doi:10.1016/j.bmc.2017.01.002
15. Mavrodi D V., Peever TL, Mavrodi OV., et al. Diversity and evolution of the phenazine biosynthesis pathways. *Appl Environ Microbiol.* 2010;76(3):866-879. doi:10.1128/AEM.02009-09
16. Hendry S, Steinke S, Wittstein K, et al. Functional analysis of phenazine biosynthesis genes in Burkholderia spp. *Appl Environ Microbiol.* 2021;87(11):e02348-20. doi:10.1128/AEM.02348-20
17. Eberl L, Vandamme P. Members of the genus Burkholderia: good and bad guys. *F1000Research.* 2016;5:F1000. doi:10.12688/f1000research.8221.1
18. Depoorter E, De Canck E, Peeters C, et al. Burkholderia cepacia complex taxon

- K: where to split? *Front Microbiol.* 2020;11:1594. doi:10.3389/fmicb.2020.01594
19. Pope CE, Short P, Carter PE. Species distribution of Burkholderia cepacia complex isolates in cystic fibrosis and non-cystic fibrosis patients in New Zealand. *J Cyst Fibros.* 2010;9(6):442-446. doi:10.1016/j.jcf.2010.08.011
 20. Medina-Pascual MJ, Valdezate S, Carrasco G, Villalón P, Garrido N, Saéz-Nieto JA. Increase in isolation of Burkholderia contaminans from Spanish patients with cystic fibrosis. *Clin Microbiol Infect.* 2015;21(2):150-156. doi:10.1016/j.cmi.2014.07.014
 21. Leong LEX, Lagana D, Carter GP, et al. Burkholderia lata infections from intrinsically contaminated chlorhexidine mouthwash, Australia, 2016. *Emerg Infect Dis.* 2018;24(11):2109-2111. doi:10.3201/eid2411.171929
 22. Green, R M, Sambrook J. Molecular Cloning: A Laboratory Manual, 4th edition. *Cold Spring Harb Lab Press.* 2012;33(1).
 23. King EO, Ward MK, Raney DE. Two simple media for the demonstration of pyocyanin and fluorescin. *J Lab Clin Med.* 1954;44(2):301-307.
 24. Dennis JJ, Zylstra GJ. Plasposons: Modular self-cloning minitransposon derivatives for rapid genetic analysis of gram-negative bacterial genomes. *Appl Environ Microbiol.* 1998;64(7):2710-2715. doi:10.1128/aem.64.7.2710-2715.1998
 25. Thomas L. The molecular basis for preservative resistance in Burkholderia cepacia complex bacteria. [Doctoral dissertation]:Cardiff University; 2011.
 26. Manoil C. Tagging exported proteins using Escherichia coli alkaline phosphatase gene fusions. *Methods Enzymol.* 2000;326:35-47. doi:10.1016/s0076-

6879(00)26045-x

27. Winsor GL, Khaira B, Van Rossum T, Lo R, Whiteside MD, Brinkman FSL. The Burkholderia Genome Database: Facilitating flexible queries and comparative analyses. *Bioinformatics*. 2008;24(23):2803-2804.
doi:10.1093/bioinformatics/btn524
28. Barrett AR, Kang Y, Inamasu KS, Son MS, Vukovich JM, Hoang TT. Genetic tools for allelic replacement in Burkholderia species. *Appl Environ Microbiol*. 2008;74(14):4498-4508. doi:10.1128/AEM.00531-08
29. Miller JH. M9 minimal medium (standard). *Cold Spring Harb Protoc*. 2010;pdb.rec122. doi:10.1101/pdb.rec12295
30. Himpsl SD, Mobley HLT. Siderophore detection using chrome azurol S and cross-feeding assays. *Methods in Molecular Biology*. 2019;2021:97-108
doi:10.1007/978-1-4939-9601-8_10
31. Vijayaraghavan P, Gnana S, Vincent P. A simple method for the detection of protease activity on agar plates using bromocresolgreen dye. *J Biochem Tech*. 2013;4(3):628-630.
32. Ha DG, Kuchma SL, O'Toole GA. Plate-based assay for swimming motility in Pseudomonas aeruginosa. *Methods Mol Biol*. 2014;1149:59-65. doi:10.1007/978-1-4939-0473-0_7
33. O'Toole GA. Microtiter dish biofilm formation assay. *J Vis Exp*. 2011;(47):2437.
doi:10.3791/2437
34. Arkin AP, Cottingham RW, Henry CS, et al. KBase: The United States Department of Energy Systems Biology Knowledgebase. *Nat Biotechnol*.

- 2018;36(7):566-569. doi:10.1038/nbt.4163
35. Kim D, Paggi JM, Park C, Bennett C, Salzberg SL. Graph-based genome alignment and genotyping with HISAT2 and HISAT-genotype. *Nat Biotechnol.* 2019;37(8):907-915. doi:10.1038/s41587-019-0201-4
 36. Pertea M, Pertea GM, Antonescu CM, Chang T-C, Mendell JT, Salzberg SL. StringTie enables improved reconstruction of a transcriptome from RNA-seq reads. *Nat Biotechnol.* 2015;33(3):290-295. doi:10.1038/nbt.3122
 37. Love MI, Huber W, Anders S. Moderated estimation of fold change and dispersion for RNA-seq data with DESeq2. *Genome Biol.* 2014;15(12):550. doi:10.1186/s13059-014-0550-8
 38. Götz S, García-Gómez JM, Terol J, et al. High-throughput functional annotation and data mining with the Blast2GO suite. *Nucleic Acids Res.* 2008;36(10):3420-3435. doi:10.1093/nar/gkn176
 39. Braga A, Faria N. Bioprocess optimization for the production of aromatic compounds with metabolically engineered hosts: Recent developments and future challenges. *Front Bioeng Biotechnol.* 2020;8:96. doi:10.3389/fbioe.2020.00096
 40. Jiang M, Zhang H. Engineering the shikimate pathway for biosynthesis of molecules with pharmaceutical activities in *E. coli*. *Curr Opin Biotechnol.* 2016;42:1-6. doi:10.1016/j.copbio.2016.01.016
 41. Minezaki Y, Homma K, Nishikawa K. Genome-wide survey of transcription factors in prokaryotes reveals many bacteria-specific families not found in archaea. *DNA Res.* 2005;12(5):269-280. doi:10.1093/dnares/dsi016
 42. Webb E, Claas K, Downs D. thiBPQ encodes an ABC transporter required for

- transport of thiamine and thiamine pyrophosphate in *Salmonella typhimurium*. *J Biol Chem*. 1998;273(15):8946-8950. doi:10.1074/jbc.273.15.8946
43. Cole L, Kramer PR. Chapter 5.2 - Vitamins and Minerals. In: *Human Physiology, Biochemistry and Basic Medicine*; 2016.
44. Hunter RC, Newman DK. A putative ABC transporter, hatABCDE, is among molecular determinants of pyomelanin production in *Pseudomonas aeruginosa*. *J Bacteriol*. 2010;192(22):5962-5971. doi:10.1128/JB.01021-10
45. Slinger BL, Deay JJ, Chandler JR, Blackwell HE. Potent modulation of the CepR quorum sensing receptor and virulence in a *Burkholderia cepacia* complex member using non-native lactone ligands. *Sci Rep*. 2019;9(1):13449. doi:10.1038/s41598-019-49693-x
46. Huber B, Riedel K, Hentzer M, et al. The cep quorum-sensing system of *Burkholderia cepacia* H111 controls biofilm formation and swarming motility. *Microbiology*. 2001;147(9):2517-2528. doi:10.1099/00221287-147-9-2517
47. Chapalain A, Vial L, Laprade N, Dekimpe V, Perreault J, Déziel E. Identification of quorum sensing-controlled genes in *Burkholderia ambifaria*. *Microbiologyopen*. 2013;2(2):226-242. doi:10.1002/mbo3.67
48. Higgins S, Heeb S, Rampioni G, Fletcher MP, Williams P, Cámara M. Differential regulation of the phenazine biosynthetic operons by quorum sensing in *Pseudomonas aeruginosa* PAO1-N. *Front Cell Infect Microbiol*. 2018;8:252. doi:10.3389/fcimb.2018.00252
49. Suvorova IA, Gelfand MS. Comparative genomic analysis of the regulation of aromatic metabolism in betaproteobacteria. *Front Microbiol*. 2019;10:642.

doi:10.3389/fmicb.2019.00642

50. Nandi M, Selin C, Brassinga AKC, et al. Pyrrolnitrin and hydrogen cyanide production by *Pseudomonas chlororaphis* strain PA23 exhibits nematicidal and repellent activity against *Caenorhabditis elegans*. *PLoS One*. 2015;10(4):e0123184. doi:10.1371/journal.pone.0123184
51. Quecine MC, Kidarsa TA, Goebel NC, et al. An interspecies signaling system mediated by fusaric acid has parallel effects on antifungal metabolite production by *Pseudomonas protegens* strain Pf-5 and antibiosis of *Fusarium* spp. *Appl Environ Microbiol*. 2016;82(5):1372-1382. doi:10.1128/AEM.02574-15
52. Schmidt S, Blom JF, Pernthaler J, et al. Production of the antifungal compound pyrrolnitrin is quorum sensing-regulated in members of the *Burkholderia cepacia* complex. *Environ Microbiol*. 2009;11(6):1422-1437. doi:10.1111/j.1462-2920.2009.01870.x
53. Hassan HM, Fridovich I. Mechanism of the antibiotic action of pyocyanine. *J Bacteriol*. 1980;141(1):156-163. doi:10.1128/jb.141.1.156-163.1980
54. Sakhtah H, Koyama L, Zhang Y, et al. The *Pseudomonas aeruginosa* efflux pump MexGHI-OpmD transports a natural phenazine that controls gene expression and biofilm development. *Proc Natl Acad Sci U S A*. 2016;113(25):E3538-E3547. doi:10.1073/pnas.1600424113
55. Meirelles LA, Newman DK. Phenazines and toxoflavin act as interspecies modulators of resilience to diverse antibiotics. *Mol Microbiol*. 2022;117(6):1384-1404. doi:https://doi.org/10.1111/mmi.14915
56. Meirelles LA, Newman DK. Both toxic and beneficial effects of pyocyanin

contribute to the lifecycle of *Pseudomonas aeruginosa*. *Mol Microbiol.* 2018;110(6):995-1010. doi:10.1111/mmi.14132

57. Lumppio HL, Shenvi N V., Summers AO, Voordouw G, Kurtz J. Rubrerythrin and rubredoxin oxidoreductase in *Desulfovibrio vulgaris*: A novel oxidative stress protection system. *J Bacteriol.* 2001;183(1):101-108. doi:10.1128/JB.183.1.101-108.2001
58. Mishra S, Imlay J. Why do bacteria use so many enzymes to scavenge hydrogen peroxide? *Arch Biochem Biophys.* 2012;525(2):145-160. doi:10.1016/j.abb.2012.04.014

CHAPTER V- CONCLUSIONS

Rhizosphere microorganisms encompass numerous beneficial microbes that improve plant growth by participating in nutrient cycling, organic matter decomposition, and mineral weathering. Other species contribute to defense responses against soilborne pathogens, impact plant development by regulating phytohormone levels, and protect plants from abiotic stress. However, although the importance of rhizosphere microbial communities has been recognized for a long time, only a handful of species were commercialized as biofertilizers or biopesticides. The idea of manipulating the rhizosphere microbiome, often termed rhizosphere engineering, provides a sustainable avenue for improving plant health¹ and is considered an important aspect of sustainable food production in the future.² However, the successful implementation of these technologies relies on understanding molecular interactions in the rhizosphere microbiome. My research aimed to address this knowledge gap by exploring the transcriptome responses of two rhizosphere bacteria to the plant rhizodeposits and redox-active microbial metabolites.

The first part of my thesis project focused on *Pseudomonas synxantha* 2-79, a model strain that exemplifies a complex of beneficial rhizobacteria associated with dryland wheat and barley grown in the arid parts of the Pacific Northwest.³ 2-79 acts as a biocontrol agent by producing redox-active phenazines against soilborne fungal pathogens that pose significant agricultural yield constraints. However, the molecular mechanisms behind the adaptation of these bacteria to the water-stressed rhizosphere remained largely unknown. In the first specific aim, I addressed this gap by focusing on *P. synxantha* 2-79 responses to root exudates of healthy barley plants (*Hordeum*

vulgare L.) and plants infected by the soilborne fungal pathogen *Rhizoctonia solani* AG-8. The targeted metabolomic analysis revealed that root exudates contain a complex mix of primary and secondary metabolites that collectively perturb hundreds of bacterial genes involved in the uptake and catabolism of C and N sources, synthesis of antimicrobial secondary metabolites, and biofilm formation. These results reveal how rhizodeposition shapes the plant microbiome by recruiting organisms involved in growth promotion and disease control and how these microbial taxa adapt themselves in the competitive rhizosphere environment.

My second aim explored the interactions between *P. synxantha* 2-79 and its typical host plant, wheat, in the event of water stress. My study identified that water stress significantly alters the wheat root exudate composition and increases the concentration of quaternary ammonium compounds (QACs) that are known to function as microbial osmoprotectants. Transcriptomic responses of the bacteria in the presence of these root exudates identified the significant upregulation of QAC uptake and catabolism genes, which indicates that the sustenance of rhizobacteria in arid regions or soils with excessive salinity depends considerably on rhizodeposition. These results may help to develop new crop varieties for dryland farming in the current era of global climate change.

The final part of my thesis project addressed the interactions of rhizobacterial species with secondary metabolites like phenazines. This study focused on *Burkholderia*, a diverse group of microorganisms, some of which act as plant-associated biocontrol agents. In contrast, others include economically important plant and animal pathogens.⁴ Many of these species produce redox-active phenazine metabolites that contribute to

biofilm formation. I aimed to characterize the regulation of phenazine production in *Burkholderia lata* 383, a member of the *B. cepacia* complex. We also investigated the defense responses of *B. lata* 383 and two phenazine-non-producing species, *B. cepacia* ATCC 25416 and *B. cenocepacia* K56-2, to phenazine toxicity. Our results identified quorum sensing as a key mechanism driving the production of phenazines in *Burkholderia*. We also revealed that phenazine resistance involves oxidative stress response and multidrug efflux by RND pumps. These results indicate that *Burkholderia* possess inherent mechanisms for self-resistance against phenazines present in the plant rhizosphere. These resilience mechanisms may also contribute to the resistance of pathogenic *Burkholderia* to medical antibiotics.

5.1 References

1. Dlamini SP, Akanmu AO, Babalola OO. Rhizospheric microorganisms: The gateway to a sustainable plant health. *Front Sustain Food Syst.* 2022;6. doi:10.3389/fsufs.2022.925802
2. Hakim S, Naqqash T, Nawaz MS, et al. Rhizosphere engineering with plant growth-promoting microorganisms for agriculture and ecological sustainability. *Front Sustain Food Syst.* 2021;5. doi:10.3389/fsufs.2021.617157
3. Parejko JA, Mavrodi D V., Mavrodi O V., Weller DM, Thomashow LS. Population structure and diversity of phenazine-1-carboxylic acid producing fluorescent *Pseudomonas* spp. from dryland cereal fields of central Washington state (USA). *Microb Ecol.* 2012;64(1):226-241. doi:10.1007/s00248-012-0015-0
4. Lauman P, Dennis JJ. Advances in phage therapy: Targeting the *Burkholderia cepacia* complex. *Viruses.* 2021;13(7):1331. doi:10.3390/v130713